SCALE INFLUENCES ON THE REPRESENTATION

OF SNOWPACK PROCESSES

by

Charles H. Luce

A dissertation submitted in partial fulfillment
of the requirements for the degree
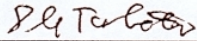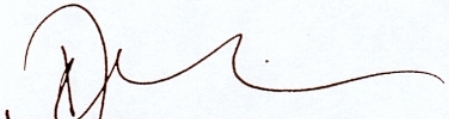
of

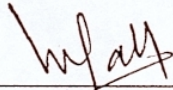DOCTOR OF PHILOSOPHY

in

Civil and Environmental Engineering

Approved:
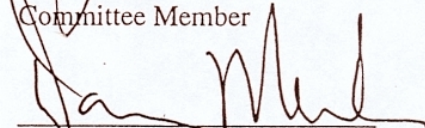
_____
David G. Tarboton
Major Professor

_____
Upmanu Lall
Committee Member

_____
Christopher M.U. Neale
Committee Member

_____
David S. Bowles
Committee Member
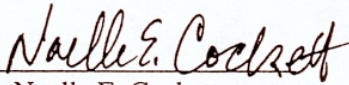
_____
Danny Marks
Committee Member

_____
Charles W. Slaughter
Committee Member

_____
Noelle E. Cockett
Interim Dean of Graduate Studies

UTAH STATE UNIVERSITY
Logan, Utah

2000

ABSTRACT

Scale Influences on the Representation

of Snowpack Processes

by

Charles H. Luce, Doctor of Philosophy

Utah State University, 2000

Major Professor: Dr. David G. Tarboton
Department: Civil and Environmental Engineering

In mountainous and high latitude regions, melting snow provides much of the
water for drinking and irrigation; it also drives the spring floods. Improved description
and modeling of the processes responsible for snowmelt are important for managing
water supplies and flood risks. This dissertation focuses on scale issues in the modeling
of snowmelt. Snow accumulation and melt is complicated, involving nonlinear energy
and mass exchanges between layers within the snow at a point. At larger scales snow
accumulates in spatially variable patterns due to wind drifting. Melt is also spatially
variable due to variable energy inputs. This variability across a range of scales and
physical mechanisms poses a challenge to model representations of snow.

This dissertation is a collection of four papers addressing some of these
challenges. The first investigates point scale processes using detailed measurements and
provides parameterizations that enable a single-layer snowpack model to reasonably

model the energy content and surface temperature of the snowpack. The remaining three papers focus on spatial variability. Detailed measurements over a 26-ha watershed are compared to model simulations showing the importance and, in this watershed, dominance of wind-induced drifting as a cause for spatial variability. The spatial variability of snow is quantified in terms of the relationship between average snow water equivalence and snow-covered area. This relationship, called a depletion curve, was incorporated into a point snowmelt model. Using a single model element, this model estimated surface water inputs over the 26-ha watershed as accurately as the point model applied on a fine grid. Depletion curves are related to, and can be derived from, the spatial probability density function of snow at peak accumulation, reducing the observational burden required to establish the depletion curve and providing improved context for understanding depletion curves. The last paper presents further theory to improve depletion curves through incorporation of the spatial distribution of radiation. The advances in methods for parameterizing snowmelt processes have application in hydrologic modeling for water resources and flood studies as well as representing the surface boundary conditions in climate models.

(202 pages)

DEDICATION

This work is dedicated to my loving family.

FRONTISPIECE

ACKNOWLEDGMENTS

Charles H. Luce

CONTENTS

LIST OF TABLES

LIST OF FIGURES

Figure   Page

CHAPTER 1

INTRODUCTION

In the fall of the year, the first snows touch the high mountaintops. From a distance it is a white frosting capping the mix of greens, yellows, and reds on the slopes below. Shortly, the mountain landscape becomes snow covered from the valleys to the ridges. As time rolls around to spring, we can watch the landscape become progressively snow free beginning on south-facing and low elevation slopes and eventually climbing back to the ridgetops.

This process also can be watched by latitude as the snow line moves south in the fall and back north in the spring. Alaska's North Slope may be covered by snow at the end of August, while high elevation areas (that will eventually be snow covered) further south are still warm. The accumulation in the southern mountains, however, may be greater so that much of the North Slope becomes snow free in the spring before the southern mountains.

We also see the same pattern at finer scales, particularly in the spring. Each spring, avid backcountry skiers must contend with taking-off and putting-on skis as their favorite trails melt-out completely in one place and have waist-deep snow in another. Often the source is variable drifting and shading caused by topography and trees.

These examples describe the visible effects of spatially varying processes leading to spatial variability in the snowcover. This spatial variability interacting with the time series of weather events yields the time series of snowmelt and streamflow that is the basis of water supplies from high elevation and high latitude areas. As will be discussed in this dissertation, knowledge only of the amount of snow in an area is insufficient for

most modeling purposes, whether the goal is to estimate snowmelt, runoff, snow-covered area, or energy and water exchanges with the atmosphere. What are the effects of this heterogeneity as we change from the point scale to larger basins? How can we revise our description of properties of the snowpack to better model the evolution of the important properties at scales of interest?

Scale issues pose important and sometimes difficult problems to the advance of hydrologic science [*Burges*, 1986; *National Research Council*, 1991]. The paired issue of subgrid variability and scale of model elements is key to improved modeling of hydrologic systems. Subgrid variability is variability occurring within a single model element that must be described by a parameterization. Darcy's law is a famous example of a parameterization describing the net effect of microscale spatial heterogeneity in pores that water must pass through when flowing through soil. The scale problem has been defined as the need to derive hydrologic models for specific scales [*Dooge*, 1986; *Beven and Fisher*, 1996; *Blöschl*, 1996]. Brutsaert [1986] called for an "appropriate level of parameterization" to solve a given hydrologic problem given available or measurable data. If our observations consist of one or a few precipitation gages and a weir measuring basin outflow, our parameterization should be constructed to the scale of the basin. This presumes we can believably scale up precipitation measurements from one or a few 8-inch orifices to the scale of the catchment, a presumption necessary even if a fine resolution distributed model were to be used. It is generally agreed that we may need to view physical processes differently at different scales and that substantial creativity may be necessary to construct such a parameterization [*Dooge*, 1986; *Beven*, 1989; *Seyfried and Wilcox*, 1995]. One of the questions that will be important in building

parameterizations for larger scale processes is in understanding which properties or state variables are important to define and describe as we increase the model integration area, or model "support."

This dissertation is about the exploration for parameterizations for snow pack models. It moves through scales of interest from describing the vertical heat flow in the snowpack, at what would be described as a point scale, to parameterizing drifting in a small basin, to providing considerations for scaling up to larger model supports. It is organized into six chapters, including this introduction and the summary. The four primary chapters are individual papers that have been published or will be submitted for journal publication.

Chapter 2 is a detailed examination of snowpack processes at the point scale, examining heterogeneity in the vertical dimension of the snowpack. The data were collected in the bottom of Cache Valley on the west edge of Logan, Utah. Much of the discussion focuses on how to describe the heat balance of a vertically integrated snowpack. State-of-the-art snowpack modeling requires a vertically distributed model such as SNTHRM [*Jordan*, 1991]. Using such a model over a watershed represents a mismatch between the detailed vertical calculations of heat flow and precision of the model calculations to the quality and resolution of data available with which to drive it. In addition, point scale vertically lumped models are useful in spatially lumped snowpack modeling. The paper also examines other aspects of the energy balance of a snowpack in a mountain valley, highlighting the importance of knowledge of fog occurrence during inversions on estimates of incoming longwave radiation.

Chapter 3 points out that basin average snowmelt cannot be described using point scale equations with basin-averaged parameters. Repeated measurements of snow water equivalence at 255 points in the Upper Sheep Creek basin of Reynolds Creek Experimental Watershed over one winter were used validate a distributed snowpack model that was then used as the basis for comparisons. Comparisons were made between the fully distributed snowpack model, which included description of spatial variation in drifting and solar radiation; a model where drifting was ignored but variability in solar radiation was modeled; a single point basin representation; and a two-patch model that breaks the basin into two regions, each modeled with the point scale model. This showed that the dominant source of spatial variability in the basin is the drifting, so much so that the model with spatially varying radiation but uniform drift performed nearly as poorly as the single point model. The two-patch representation was also fairly poor because of the extreme heterogeneity caused by the drifting.

Chapter 4 describes the development and testing of a parameterization based on differential accumulation that successfully described the evolution of the snowpack in Upper Sheep Creek. The parameterization was based on the depletion curve concept that heretofore has been used to estimate runoff from snowmelt. A depletion curve is a relationship between snow-covered area and the basin average snow water equivalence. By assuming that areas with shallowest snow melt first, we showed how to calculate the depletion curve from information about the probability density function of snow water equivalence at peak accumulation.

Chapter 5 examines the development of parameterizations for snowmelt in a more general sense by describing how different sources of variability might interact. Chapters

3 and 4 show that drifting is the primary effect on spatial variability. Chapter 5 explicitly incorporates differential solar radiation into the depletion curve concept to improve the parameterization. This addition of differential energy input was added based on the idea that the change in the variance (spatially sampled) of snow water equivalence is related to the covariance of snow water equivalence and its accumulation or melt. If areas with deep snow receive a greater precipitation depth during an event than areas with shallow snow, the variance increases. Likewise, if areas with shallow snow receive more sun, the variance will (at least temporarily) increase.

The four chapters show an increase in scale from a discussion of issues important for point scale modeling, to small basin scale modeling, to modeling of larger basins or climate grid cells. Each stands as a separate contribution, but there is also an evolution of thought apparent among them. The actual writing sequence was 3,4,2,5, but they are set here according to the spatial scales addressed. Taken together the papers are about the opportunities for learning inherent in the attempt to scale up snowmelt models. The analyses and lessons herein provide insights about spatial patterns that are helpful to those who work with snowmelt problems.

REFERENCES

Beven, K., Changing ideas in hydrology—the case of physically-based models, *J. Hydrol.*, *105*, 157-172, 1989.

Beven, K., and J. Fisher, Remote sensing and scaling in hydrology, in *Scaling up in Hydrology using Remote Sensing*, edited by J. B. Stewart, E. T. Engman, R. A. Feddes and Y. Kerr, pp. 1-18, John Wiley and Sons, Chichester, 1996.

Blöschl, G., *Scale and Scaling in Hydrology*, Habilitationsschrift, Weiner Mitteilungen Wasser Abwasser Gewasser, Wien, 1996.

Brutsaert, W., Catchment-scale evaporation and the atmospheric boundary layer, *Water Resour. Res.*, *22*, 39S-45S, 1986.

Burges, S. J., Trends and directions in hydrology, *Water Resour. Res.*, *22*, 1S-5S, 1986.

Dooge, J. C. I., Looking for hydrologic laws, *Water Resour. Res.*, *22*, 46S-58S, 1986.

Jordan, R., A one-dimensional temperature model for a snow cover, technical documentation for SNTHERM.89, *Special Technical Report 91-16*, US Army CRREL, Hanover, N.H., 1991.

National Research Council, *Opportunities in the Hydrologic Sciences*, National Academy Press, Washington, DC, 1991.

Seyfried, M. S., and B. P. Wilcox, Scale and the nature of spatial variability: Field examples having implications for hydrologic modeling, *Water Resour. Res.*, *31*, 173-184, 1995.

CHAPTER 2

SNOWPACK ENERGY FLUXES IN A LARGE MOUNTAIN VALLEY[1]

Abstract. Detailed measurements of the energy balance of a snowpack in a mountain

valley are used to 1) characterize relative contributions from different components of the

energy budget at a valley site, 2) compare characteristics of the valley floor energy

balance to those of a site part way up the valley sides, 3) test alternative models of

internal snowpack heat conduction and ground heat flux, 4) examine the sensitivity of

turbulent flux estimates to stability corrections under common weather conditions in a

valley, 5) test a simple albedo model, and 6) assess the uncertainty in incoming longwave

radiation. The dominant feature of the season was the long cold periods when there were

temperature inversions in the valley. The inversion muted most fluxes but increased the

ground heat flux, and the cumulative ground heat flux was comparable in magnitude with

other cumulative fluxes. During one brief warming, the inversion broke and the turbulent

flux was large, and at the end of the season, net radiation increased dramatically with

clearing of the inversion. The inversion kept a snowpack in the valley bottom one month

after the snowpack melted on benches on the valley sides. The long cold periods

provided opportunities to test models of heat conduction within and below the snowpack.

Describing the heat flux with a sinusoidal model shows promise for estimation of the heat

flux near the surface of the snowpack and the ground heat flux, but more work is needed

to generalize the model beyond periods with no snowmelt. During the period of the cold

---

[1] Coauthored by Charles H. Luce and David G. Tarboton.

inversion, turbulent transfers were very sensitive to estimates of the stability correction, but during the largest turbulent heat transfer event, the stability corrections were negligible. A test of a simple albedo model showed good agreement for daily time scale variations caused by changes in the angle of incidence, but poor estimates of long term variations in albedo caused by changes in the surface. Uncertainty in incoming longwave radiation was great because the airmass in the inversion layer could rapidly change from fog to clear, and the effective emissivity of the atmosphere is very sensitive to the presence of liquid water droplets. Uncertainty is great enough that direct observation of incoming longwave radiation or of cloudiness may be needed to accurately describe the energy balance of a valley under an inversion. A pattern of cloudiness could be seen with night and morning fog and relatively clear skies typical of afternoon and early evening. In summary, the presence of a persistent inversion was a very important feature in the energy balance of the snowpack in Cache Valley during the winter of 1993, and information gained from monitoring of parts of the energy balance at a site in the valley is important for improving vertically lumped snowpack models and for improving spatial representations of climate in valleys for spatially lumped and distributed models.

1. INTRODUCTION

Water supply at high elevations and high latitudes is closely tied to the accumulation and melt of seasonal snowpacks. Snow cover energy exchanges govern generation of snowmelt that provides runoff and water supply in these regions. These energy exchanges affect atmospheric water and temperature. Detailed measurements of the energy balance of a snowpack are required to further the goals of better understanding

and modeling snow cover energy exchanges. There are many contributions on the subject in the research literature [e.g., *Male and Granger*, 1981; *Marks and Dozier*, 1992; *Dingman*, 1994; *Tarboton*, 1994], and many new questions arise as the science of hydrology advances. An underlying theme of much hydrologic research is to learn how changes in scale of analysis change the nature of the hydrologic questions [*Dooge*, 1986; *Eagleson*, 1986; *Seyfried and Wilcox*, 1995]. In this regard two very interesting problems to explore using detailed energy and state measurements at a site are describing heat conduction internal to the snowpack based on lumped snowpack state variables, and understanding the role of temperature inversions on spatial and temporal patterns of incoming longwave radiation, temperature, and snowmelt.

Modeling of the conductive heat flux through the snowpack is a complex problem. Internal conductive heat fluxes depend on the previous history of heating and cooling at the surface, and in turn affect the heating and cooling at the surface. Some snowmelt models use finite difference solutions of the heat equation [*Yen*, 1967; *Anderson*, 1976; *Hanks and Ashcroft*, 1980; *Flerchinger*, 1987; *Jordan*, 1991]. This is called a vertically distributed solution. It is well recognized that inaccuracies in describing internal snowpack properties may lead to substantial errors in estimating the distributed snowpack temperature [*Arons and Colbeck*, 1995]. This is conceptually similar to problems faced by other distributed hydrologic models where distributed predictions may be in error while the lumped output is reasonably close to observations [*Kirnbauer et al.*, 1994; *Beven*, 1995; *Blöschl*, 1996]. There may be value in avoiding unnecessary complexity in the model that is difficult to parameterize if there is no actual need to know the vertically distributed snowpack temperatures. Vertically lumped

snowpack models have also been used [*Blöschl and Kirnbauer*, 1991; *Tarboton et al.*, 1995; *Tarboton and Luce*, 1996]. By examining temperature data from a snowpack, we can compare alternative parameterizations used to describe the heat flux into and out of the snowpack at the surface when the snowpack is considered a single element instead of as a series of layers.

There are unique aspects of the energy balance in large mountain valleys, and knowledge of how valleys differ from ridges and hillsides is important when modeling snowmelt over a basin [*Barry*, 1992]. Temperature inversions, night and early morning fog, low wind speeds, and shallow snowpacks are among the characteristics one might expect when working in mountain valleys. One of the chief difficulties faced in modeling distributed snowpack accumulation and melt has been in distributing the weather [*Kirnbauer et al.*, 1994]. How the weather varies over a snow-covered landscape is critical both to improving distributed models and models covering whole basins. Key questions exist about how great an influence inversions have on components of the snowpack energy balance and how to better predict conditions of reduced visibility.

Examination of the energy balance at a site provides insights about the magnitude of the many energy fluxes at such sites [e.g., *Zuzel and Cox*, 1978; *Male and Granger*, 1981; *Marks and Dozier*, 1992; *Cline*, 1997, among others]. Some of the cited studies have examined the special situation of the snowpack studied. In this paper we examine a set of detailed energy state and flux measurements taken in a mountain valley. The measurements were originally presented in *Tarboton* [1994], where they were used to validate the Utah Energy Balance Model (UEB). This paper presents a more thorough data analysis with the purpose of better characterizing the nature of energy exchanges

with the atmosphere at a site in a large mountain valley. We also explored in greater

depth several problems of interest to snowpack modelers. In addition to the focus on heat

conduction at the snowpack surface and the uncertainty in incoming longwave radiation

at a valley bottom site, we briefly examine modeling of ground heat flux, snowpack

albedo, and stability corrections for turbulent transfers.

2. THEORY

2.1. Heat Conduction Internal to the Snowpack

The exchange of heat between the snowpack and the atmosphere is largely

governed by the snow surface temperature and the driving climatic variables. If we

accept an approximation of the snowpack surface as being thin, with nearly no mass, the

snow surface temperature has a value that balances heat fluxes from the atmosphere with

heat conduction into the snowpack [*Tarboton et al.*, 1995; *Tarboton and Luce*, 1996].

Given what we know about penetration of radiation into the snowpack [*Warren*, 1982]

and movement of air into the snowpack [*Colbeck*, 1989], the approximation is not

perfect, but is conceptually useful. Under dry snow conditions, the net atmospheric

exchange has a nearly linear relationship with the surface temperature that is fairly well

defined. Conduction of heat from the snow surface into the snowpack, however, depends

on a complex history of previous heat exchanges and surface temperatures.

If the heat flux into the snowpack were steady state and snowpack thermal

properties homogeneous, the temperature profile would be linear and the temperature

gradient constant with depth. Because snow surface heating varies dramatically over the

course of a day, and over longer time periods for that matter, the temperature profile with

depth is decidedly nonlinear, and much of the pattern is caused by temporal fluctuations

of heating. To calculate heat conduction into the snowpack based on the complex history

of surface temperatures snowpack heat models and snowmelt models frequently use finite

difference schemes [*Yen*, 1967; *Anderson*, 1976; *Blöschl and Kirnbauer*, 1991; *Jordan*,

1991; *Gray et al.*, 1995; *Marks et al.*, 1999]. The finite difference models keep track of

heat stores and varying gradients with depth using short linear approximations, with more

elements near the surface where the temperature profile is most nonlinear. In addition,

these finite difference models may keep track of changes in snow properties within layers

based on models of snow metamorphism [*Colbeck*, 1982; *Jordan*, 1991; *Arons and

Colbeck*, 1995]. The distributed temperature and snow property information internal to

the snowpack is useful in some applications, such as determining hoar crystal

development at depth for snowpack strength. However, for most snowmelt modeling

purposes, the heat flux at the surface and the base of the snowpack (or other suitable

control volume) are the only pieces of information required, and they depend on the

temperature gradient and the properties of the snow at the surface and base.

Because inaccuracies in the modeling of internal snowpack properties could lead

to substantial errors in estimating the distributed snowpack temperature [*Arons and

Colbeck*, 1995], it is desirable to have a minimum of model complexity. Also, vertical

integration of the snowpack energy distribution may be an important initial step in

constructing spatially integrated models [*Horne and Kavvas*, 1997]. There is also the

bonus that substantial computational savings could be realized if we could calculate the

heat flux into the snowpack without the burden of describing the internal variations in

detail. Some have investigated the problem from the point of view of minimizing the

number of layers needed while still retaining essentially a finite difference solution [*Jin et al.*, 1999; *Marks et al.*, 1999]. One of the primary reasons cited for the poor performance of single-layer models in comparative validations is poor representation of internal snowpack heat transfer processes [*Blöschl and Kirnbauer*, 1991; *Koivasulo and Heikinheimo*, 1999]. They have also specifically cited the errors being most pronounced during cold periods before melt occurs, indicating that heat flow more than water flow may be to blame. This raises the question of whether single-layer representation of the snowpack is a feasible goal or, phrased another way, whether the models examined had errors in the specific derivation of their single-layer approach that can be overcome. Given that the source of the strongest nonlinearities in the snowpack temperature profile are daily temperature fluctuations at the surface, which have a sinusoidal pattern, it seems reasonable to use this to formulate a solution to the surface and basal heat fluxes for a single-layer snowmelt model. The force-restore approach to estimating snow surface heat flux [e.g., *Deardorff*, 1978; *Dickinson et al.*, 1993; *Hu and Islam*, 1995] assumes that the driving flux at the surface is sinusoidal. Such an assumption may allow for significant simplification of heat flow modeling compared to finite difference procedures, while still retaining important information about the process.

We can describe heat flow in the snowpack approximately using the diffusion or heat equation and assuming homogeneity of properties [*Yen*, 1967],

$$\frac{\partial T}{dt} = k \frac{\partial^2 T}{\partial z^2} \tag{1}$$

where T is the temperature (C), t is time (s), z is depth (m), and k is the thermal diffusivity ($m^2 \, s^{-1}$). Thermal diffusivity is related to thermal conductivity and specific heat through

$$k = \frac{\lambda}{C\rho} \tag{2}$$

where λ is the thermal conductivity ($J \, m^{-1} \, K^{-1} \, s^{-1}$), C is the specific heat ($J \, kg^{-1} \, K^{-1}$), and ρ is the density ($kg \, m^{-3}$). For semi-infinite boundary condidtions ($0 < z < \infty$) with a sinusoidal temperature fluctuation at the upper boundary,

$$T(0,t) = \bar{T} + A\sin(\omega t) \tag{3}$$

the differential equation (1) has a solution [*Berg and McGregor*, 1966]

$$T(z,t) = \bar{T} + A\exp\left(-z\sqrt{\frac{\omega}{2k}}\right)\sin\left(\omega t - z\sqrt{\frac{\omega}{2k}}\right) \tag{4}$$

In this solution, A is the amplitude of the diurnal temperature fluctuation at the surface (C) and ω is the diurnal frequency (radians s^{-1}). $\bar{T}$ is the time average temperature at the upper boundary (C), and when there is no other gradient superimposed on the daily oscillations, it is also the depth averaged temperature. Note that the diurnal damping depth, d_1, the depth at which the amplitude is 1/e times the surface amplitude, is

$$d_1 = \sqrt{\frac{2k}{\omega_1}} \tag{5}$$

where the subscript 1 denotes one day. Equation 4 may be rewritten as

$$T(z,t) = \overline{T} + Ae^{-\frac{z}{d_1}} \sin\left(\omega_1 t - \frac{z}{d_1}\right) \tag{6}$$

clarifying the relationship between depth and amplitude and phase shift in the diurnal

temperature pattern at each depth.

The heat flux is the thermal conductivity times the temperature gradient

$$Q_c(z,t) = -\lambda \frac{\partial T}{\partial z} = \frac{\lambda A}{d_1} e^{-\frac{z}{d_1}} \left[\sin\left(\omega_1 t - \frac{z}{d_1}\right) + \cos\left(\omega_1 t - \frac{z}{d_1}\right)\right] \tag{7}$$

The surface heat flux is

$$Q_{cs} = -\lambda \frac{dT}{dz}(0,t) = \frac{\lambda A}{d_1}[\sin(\omega_1 t) + \cos(\omega_1 t)] = \frac{\sqrt{2}A\lambda}{d_1} \sin\left(\omega_1 t + \frac{\pi}{4}\right) \tag{8}$$

showing that the surface temperature lags the surface heat flux by $\pi/4$ radians, which is

1/8 of a cycle or 3 hours. Equation 8 suggests that simplifications estimating the heat

flux into the snowpack based on the difference between the snowpack average and

surface temperatures such as

$$Q_{cs} = \frac{\lambda}{d_1}(T_s - T_{ave}) \tag{9}$$

where T_{ave} is the vertically averaged snowpack temperature, would be incorrect.

From equation 7, recognizing that $\omega\cos(\omega t)$ is the derivative of $\sin(\omega t)$, and

substituting equation 6 we can derive an alternative method to estimate the surface heat

flux

$$Q_c(z,t) = \frac{\lambda}{d_1}\left(\frac{1}{\omega_1}\frac{\partial T(z,t)}{dt} + T(z,t) - \bar{T}\right) \qquad (10)$$

which is the basis for the force restore method to estimate the surface heat flux [c.f. equation 10 of *Hu and Islam*, 1995]. Applied at the surface and using a finite difference approximation for $\partial T_s / \partial t$ results in an estimate

$$Q_{cs} = \frac{\lambda}{d_1}\left(\frac{1}{\omega_1 \Delta t}\left(T_s - T_{s_{lag1}}\right) + \left(T_s - \bar{T}\right)\right) \qquad (11)$$

where Δt is the measurement interval, and T_s is the surface temperature. While $\bar{T}$ is specifically identified as the time average temperature in equation 3, in typical application, the value of $\bar{T}$ is taken as the average temperature of the medium with depth [see *Hu and Islam*, 1995, for example], denoted in this paper as T_{ave}. A quick preview to Figure 2-2b shows that this is probably a poor approximation because the temperature gradient with depth does not cycle on a daily time scale. The diurnal cycle is superimposed on a strong upward temperature gradient with what appears to be a weekly time scale. There are lower frequency fluctuations, such as the annual cycle, causing temperature variation with depth and thus heat fluxes. In fact, there may be greater power in the lower frequency variability. We can superimpose the heat fluxes due to lower frequency variability on equation 11 using the gradient in daily average temperature to estimate the net result of lower frequency variability. We roughly approximate the superimposed gradient using the difference in the daily average surface temperature, $\bar{T}_s$, and the daily average depth average snowpack temperature (estimated

from the energy state of the snowpack), $\bar{T}_{ave}$, over a distance d_{lf}, the low frequency

damping depth. This results in

$$Q_{cs} = \frac{\lambda}{d_1}\left(\frac{1}{\omega_1 \Delta t}\left(T_s - T_{s_{lag1}}\right) + \left(T_s - \bar{T}_s\right)\right) + \frac{\lambda}{d_{lf}}\left(\bar{T}_s - \bar{T}_{ave}\right) \tag{12}$$

where

$$d_{lf} = \sqrt{\frac{2k}{\omega_{lf}}} \tag{13}$$

This equation associates a frequency, ω_{lf}, with the distance d_{lf} used in the daily average

gradient estimate. The thermal properties of the snowpack are the same for both low and

high frequency forcing; however, the appropriate frequency to describe the low frequency

contribution, ω_{lf}, is less clear. In this paper, ω_{lf} is fitted to observations.

Large and fast variations in the snowpack surface temperature and strong

nonlinearities in the process make finding the average temperature of the top few

centimeters of snow difficult. Using equation 6 to describe temperature variation with

depth, the average temperature over a layer of snow is given by

$$\langle T_{sl} \rangle = \frac{\int_0^{z_b} \bar{T}(z) + Ae^{-\frac{z}{d_1}} \sin\left(\omega_1 t - \frac{z}{d_1}\right) dz}{\int_0^{z_b} dz} \tag{14}$$

where z_b is the depth of the bottom of the layer, $\langle T_{sl} \rangle$ is the depth averaged temperature

of the surface layer between $z = 0$ and z_b, and $\bar{T}(z)$ is the average temperature varying on

a lower frequency, for example the mean daily temperature, at depth z. Assuming a

linear relationship of the time average temperature with depth over the range of the

integral,

$$\langle T_{sl} \rangle = \tfrac{1}{2}\left(\overline{T}_s + \overline{T}_b\right) - \frac{A}{z_b/d_1}\left[e^{-\frac{z}{d_1}}\left(\sin\left(\omega_1 t - \tfrac{z}{d_1}\right) - \cos\left(\omega_1 t - \tfrac{z}{d_1}\right)\right)\right]_0^{z_b}$$

$$= \tfrac{1}{2}\left(\overline{T}_s + \overline{T}_b\right) - \frac{A}{z_b/d_1}\left[e^{-\frac{z_b}{d_1}}\left(\sin\left(\omega_1 t - \tfrac{z}{d_1}\right) - \cos\left(\omega_1 t - \tfrac{z}{d_1}\right)\right) - \left(\sin(\omega_1 t) - \cos(\omega_1 t)\right)\right] \quad (15)$$

$$= \tfrac{1}{2}\left(\overline{T}_s + \overline{T}_b\right) + \frac{A}{\sqrt{2}\,z_b/d_1}\left[\sin(\omega_1 t - \tfrac{\pi}{4}) - e^{-\frac{z_b}{d_1}}\sin\left(\omega_1 t - \tfrac{z_b}{d_1} - \tfrac{\pi}{4}\right)\right]$$

noting the identities for temperature at the surface and the temperature at z_b, and

recognizing that a phase change of $-\pi/4$ represents 3 hours earlier yields

$$\langle T_{sl} \rangle = \tfrac{1}{2}\left(\overline{T}_s + \overline{T}_b\right) + \frac{1}{\sqrt{2}\,z_b/d_1}\left[T_s\left(t - 3hr\right) - T_b\left(t - 3hr\right) - \overline{T}_s + \overline{T}_b\right] \quad (16)$$

where $\overline{T}_s$ is the time averaged surface temperature and $\overline{T}_b$ is the time averaged

temperature at depth z_b (we used the 24-hour average centered on the time of interest for

our application). Equation 16 is approximate because of the assumptions regarding

sinusoidal temperature fluctuations in the derivation of equation 6. Equation 16 is also in

error in so far as there are lower frequency variations in temperature, i.e., $\overline{T}_s$ and $\overline{T}_b$ are

not constant.

Equations 1-16 represent a thorough description of how snowpack temperatures should behave if the sinusoidal forcing model represents a reasonable approximation of the heat conduction processes. One of the primary clues we can use from temperature measurements in the snowpack is the relative phase and amplitude of the diurnal wave as it passes through the snowpack. Table 2-1 presents a brief summary for the reader's later reference while the equations are still fresh.

2.2. Incoming Longwave Radiation and Valley Inversions

Temperature inversions are so named because in a shallow layer of the atmosphere above the valley floor, temperature increases with elevation. This is a very stable configuration for the atmosphere and inhibits turbulent exchange of valley air with the overlying airmass. This aspect of inversions makes them notorious for trapping pollutants and exacerbating air pollution problems in many cities. Because water vapor is also held in this layer, night and early morning fog are common as the layer cools at night and warms during the day primarily by radiant energy exchanges. It is probably clear from these characteristics that inversions have a pronounced effect on the snowpack energy balance and probably play an important role in the spatial patterns of snowmelt.

Table 2-1. Theoretically Derived Relative Phase and Amplitude of Various Observations Used Later in Dissertation.

Measurement	Relative Phase	Relative Amplitude	Equation
Surface Heat Flux	ϕ	$\sqrt{2}\,A\,\lambda\,/\,d_1$	
Surface Temperature	$\phi - \pi/4$	A	8
Temperature at z	$\phi - \pi/4 - z/d_1$	$A e^{-z/d_1}$	6, 8
Average snowpack temperature (z/d > 3)	$\phi - \pi/2$		15
Heat flux at z	$\phi - z/d_1$	$\sqrt{2}\,A\,\lambda\,e^{-z/d_1}\,/\,d_1$	7

Valleys can cover a large part of the landscape in many regions of the world, and only a small amount of topographic relief is needed to create frequent winter inversions. During cold clear periods, strong radiant cooling of the surface cools the air close to the surface, and unless there is a strong synoptic wind, the cool air stays close the surface and "drains" into the lowest areas. Inversions occur in narrow and broad mountain valleys and even in small valleys in hilly terrain. Estimation of snowmelt in either distributed or lumped snowmelt models requires a clear understanding of how the energy balance in valleys differs from sites with better exchange with the atmosphere.

There are difficulties estimating and measuring incoming longwave radiation during the winter in valleys. Radiation instruments may suffer problems under inversions. Globes on net-radiometers and pyrgeometers are prone to developing frost. These covers, normally transparent to longwave radiation, become opaque to longwave radiation when covered with frost. Pyranometers are affected less by this problem because the thin frost is not opaque in the shortwave part of the spectrum. Humidity instruments have poorer precision and accuracy under nearly saturated conditions, and even some of the better instruments are not reliable above 95% relative humidity. Methods to estimate incoming longwave radiation based on surface temperature and humidity are available for clear sky conditions [*Idso and Jackson*, 1969; *Brutsaert*, 1975; *Marks*, 1978; *Satterlund*, 1979]. These assume a standard temperature lapse rate to develop an effective atmospheric emissivity. Because the strength and depth of the inversion are uncertain and because shallow cloud or fog layers may form at the top or bottom of the inversion layer, the integrated temperature and emissivity of the air mass above a site may not be related to surface temperature and humidity. *Bristow and Campbell* [1984] give a method for

estimating atmospheric transmissivity and hence cloud cover based on the daily

temperature range from the idea that when it is cloudy, temperature fluctuations are

damped. When the cloudiness is caused by large temperature fluctuations, as is the case

with fog in inversions, the method is not reliable.

Lacking measurements or a reasonable basis for estimating incoming longwave

radiation, we cannot close the energy balance. However, we can use measurements of

the snowpack temperature, measurements of other components of the energy balance, and

an understanding of longwave radiation from the atmosphere to deduce the incoming

longwave. From this information we can derive insights about incoming longwave

radiation in a valley under an inversion.

3. METHODS

3.1. Site Description

The measurements were made west of Logan, Utah, near the center of Cache

Valley, situated in the Wasatch Mountains, east of the Great Salt Lake in Utah (Figure 2-

1). Cache Valley is oriented north and south between two high ranges on the east and

west, about 2000 m higher than the valley floor. The valley is similar to many valleys

formed by faulting in the Basin and Range Province of the western United States. It is

roughly 15 km wide at Logan, and about 110 km long. Many streams feed the valley and

drainage is through a canyon on the west side. The valley bottom is flat and is mostly

covered by wetlands and related vegetation. Much of the land near the valley bottom has

been converted to pasture land through the use of drainage canals. Measurements were

taken at the Utah State University Research Drainage Farm, which was instrumented
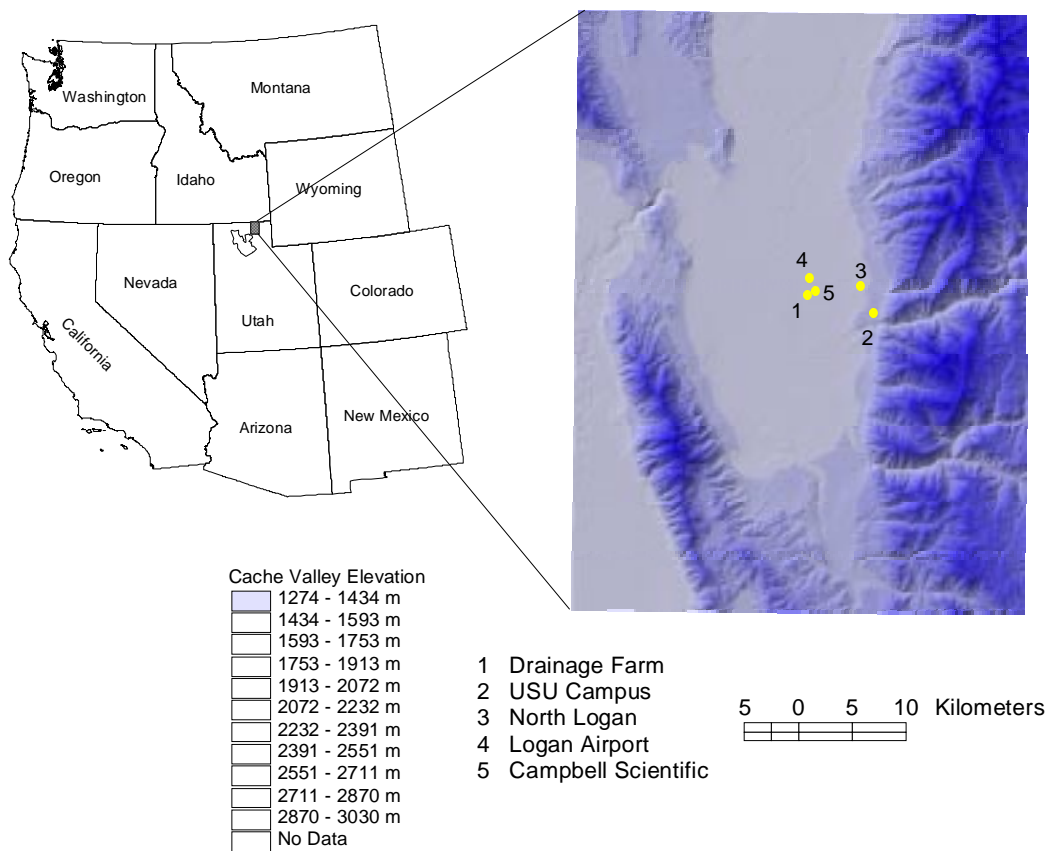
Figure 2-1. Location map showing location of Cache Valley in the Western United States and the location of several sites referenced in the dissertation.

to measure the effects of the wetland-to-pasture conversion. The ground at the site has a loamy soil, rich in organics and a cover of short grass.

3.2. Snowpack Energy Balance

The energy balance of a snowpack is given by

$$\frac{dU}{dt} = Q_{si} - Q_{so} + Q_{li} - Q_{lo} + Q_{ts} + Q_{tl} + Q_p - Q_m + Q_g \qquad (17)$$

where, U is the snowpack energy content (kJ/m^2), Q_{si} is incoming solar radiation, Q_{so} is reflected solar radiation, Q_{li} is incoming longwave radiation, Q_{lo} is outgoing longwave radiation, Q_{ts} is turbulent transfer of sensible heat, Q_{tl} is turbulent transfer of latent heat, Q_p is heat advected with precipitation, Q_m is heat advected with melt water, and Q_g is heat conducted from the ground. We directly measured Q_{si}, Q_{so}, Q_{lo}, Q_g, and dU/dt based on temperature changes. Q_{ts} and Q_{tl} were inferred from wind speed, temperature, and humidity measurements at multiple levels above the snowpack using aerodynamic formulae. Q_p was inferred from precipitation and temperature measurements. Q_m was not measured, but can be inferred from decreasing snow water equivalence. Q_{li} was calculated as the remainder of the energy balance bounded by temperature and emissivity estimates for the atmosphere over the snowpack. Where the remainder was either greater or less than could be made up by the incoming longwave, the differences were attributed to phase changes in the snowpack. We examined the relationship of phase changes to time of day and melt patterns to establish the validity of this assumption. Net radiation (Qsi-Qso+Qli-Qlo) was also measured; however, these measurements suffered from problems due to snow and frost on the instruments, making correct readings difficult to interpret and hampering inference of Q_{li} from radiation measurements alone.

3.3. Temperature and Heat Conduction in the Snowpack

Snowpack and shallow soil temperatures were measured using eight copper-constantin thermocouples and an infrared thermometer. Two thermocouples were placed below the ground surface at depths of 2.5 and 7.5 cm. Another thermocouple was placed at the ground surface, and the remaing five thermocouples were placed at 5, 12.5, 20,

27.5, and 35 cm above the ground surface on a ladder constructed of fishing line. The raw thermocouple measurements showed high frequency, large magnitude temperature variations simultaneously through the snowpack, and temperatures greater than 0°C in some cases (Figure 2-2a). The simultaneity was a clue that perhaps the reference thermistor on the face plate of the datalogger gave inadequate correction for voltages created where the thermocouples connected to the metal of the datalogger. Such voltages would depend on the temperature at the connection, which can vary during the day as the datalogger enclosure is heated and cooled. We assumed that the temperature at the thermocouple 7.5 cm below the ground surface would have nearly no diurnal variation and set the temperature for this thermocouple as a linear interpolation of the daily average temperature. The voltage differences between the recorded readings and the interpolated readings were subtracted from the other thermocouple readings to produce a corrected temperature trace for each thermocouple (Figure 2-2b). The fact that the high frequency variations were simultaneous through such a strong insulator as a snowpack lends credence to the explanation that voltages generated at the datalogger caused them. For future investigations, it might be more useful to place the reference thermistor with the thermocouple lowest in the soil; then differences between thermocouple voltages can be used to estimate temperature differences between the thermistor and each thermocouple.

Snowpack surface temperature was measured with two Everest Interscience model 4000 infrared thermometers with 15-degree field of view. These instruments measure upwelling longwave radiation and assume an emissivity of 0.99 to estimate the snowpack temperature. Snowpack emissivity in the longwave part of the spectrum is between 0.988 and 0.985 [*Marks and Dozier*, 1992].
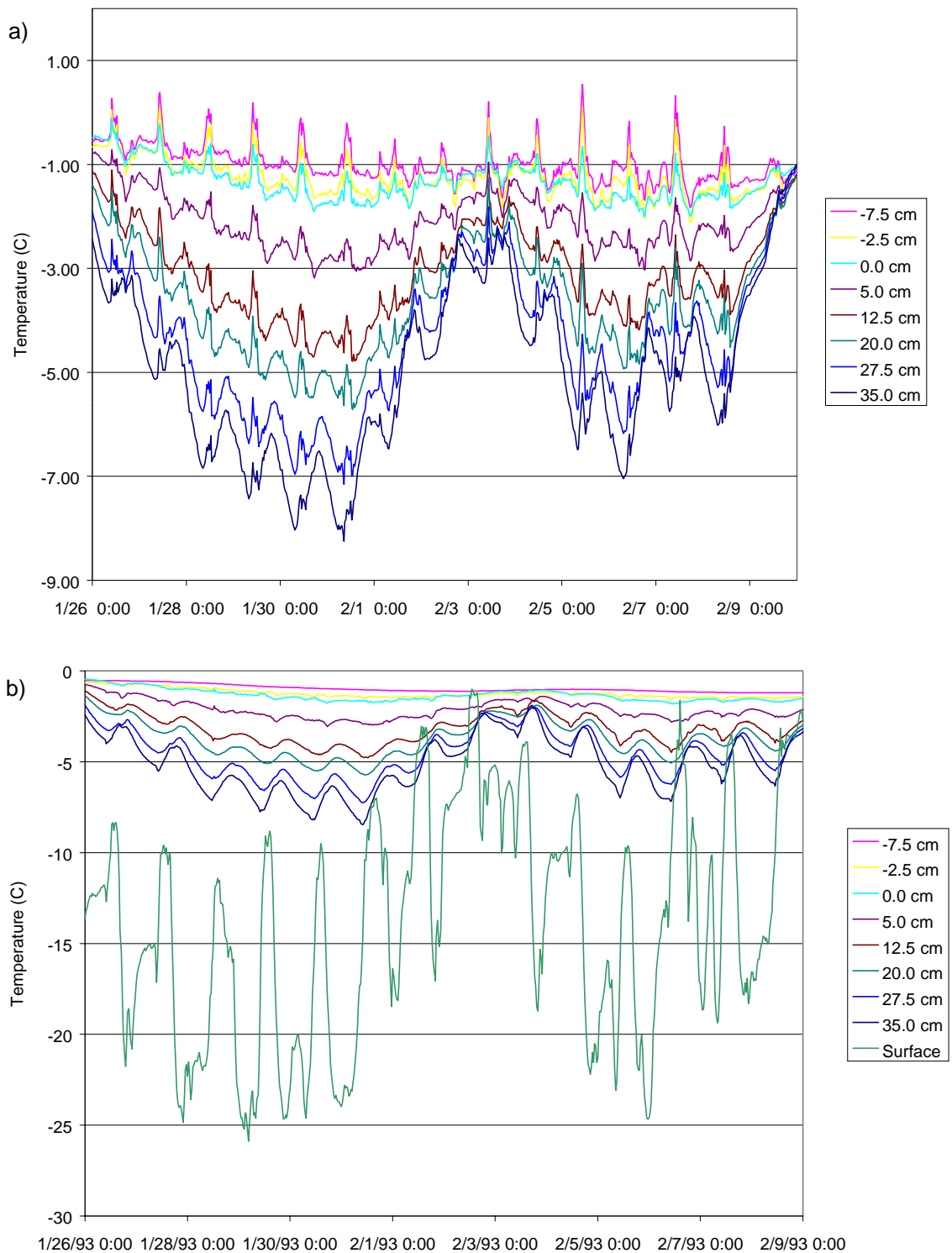
Figure 2-2. a) Raw thermocouple traces and b) corrected thermocouple traces.

Ground heat flux was measured with a REBS ground heat flux plate placed at 10 cm depth in the soil. The heat flux plate gives heat conduction from the ground into the snowpack as positive.

We examined the temperature patterns over the first 8 days of the study period to examine how well the heating and the cooling of the snowpack can be described as a sinusoidal process. We also wanted to confirm that the large phase shift and amplitude change between the surface temperature and uppermost thermocouple (about 4 cm depth) was reasonable. We used Fourier analysis to estimate the amplitude and phase associated with each temperature trace. To do this, we performed a Fourier transform with a Parzen window [*Press et al.*, 1992] spanning the full 8 days (192 hours). The results gave amplitude, A, and relative phase, ϕ, for each temperature trace, and the differences were used to infer z/d_1 from equation 6.

A function spanning the full 8-day (192-hour) period length, L, may be represented by its Fourier series

$$f(t) = \bar{f}(t) + \sum_{k=1}^{\infty} a_k \cos(k\omega_0 t) + b_k \sin(k\omega_0 t) \tag{18}$$

where

$$\omega_0 = \frac{2\pi}{L} \tag{19}$$

The Fourier coefficients, a_k and b_k, quantify the amplitude and phase associated with each frequency $\omega_k = k\omega_0$ that is present in the Fourier decomposition of the function. They may be estimated from discrete data sampled on equal time steps, Δt, by

$$a_k = \frac{\sum_{j=0}^{n-1} f_j w_j \cos(\omega_k j \Delta t)}{\sum_{j=0}^{n-1} w_j} \qquad (20)$$

$$b_k = \frac{\sum_{j=0}^{n-1} f_j w_j \sin(\omega_k j \Delta t)}{\sum_{j=0}^{n-1} w_j} \qquad (21)$$

[*Press et al.*, 1992] where n is the number of observations ($n = L/\Delta t$), and w_j are the weights applied to each observation using a window function. For our analysis, we used a Parzen window, which gives the weights as

$$w_j = 1 - \left| \frac{j - \frac{1}{2}(n-1)}{\frac{1}{2}(n+1)} \right| \qquad (22)$$

[*Press et al.*, 1992]. The purpose of windowing the data is to reduce biases towards higher frequencies from edge effects caused by the discontinuities at the beginning and end of the analysis period. In our analysis, we are interested in the diurnal frequency, with period, T = 24 hours. For an analysis window of 192 hours, this corresponds to a k of 8. We estimated a_8 and b_8 from equation 20 and 21. Noting that

$$a_8 \cos(8\omega_0 t) + b_8 \sin(8\omega_0 t) = A \sin(8\omega_0 t + \phi) \qquad (23)$$

we can calculate

$$A = \sqrt{a_8^2 + b_8^2} \qquad (24)$$

and

$$\phi = \frac{a_8}{|a_8|} \cos^{-1}\left(\frac{b_8}{A}\right) \tag{25}$$

For negative values of ϕ, we added 2π. The difference in the value of ϕ at one layer and the value of ϕ at another is an estimate of the value of $-z/d_1$ from equation 6 for the intervening snow. Similarly, the value of z/d_1 for snow between two measurements can be estimated from the natural log of the ratios of the amplitude of the lower measurement to the amplitude of the upper measurement. Knowing the vertical position of each measurement in the snowpack, we obtained an estimate of d_1, which was used along with the measured average snowpack density of 0.4 Mg/m^3 and specific heat of ice, 2.09 kJ/kg, to estimate the conductivity, λ, from equation 2. The conductivity and damping depth were used in equation 12. ω_{lf} in equation 13 was then fitted.

The energy content of a control volume comprising the snow and soil above the heat flux plate buried at 10 cm was estimated from the average snowpack temperature, the average soil temperature, and the snowpack surface temperature. For layers of the snowpack and soil between thermocouples, we used the average temperature between the thermocouples. The average temperature of the surface layer calculated from equation 16 was given a weight equal to the depth of the layer divided by the total depth of the snowpack for the computation of the weighted average temperature of the snowpack. Taking 0°C ice as having 0 energy content, for $U < 0$,

$$U = \langle T_{snow} \rangle W_{snow} \rho_w C_{ice} + \langle T_{soil} \rangle \rho_{soil} C_{soil} D_e \tag{26}$$

where $\langle T_{snow} \rangle$ is the depth averaged snow temperature as $\langle T_{soil} \rangle$ is the depth averaged soil

temperature over the depth of the soil above the heat flux plate, D_e (0.1 m), W_{snow} is the

water equivalence of the snowpack, ρ_w is the density of water (1 Mg/m^3), ρ_{soil} is the

density of soil (1.7 Mg/m^3), C_{ice} is the specific heat of ice (2.09 kJ/kg) and C_{soil} is the

specific heat of soil (2.09 kJ/kg). Note that this measure of the energy content can only

record energy content when there is no water in the snowpack, thus it can only calculate

U<0. For periods when this calculation results in a value close to 0, there is probably

liquid water in the snowpack, and the value of U may be much higher.

3.4. Shortwave Radiation

The shortwave energy balance was measured with two Licor silicon

pyranometers, one pointing down, and the other up. Both pyranometers were calibrated

through the season with an Eppley black and white pyranometer facing upwards for a part

of the season and facing downwards for the rest. Our preliminary estimates of reflected

shortwave were low, and we received more than expected when the instruments were

installed. Consequently voltages from the radiometer reading reflected shortwave were

occasionally out of range during the brightest part of a few days. We interpolated albedo

from earlier and later in the day using a slightly modified version (described below) of

the model of *Dickinson et al.* [1993] to describe the daily variation in albedo caused by

changing sun angles. Measurements in the morning and afternoon were used to calibrate

the model each day it was needed. We described the daily variation in albedo as

$$\alpha = \alpha_d + f(\psi)(\alpha_{max} - \alpha_d) \tag{27}$$

where α_d was taken as the daily observed average minimum albedo (averaged during peak solar angles of the day), α_{max} was the observed maximum for the day, and

$$f(\psi) = \begin{cases} \dfrac{1}{2}\left[\dfrac{3}{1+4\cos(\psi)} - 1\right] & \text{for } \cos(\psi) < 0.5 \\ 0 & \text{otherwise} \end{cases} \tag{28}$$

where ψ is the illumination angle relative to the surface normal. The modification was in using α_{max} in place of $(0.4 + 0.6\alpha_d)$ as an estimate of the daily maximum albedo. We also compared observed values of α_d to values predicted by *Dickinson et al.* [1993] based on the age and temperature history of the snow surface. *Dickinson et al.* [1993] give

$$\alpha_d = \frac{1}{2}\left[\alpha_{v0} + \alpha_{ir0} - \frac{\tau}{1+\tau}(\alpha_{v0}C_v + \alpha_{ir0}C_{ir})\right] \tag{29}$$

where α_{v0} (=0.95 by *Dickinson et al.* [1993] and calibrated to 0.85 by *Tarboton and Luce* [1996] for data from the Sierras) is the fresh snow reflectance for visible light (<0.7μm), α_{ir0} (=0.65) is the fresh snow reflectance in near infrared part of the solar spectrum (<0.7μm), C_v=0.2 and C_{ir}=0.5 are parameters quantifying the sensitivity of the albedo to snow surface aging, and τ is the non-dimensional snow surface age

$$\tau = \frac{\displaystyle\int_0^t r_1 + r_1^{10} + 0.03 \, dt}{\tau_0} \tag{30}$$

where t is the time since the last snowfall event in seconds, τ_0 is 10^6 seconds, and

$$r_1 = \exp\left[5000\left(\frac{1}{273.16} - \frac{1}{T_s}\right)\right] \tag{31}$$

where T_s is the surface temperature (K). The integral (30) was evaluated numerically in half-hour time steps. During snowfall, τ is reduced

$$\tau = \tau_i\left(1 - \frac{P_s}{0.01}\right) \tag{32}$$

where τ_i is the initial value of τ before snowfall, and P_s is the depth of snowfall water equivalent (m). Equation 32 was evaluated in half-hour time steps. τ has a minimum value of 0. Thus if 0.01 m of snow water equivalence falls the surface will be considered "fresh snow."

3.5. Turbulent Transfer

Turbulent transfers of latent and sensible heat were estimated from aerodynamic formulae. Four R.M. Young cup-type anemometers measured the wind speed at 0.6, 0.9, 1.4, and 2.4 m above the snow surface, and four Vaisala HMP-35C temperature and humidity probes measured temperature and relative humidity at the same elevations. The minimum wind speed that could be measured by the anemometers is 0.4 m/s. According to manufacturer specifications, the HMP-35C measures temperature with a precision of $\pm0.4°C$ worst case or $\pm0.2°C$ typical, and it measures relative humidity with a precision of $\pm2\%$ RH for 0-90% RH and $\pm3\%$ RH for 90-100% RH. Relative humidity measurements reported by the probe are relative humidity relative to the saturation vapor pressure over liquid water and required correction for the vapor pressure over ice at the

same temperature. The probe at 1.5 m reported incorrect values and was calibrated and

corrected values were estimated. The snowpack was close to 0.4 m in depth through

much of the measurement period, and the heights of the instruments over the snowpack

were 0.2, 0.5, 1.0, and 2.0 m above the snowpack surface. The estimates of the latent and

sensible heat fluxes between any two sensors or between any sensor and the snow surface

were estimated by bulk aerodynamic formulae

$$Q_{ts} = \rho_a C_p k^2 \frac{u_2 - u_1}{\phi_M [\ln(z_2) - \ln(z_1)]} \frac{T_2 - T_1}{\phi_H [\ln(z_2) - \ln(z_1)]} \tag{33}$$

$$Q_{tl} = \rho_a L_v k^2 \frac{u_2 - u_1}{\phi_M [\ln(z_2) - \ln(z_1)]} \frac{q_2 - q_1}{\phi_E [\ln(z_2) - \ln(z_1)]} \tag{34}$$

where Q_{ts} is the turbulent flux of sensible heat, Q_{tl} is the turbulent flux of latent heat, z_i is

the instrument height for instrument i (taken to be z_0 when the flux between the surface

and instrument is calculated, see below for estimation of z_0), u_i is the wind speed at

instrument i (0 at the snow surface), T_i is temperature at the instrument (taken from

upwelling longwave sensor for snow surface), q_i is the specific humidity at the instrument

(assumed saturated at the snow surface based on snow surface temperature), ρ_a is the

density of air, C_p is the specific heat of air at constant pressure, L_v is the latent heat of

vaporization of ice, k is von Karman's constant, and ϕ_M, ϕ_H, and ϕ_E are the stability

functions for momentum, sensible heat, and water vapor.

The stability functions were estimated from simple parameterizations using the

bulk Richardson number,

$$R_i = \frac{gz_m(T_a - T_s)}{\frac{1}{2}(T_a + T_s)u^2} \tag{35}$$

where g is gravity (m/s^2), z is the height of the instruments (m), T_a is the air temperature

(K), T_s is the snow surface temperature (K), and u is the wind speed (m/s). Often the

airmass above a snow surface is stable because the surface is colder than the air above,

and buoyant forces counter the viscous shear forces ($R_i > 0$) and transfers are damped

compared to the neutral aerodynamic calculations. For stable conditions, we used the

approximation of *Price and Dunne* [1976]

$$\frac{1}{\phi_M \phi_H} = \frac{1}{\phi_M \phi_E} = \frac{1}{1 + 10R_i} \tag{36}$$

For unstable conditions ($R_i < 0$),

$$\phi_M = (1 - 16R_i)^{-0.25} \tag{37}$$

$$\phi_H = \phi_E = (1 - 16R_i)^{-0.5} \tag{38}$$

[*Dyer and Hicks*, 1970; *Anderson*, 1976; *Jordan*, 1991]. Because guidance for estimating

turbulence under extremely unstable conditions is poor, we capped the value of $\phi_M \phi_H$ at

1/3, which occurs near $R_i = -0.2$. Beyond this the approximations for equations 37 and 38

allowing use of the Richardson number in place of the Monin-Obukhov similarity length

become poor. *Anderson* [1976] shows that iterative solutions of *Deardorff's* [1968]

empirical equations begin to level off for more strongly unstable situations as a value of

1/3 is approached.

The log(distance) difference is much greater between the surface and any of the sensors than between any two sensors. The expected differences in temperature and humidity between any two sensors was frequently close to the precision of the temperature-humidity probe, sometimes suggesting inconsistent gradients between sensors. We therefore used the average of the fluxes calculated between each sensor and the surface to estimate fluxes over time and calibrated the z_0 value so that the long term average flux calculated in this manner was the same as the season average flux between the lowest and highest sensor. This yielded a z_0 value of 10 mm, greater than some estimates, but within the range reported in the literature [*Anderson*, 1976; *Dunne et al.*, 1976; *Jordan*, 1991; *Morris*, 1991].

3.6. Other Measurements

Precipitation was measured in an unshielded heated tipping bucket gage. Given the possibility of undercatch, we also examined precipitation accumulating on a weighing lysimeter with no outflow.

Hourly solar radiation and temperature data were collected at other weather stations in Cache Valley at the same time (Figure 2-1). The Utah State University Campus Station is about 5.1 km to the east and 150 m higher in elevation than the research drainage farm. Daily precipitation and snowpack depth were also collected at this station. Campbell Scientific maintains a station 1.2 km east of the study site and at roughly the same elevation. The USU Experimental Farm is 4.7 km to the east and 50 m higher in elevation on the east side of the valley. Observations of visibility and sky conditions were collected at the Logan-Cache airport, which is also near the valley bottom and 2.4 km to the northeast.

4. RESULTS AND DISCUSSION

4.1. Temperature Changes in the
Snowpack

Figure 2-3 shows the snowpack energy content as measured by snowpack

temperature (liquid water content of pack was not measured) over the study period.

Where U is close to 0 on this graph indicates times when there is probably liquid water in

the snowpack, and U may be positive. Figure 2-4 shows the magnitude of heat fluxes at

the surface of the snowpack inferred from equation 17 and measured ground heat flux

necessary to explain the observed changes in temperature. During the first two weeks of

the period, all parts of the snowpack were below freezing, so the energy content as

measured by the temperature is an accurate description of the energy of the snowpack.

During this period, there is an opportunity to examine how to model changes in

snowpack energy that relate to the average snowpack temperature. Two important

processes are conduction of heat from the surface and conduction of heat through the

ground, or ground heat flux.
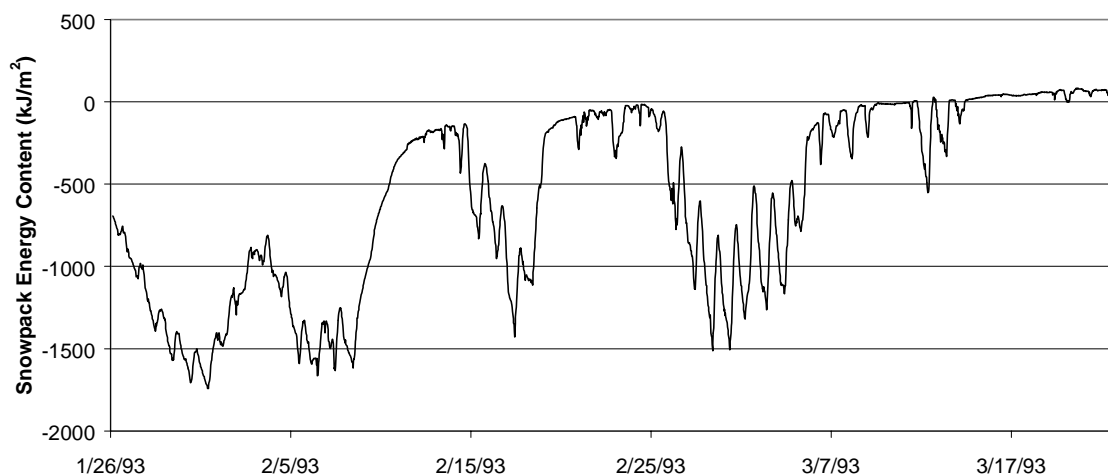
Figure 2-3. Snowpack energy content over time.
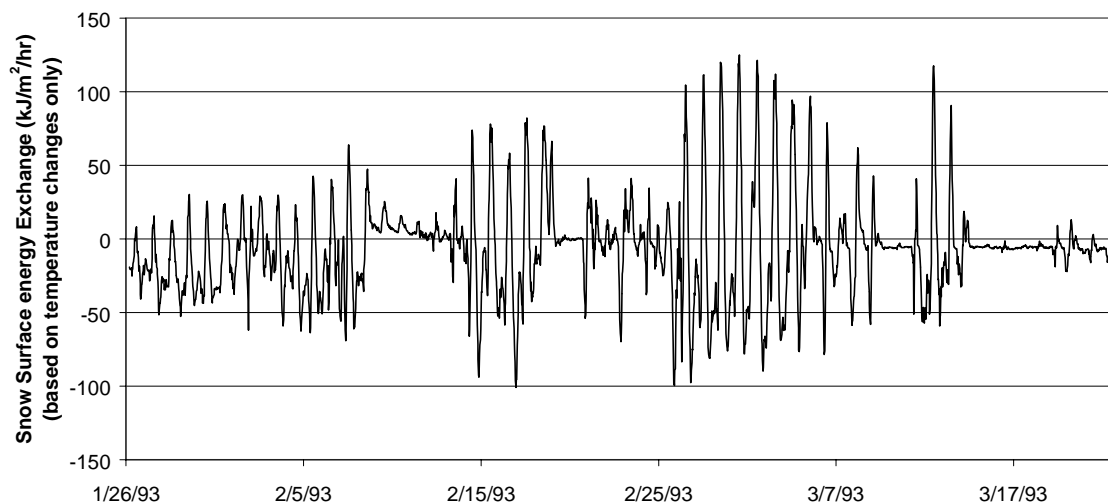
Figure 2-4. Snowpack surface energy fluxes over duration of study period reported at half-hourly intervals.

Some information may be gleaned from a Fourier transform of temperature data at the daily frequency. We examined the implied snowpack thermal properties between the surface and each thermocouple (Table 2-2a) and the thermal properties between each thermocouple (Table 2-2b) using both phase shifts and amplitudes. Table 2-2 reports the average phase and amplitude from the Fourier analysis of diurnal frequency between January 26 and February 2, 1993. For reference, the formula used by *Anderson* [1976] to estimate thermal conductivity gives 0.53 W/m/K at this density and the formula used by *Jordan* [1991] gives 0.61 W/m/K. *Sturm and Johnson* [1992] observed thermal conductivity values between 0.5 and 0.8 W/m/K in snow with a density close to 0.2 Mg/m^3. Anderson and Jordan both state that the effective thermal conductivity of air in a snowpack is about 0.02 W/m/K. Also for reference, *Hu and Islam* [1995] give a diurnal damping depth of about 5 cm for dry clay and about 20 cm for stone. The properties for the upper snow layers differ from those of the lower layers. Although the heat equation

Table 2-2. Analysis of Phase Shifts and Amplitude Changes with Depth in the Snowpack for A) Effective Parameters Between the Surface and Each Thermocouple and B) Parameters of Each Increment Between Temperature Measurements in Layers

A) Bulk Properties Surface to z

Phase Shift Analysis						Amplitude Analysis						
z	phi	z/d1	d1	K	λ	z	Amplitude	exp(z/d1)	z/d1	d1	K	λ
cm	radians		cm	cm^2/hr	W/m/K	cm	C			cm	cm^2/hr	W/m/K
0	4.23	0.00				0	5.52	1.00	0.00			
4	2.48	1.75	2.29	0.69	0.016	4	0.81	0.15	1.92	2.08	0.57	0.013
11.5	2.19	2.04	5.64	4.17	0.097	11.5	0.59	0.11	2.23	5.16	3.48	0.081
19	1.78	2.44	7.78	7.93	0.184	19	0.35	0.06	2.75	6.92	6.26	0.145
26.5	1.47	2.75	9.63	12.13	0.282	26.5	0.28	0.05	2.97	8.91	10.39	0.241
34	0.62	3.61	9.43	11.63	0.270	34	0.11	0.02	3.96	8.58	9.64	0.224
39	0.02	4.21	9.27	11.25	0.261	39	0.04	0.01	4.86	8.02	8.42	0.196

B) Properties Between Measurements

Phase Shift Analysis						Amplitude Analysis						
z	phi	Δ z/d1	d1	K	λ	z	Amplitude	exp(Δ z/d1)	Δ z/d1	d1	K	λ
cm	radians		cm	cm^2/hr	W/m/K	cm	C			cm	cm^2/hr	W/m/K
0	4.23					0	5.52					
4	2.48	1.75	2.29	0.69	0.016	4	0.81	0.15	1.92	2.08	0.57	0.013
11.5	2.19	0.29	25.83	87.31	2.028	11.5	0.59	0.73	0.31	24.33	77.50	1.800
19	1.78	0.40	18.61	45.34	1.053	19	0.35	0.60	0.52	14.52	27.61	0.641
26.5	1.47	0.31	24.04	75.65	1.757	26.5	0.28	0.80	0.23	32.93	141.96	3.297
34	0.62	0.85	8.79	10.11	0.235	34	0.11	0.37	0.99	7.59	7.55	0.175
39	0.02	0.60	8.33	9.08	0.211	39	0.04	0.41	0.90	5.56	4.04	0.094

(1) assumed homogeneity of snowpack thermal properties, for heat conduction problems, it has been established that a non-homogeneous system can be represented by effective parameters in the heat equation [*Hanks and Ashcroft*, 1980, p. 140]. Both the phase analysis and the amplitude analysis show a very low conductivity in the top 4 cm, underlain by 22.5 cm of high conductivity snow, which overlies 12.5 cm of snow with low to moderate thermal conductivity. We could characterize this as a nugget of resistance near the top of the snowpack with relatively conductive snow below. Strong temperature gradients near the surface of the snowpack may have promoted hoar frost development and destruction of bonds between snow grains, hampering conduction of heat. Even so, the estimated effective thermal conductivity is less than the effective thermal conductivity of air in a snowpack, which includes accounting of water vapor

diffusion through the air [*Yen*, 1967]. This estimate is unrealistically low. A possible

reason for the low estimate is that the estimate of the position of the thermocouple in the

snowpack was imprecise because the line by which the thermocouple was held may have

sagged and because the snow depth measurement was taken as the average of several

measurements a short distance away from the thermocouple ladder to avoid disturbing the

thermocouples. If the first thermocouple were at depth of 5 or 6 cm, the estimate of the

surface conductivity would be 0.025 or 0.036 W/m/K, respectively, and the estimate of

the conductivity of the next layer would be 1.523 or 1.090, respectively. This sensitivity

of the estimate to the precise thermocouple depth below the surface suggests that future

studies should have a means to estimate the thermocouple position with precision.

Although the depth of the first thermocouple may be in error, we used it for lack of

another measurement. Sensitivity to imprecision in the depth estimate decreases with the

depth of the thermocouple.

      Given the large phase shift and the strong damping in the upper layer, there exists

a concern that the infrared thermometer was not reading the surface temperature of the

snowpack, but the air temperature of the air between the lens and the snowpack. We

believe that the infrared thermometer correctly observed the snowpack surface

temperature for the following reasons. Equation 8 suggests that the surface temperature

should lag the surface heat flux by 3 hours. Incoming solar radiation (which we will later

show is the largest part of the surface heat flux) peaks at about 12:30 in the afternoon

(because Logan is west of the reference meridian for the time zone). The surface

temperature peaks between 2:00 and 4:30 every day during the period, most commonly at

3:00 in the afternoon. Analysis of phase differences shows a phi of 4.595 radians for

solar radiation and a phi of 4.225 radians for the surface temperature, giving a 1.5-hour

estimate of the delay. Based on equation 15, we expect the average snowpack

temperature to lag behind the surface temperature by just less than $\pi/4$ radians, depending

on z/d_b. The average snowpack temperature (phi=3.513) calculated from the average

snowpack energy content (equation 26) lagged the surface temperature by 0.71 radians,

or about $0.9\pi/4$. So the large phase difference between the surface temperature

measurement and the first thermocouple measurement was not because the surface

temperature measurement was early, but because heat transfer between the surface and

the first thermocouple was slow. The amplitude analysis is consistent with this reasoning,

showing strong damping in the upper layer because of slow heat transfer.

As originally developed, the Utah Energy Balance Model [*Tarboton*, 1994;

Tarboton et al., 1995; *Tarboton and Luce*, 1996] estimated that the conduction of heat

from the surface into the snowpack was a function of the difference between the average

snowpack temperature (as estimated from the energy content) and the surface

temperature (equation 9). There was some concern that this formulation might be

inadequate based on the results of *Tarboton* [1994] showing that snowpack energy

content was underestimated during the long cold period examined here. The classical

force restore approach (equation 11) and the modified force-restore approach (equation

12) appeared to be promising alternatives requiring few additional state variables or

parameters, so we compared those solutions to the original simpler parameterization. To

perform the comparison, we constructed a simple energy balance model for the snowpack

using the observed ground heat fluxes and the observed surface temperatures over time

substituted into equations 9, 11, and 12, hereafter referred to as the T_{ave} model, the force-

restore model, and the modified force restore model. In equation 11, we substituted T_{ave} in place of $\overline{T}$, per the general assumption that the time average at the surface is the same as the depth average temperature. Where the models required a value for T_{ave}, the modeled energy content was used, so that the model energy content evolved based on observed surface temperature and ground heat flux. In equations 9 and 11, λ was calibrated so that the minimum modeled average temperature matched the minimum observed average temperature. We calibrated a value of λ for both models at 0.0045 W/m/K. In the modified force-restore model, we used a value of 0.016 W/m/K for λ estimated from the Fourier transform analysis (Table 2-2a). ω_{lf} was calibrated to give a period of 4 days. Until further study provides more specific guidance, ω_{lf} may be considered an adjustable parameter to fit the observed data. *Tarboton* [1994] used a value of 0.8 W/m/K for λ, which is more in keeping with the literature cited earlier, but did not match our measurements. In their analysis, when this value was used, modeled surface temperatures were only slightly damped, but average snowpack temperature was dramatically underestimated during the cold period analyzed here. They may have been using low estimates of incoming longwave radiation, which allowed agreement with one observable variable, but yielded poor predictions of another variable.

Figure 2-5 shows the relative performance of the three calibrated models over the 2-week period. The modified force-restore approach shows a pattern very similar to the observations, although the modified force restore based energy content precedes the observations. Performance of the unmodified force restore is similar to, but slightly better than, the simpler T_{ave} model. Examining fluxes directly (Figure 2-6) shows the phase shift again and the relative magnitudes of the fluxes estimated by the models. The
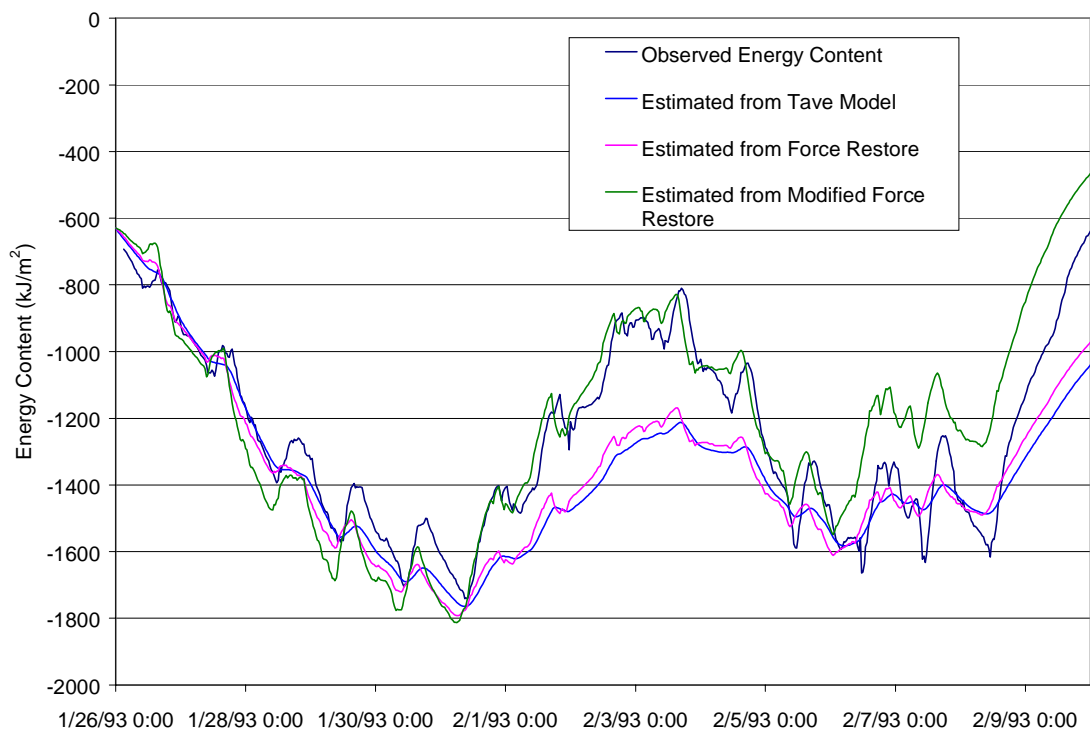
Figure 2-5. Measured and modeled energy content during first 2 weeks.
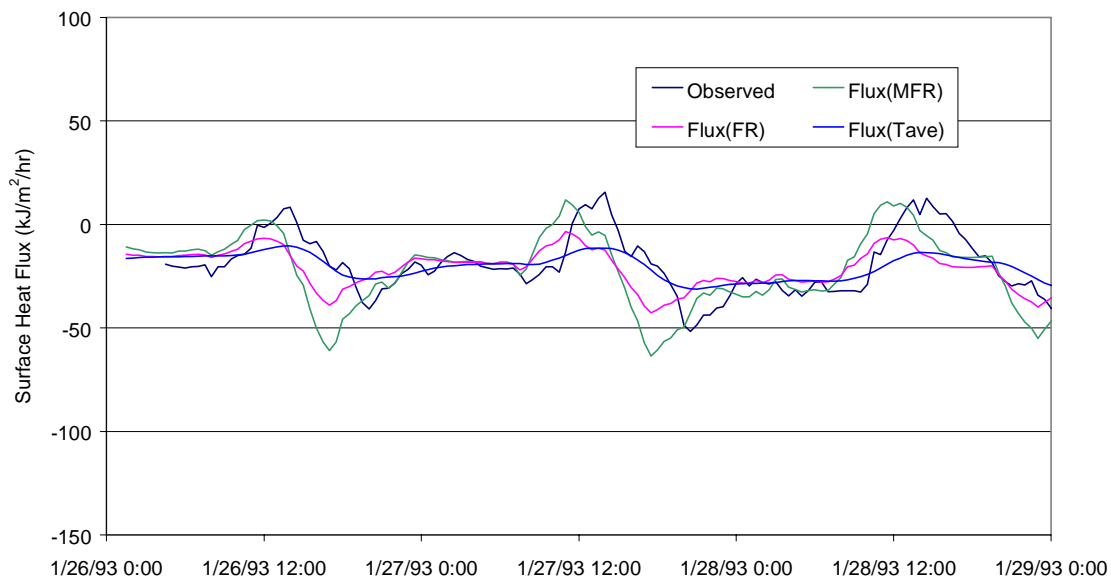
Figure 2-6. Surface conduction heat flux compared to models over first 3 days.

T_{ave} model appears to be in phase with observations, but the amplitude is too small to explain any daily warming. Equations 9 and 12 would suggest that the modified force restore is a force-restore equation superimposed on equation 9, and the differences in model behavior are consistent with this interpretation.

Differences in the timing seen in Figures 2-5 and 2-6 support the idea that the depth of the uppermost thermocouple was greater than estimated. If the thermocouple were deeper below the surface, the weight of the surface layer in the calculation of the snowpack energy content would be greater, and the daily oscillations of the observed average and flux would be greater in magnitude and earlier. The Fourier analysis would give greater values for the conductivity, allowing the modeled oscillations to keep pace with the observed magnitude of the oscillations. The timing of modeled oscillations would not be affected.

The modified force restore is based on the idea of a force restore parameterization with an imposed temperature gradient and therefore, an imposed heat flux. Under steady state conditions, that imposed flux should be equivalent to the ground heat flux, because there is insufficient heat storage occurring in the snowpack to have different fluxes at the ground heat flux plate and the snow surface for an extended period of time. If equation 12 accurately portrays the heat flux, then, there should be some equivalence between the second term on the right side of equation 12 and the ground heat flux measured at the plate, G. The reality of the situation, however, is that the imposed flux is not perfectly steady state, but varies with some period, and so does the ground heat flux. According to equation 7, substituting ω_{lf} for ω_{l} and d_{lf} for d_{l}, because we are now working with time-
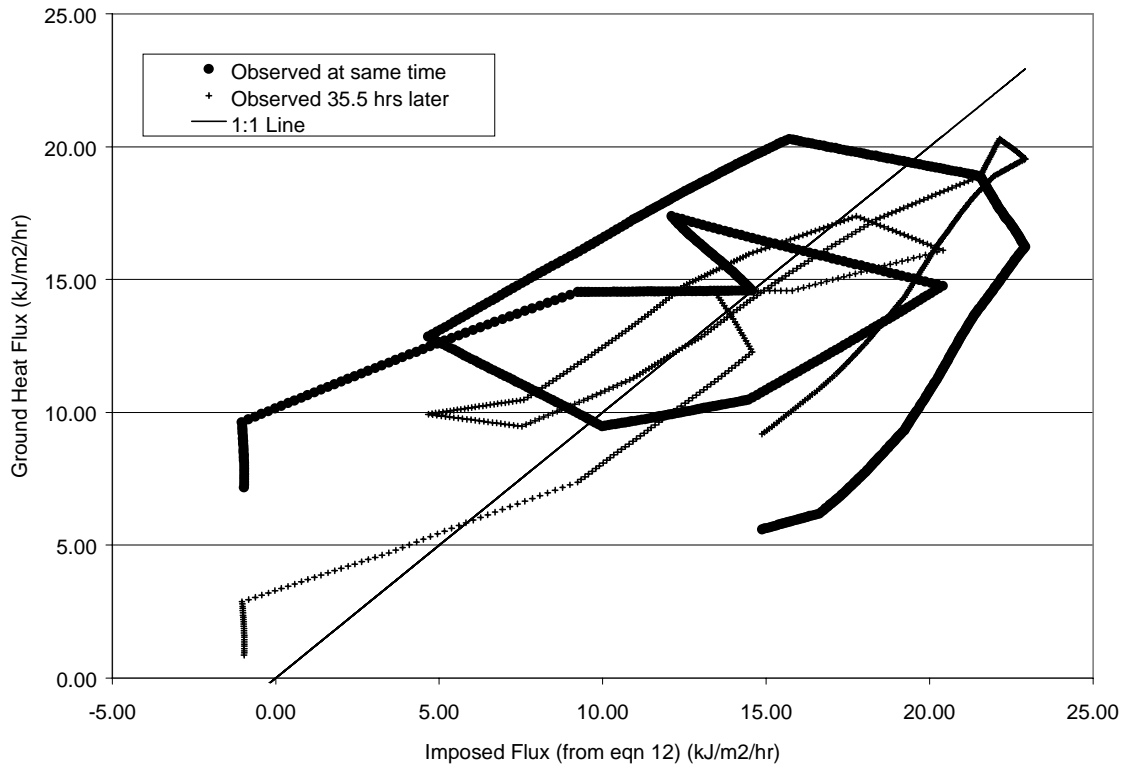
Figure 2-7. Ground heat flux compared to low frequency contribution to the surface heat flux at the same hour and lagged by 35.5 hours.

averaged temperatures and fluxes (as a rough approximation we can consider the data to have passed through a low pass filter), the ground heat flux should lag behind the surface heat flux by z/d_{lf} radians. From our fitting, ω_{lf} is $\frac{1}{4}$ ω_1, so d_{lf} should be twice d_1 and z/d_{lf} should be $\frac{1}{2}$ of z/d_1. From Table 2-2a, we can estimate that z/d_1 might be between 5 and 7 at a depth of 10 cm into the soil, so that z/d_{lf} should be between 2.5 and 3.5. Figure 2-7 shows the flux calculated from the second term of equation 12 at the surface versus the smoothed ground heat flux (frequencies below daily removed) at the same time (big loops) and lagged by 35.5 hours (2.32 radians), which is the lag with the best fit. The ground heat flux may be a bit early because of errors in depth measurement and because

there are variations at yet lower frequencies slightly advancing the ground heat flux. This shows that a directly steady state relationship should not be assumed, and that the frequency and power relationship implied by a sinusoidal model is reasonable. The close correspondence between the calculated low-frequency imposed flux and the lagged observations of ground heat flux along the 1:1 line provides additional support to the use of the modified force-restore model.

4.2. Ground Heat Flux

Because the magnitude of the ground heat flux is generally small compared to other fluxes, it is sometimes treated simplistically or ignored [*Male and Granger*, 1981; *Marks and Dozier*, 1992; *Tarboton and Luce*, 1996; *Albert and Krajewski*, 1998]. In finite difference heat flow models, the ground heat flux is modeled with the rest of the internal heat transfers in the snowpack as a function of the deep soil temperature. In single-layer models, one approximation of the ground heat flux is an average over a season [*Tarboton and Luce*, 1996]. The values of the heat flux are small relative to other heat fluxes like net radiation, but ground heat flux is consistently positive, so the cumulative error may be substantial. For example, the average ground heat flux for the period January 26 to March 21 is 7.03 kJ/m^2/hr, while the average ground heat flux for the period January 26 to February 10 is 13.23 kJ/m^2/hr. Over this period, the difference amounts to a cumulative error of 2380 kJ/m^2, roughly equivalent to 4°C averaged over the snow and top 10 cm of soil, on February 10. The cumulative average flux agrees with the measured cumulative flux at the beginning and end of the time period (January 26 to March 21) and is at maximum disagreement on February 10.
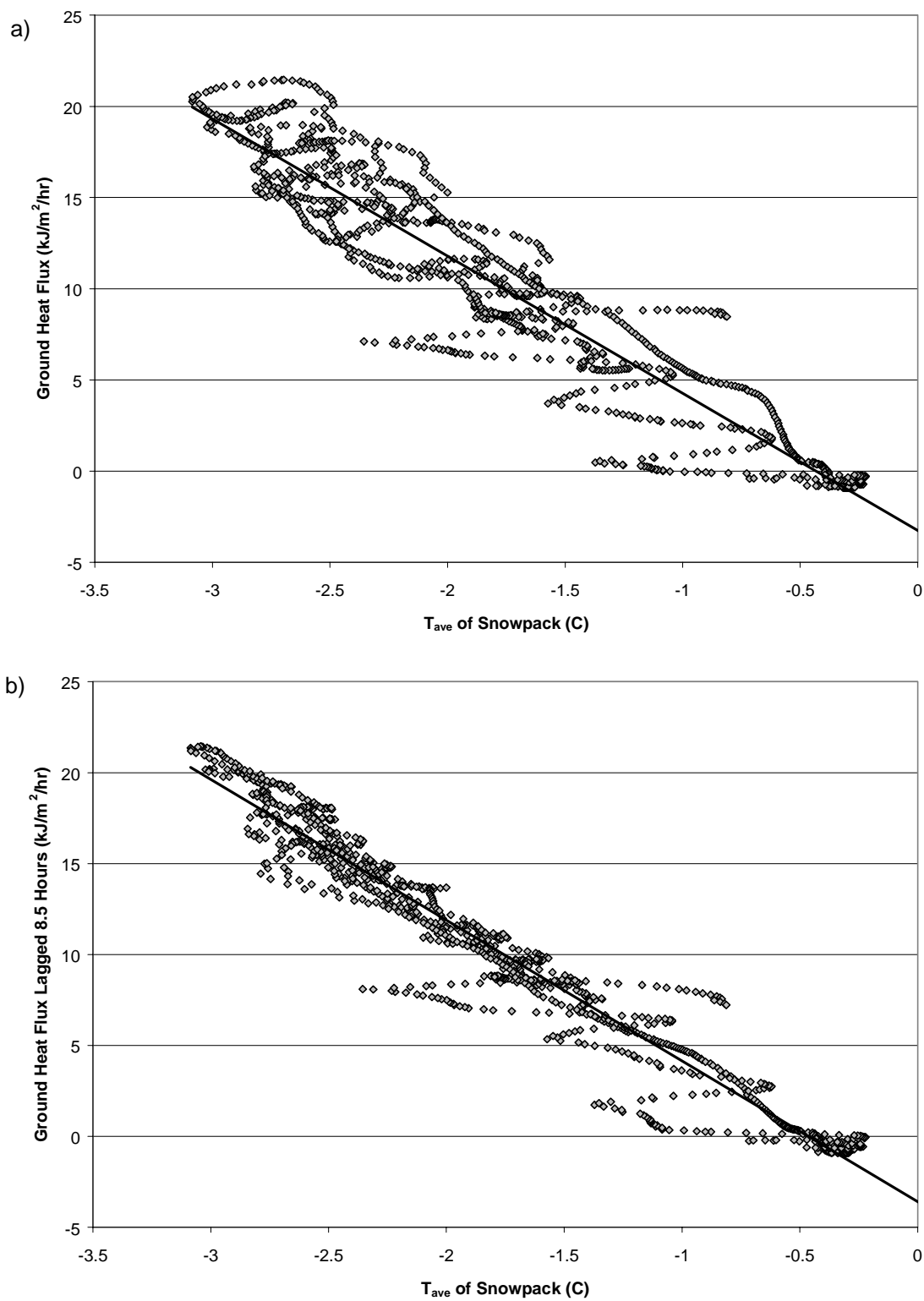
Figure 2-8. Ground heat flux vs. snowpack energy content over 2 weeks a) without lags and b) lagged by 8 hours.

Another simple approximation is that the ground heat flux is the thermal conductivity times the temperature gradient [e.g., *Marks and Dozier*, 1992]. This would lead to an expectation that the ground heat flux measured 10 cm below the ground surface might be correlated to the average snowpack temperature (or snowpack energy content). Figure 2-8a shows that the ground heat flux is strongly negatively correlated with the energy content of the snowpack. Also visible in Figure 2-8a are daily "loops." Because of the sinusoidal forcing, the gradient at the base of the snowpack or the level in the soil being examined may not be well approximated by the simple difference in temperatures divided by the distance. Equation 15 states that the average snowpack temperature should lag $\pi/4$ radians behind the surface temperature for z/d_1 large, and equation 8 suggests that the surface temperature should lag $\pi/4$ radians behind the surface heat flux. The ground heat flux should lag z/d_1 radians behind the surface heat flux (equation 7). Therefore, the ground heat flux, Q_{cg}, should lag the average temperature by $(z/d_1-\pi/2)$ radians. Direct extrapolation of Table 2a gives a rough estimate of z/d_1 between 5 and 7. The correlation was best for $z/d_1 = 3.8$, corresponding to a correlation between the average snowpack temperature and the ground heat flux 8.5 hours later (Figure 2-8b). The ground heat flux is again a bit early (see analysis above for low frequency) because of the influence of lower frequencies, and as mentioned earlier, the calculated average snowpack temperature may be a little late. The correlation covers the period from January 26, 1993 to February 19, 1993, when the first significant rainfall and melt occurred; so includes significant warming and cooling lasting several days. During melt events, advective heat transport is the dominant mechanism, and is not measured by the flux plate. The strong linearity of the relationship suggests that a simple model for

ground heat flux during cold weather could be developed to improve models without

finite difference approximations for the ground heat flux [e.g., *Tarboton and Luce*, 1996;

Albert and Krajewski, 1998; *Jin et al.*, 1999; *Marks et al.*, 1999]. If we posit a

relationship

$$G = \frac{\lambda}{d_e}\left(T_{ref} - T_{ave}\right) \tag{39}$$

where λ is the appropriate thermal conductivity, d_e is an effective depth for the transfer,

T_{ref} is a reference temperature (presumably related to the deep soil temperature) and T_{ave}

is the average snowpack temperature. For the regression shown in Figure 2-8b, this

would imply a value of 2.14 W/m^2/K for λ/d_e and –0.45°C for T_{ref}. *Hanks and Ashcroft*

[1980] give examples of 1.67 to 2.09 W/m/K for soil heat conductivity in the Logan area,

and the regression implies an effective depth on the order of a meter or a little less. The

negative value for T_{ref} is small in magnitude and may be close to the monthly mean

temperature at or near 10 cm. Notably at later dates, after some warming of the soil, the

ground heat flux is roughly 5 kJ/m^2/hr for average snowpack temperatures close to 0°C.

This suggests that if this relationship were used, T_{ref} would need to vary appropriately

through the season. In the case of estimating the ground heat flux, there is once again a

suggestion that low frequency (relative to diurnal) forcing may be responsible for the

observed fluxes.

4.3. Turbulent Transfer

Net turbulent transfer for the period of the study is shown in Figure 2-9. The

effect of the stability corrections were substantial (Figure 2-10) causing an increase in the
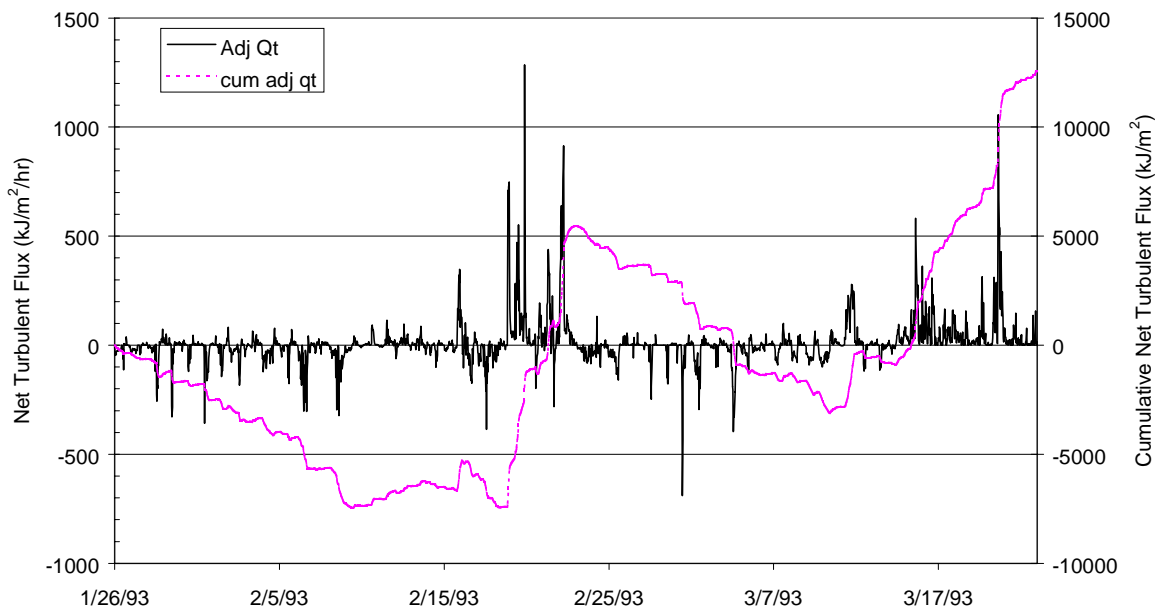
Figure 2-9. Net turbulent transfer and cumulative net turbulent transfer over time.
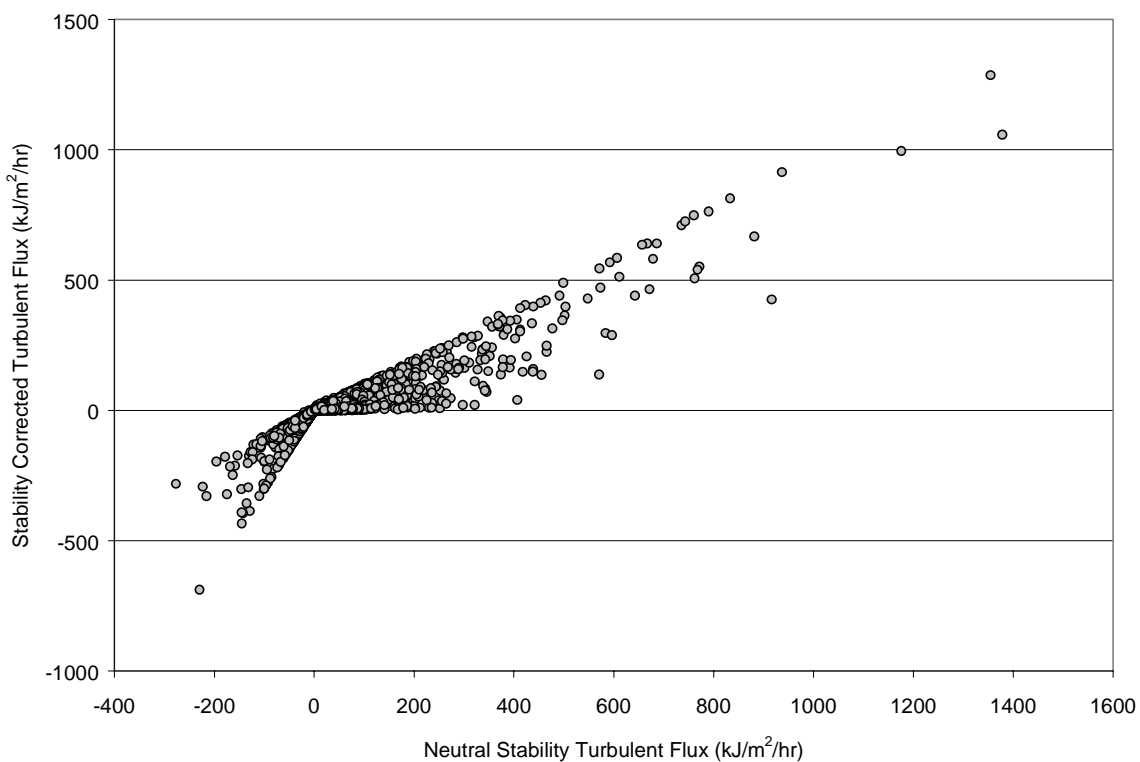
Figure 2-10. Neutral turbulent transfer versus turbulent transfer adjusted for stability.

heat flux out of the snowpack when the snow would warm during the day and a decrease in the heat flux into the snowpack as the snowpack cooled. Turbulent fluxes during the largest heating events were largely unaffected because of the large wind speeds.

Over much of the period, wind speeds were low and turbulent fluxes were not a large portion of the energy balance. During this period, the estimated net turbulent flux is generally more negative than positive because we calculated negative Richardson numbers. The negative Richardson numbers are calculated when the snow surface is warmer than the air above and indicate that the difference in temperatures is creating instability in the shallow airmass above the snowpack. Simultaneously during this period, the valley is under a strong inversion, implying a very stable airmass at the larger scale. Without direct measurements of the fluxes, it is not clear whether the stability at the larger scale will dominate over the very shallow instability represented by the snowpack to air temperature differences.

The long periods of low turbulent transfer are periodically interrupted by brief periods of strong turbulent transfer. As mentioned above, these periods of strong turbulent transfer are affected little by assumptions about stability. While the cumulative positive turbulent transfer during these brief windy periods is greater than the cumulative negative turbulent transfer during cold, still conditions, the difference is not great. An important unanswered question is whether the apparent shallow instability or the larger scale stability associated with the inversion determines turbulent transfer during the calm periods. The answer to this question is important in understanding the cumulative influence of the net turbulent transfer over the season.

4.3. Shortwave Radiation

Incoming shortwave radiation over the period of study is shown for the study site, a nearby site at Campbell Scientific, and at the Utah State University campus (Figure 2-11). The comparison shows that the inversion and foginess may reduce solar radiation slightly at the sensors in the valley (Campbell and Drainage Farm) during otherwise sunny days. This is not unreasonable considering the high reflectance of fog and clouds close to the ground. There is good agreement between all sensors on cloudier days. Within-day patterns of albedo seem to be reasonably well represented by the model of
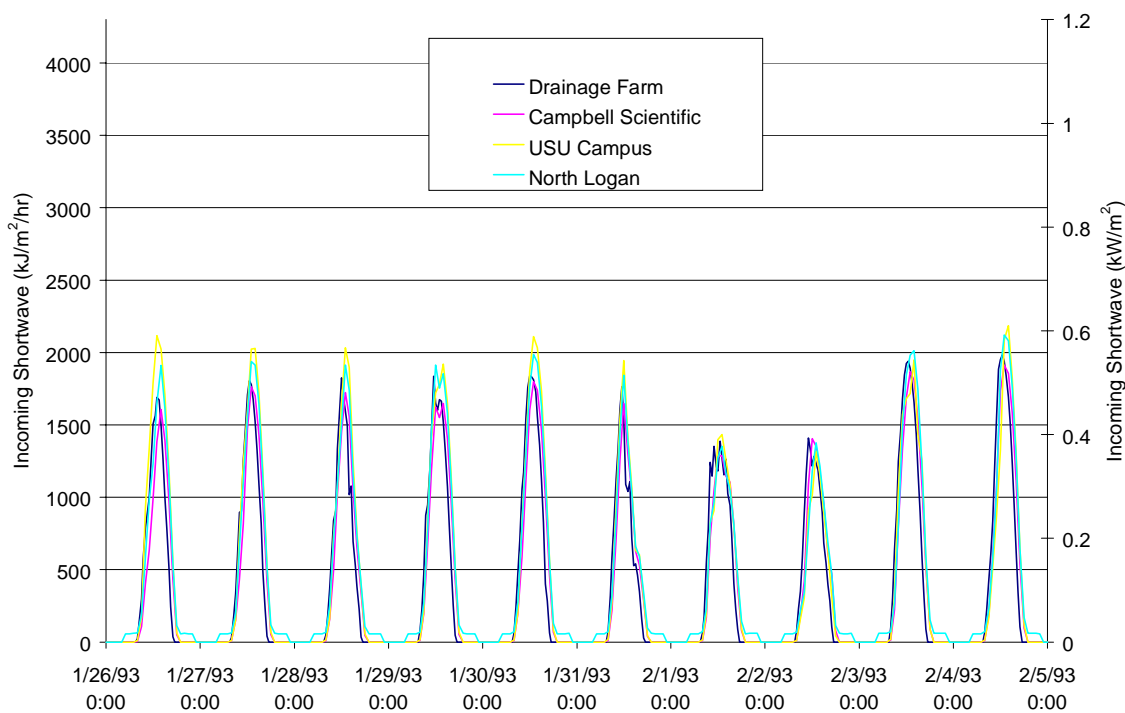
Figure 2-11. Incoming shortwave at Drainage Farm, Campbell Scientific, USU campus, and North Logan Experimental Farm. Note that incoming solar radiation at the higher elevation North Logan and USU campus sites is sometimes greater than at the other sites.
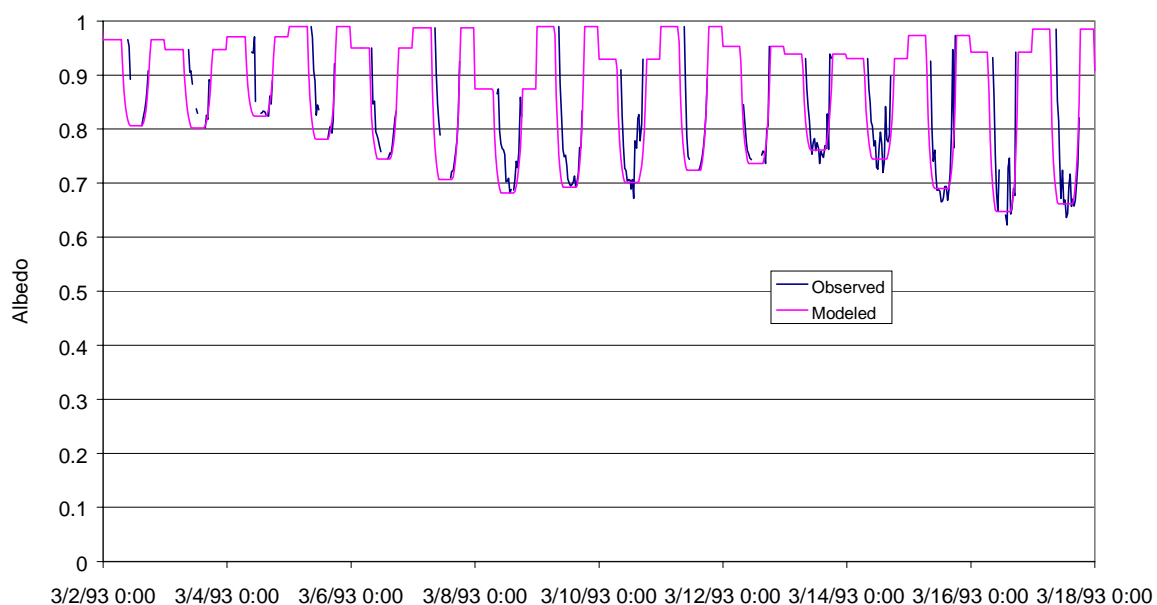
Figure 2-12. Interpolated and measured albedo variations over several days.

Dickinson et al. [1993] when the observed daily minimum albedo is input (Figure 2-12).

Looking at a longer scale, the pattern of daily minimum albedo (when the sun is at a high

angle) shows the general expected pattern of periodic increases followed by a gradual

decay (Figure 2-13). The value of $\alpha_{v0} = 0.85$ calibrated using data from the Central

Sierra Snow Laboratory in Norden, California, and suggested for use in UEB [*Tarboton*,

1994; *Tarboton et al.*, 1995; *Tarboton and Luce*, 1996] gives low values of the daily

minimum albedo. The value of $\alpha_{v0} = 0.95$ suggested by *Dickinson et al.* [1993], while

better, is still low through much of the season, showing good matches only during the

period of strongest melt. Similar results were seen in observations by *Koivusalo and*

Heikinheimo [1999]. Figure 2-14 shows the net shortwave estimated for the period of the

study. At the peak of the day, net shortwave radiation can be one of the largest

contributors to the snowpack energy balance.
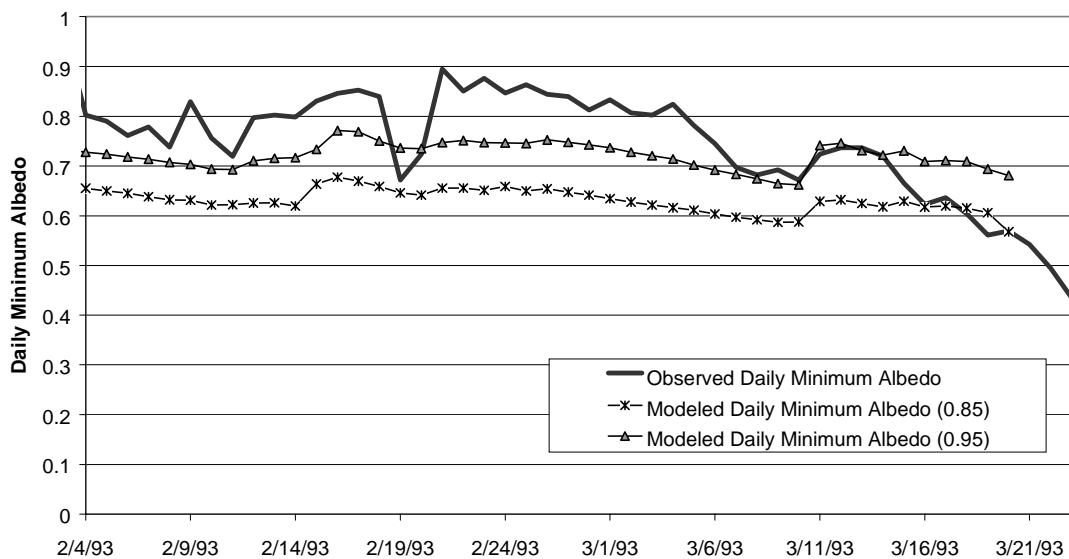
Figure 2-13. Daily minimum albedo over study period, modeled and measured.
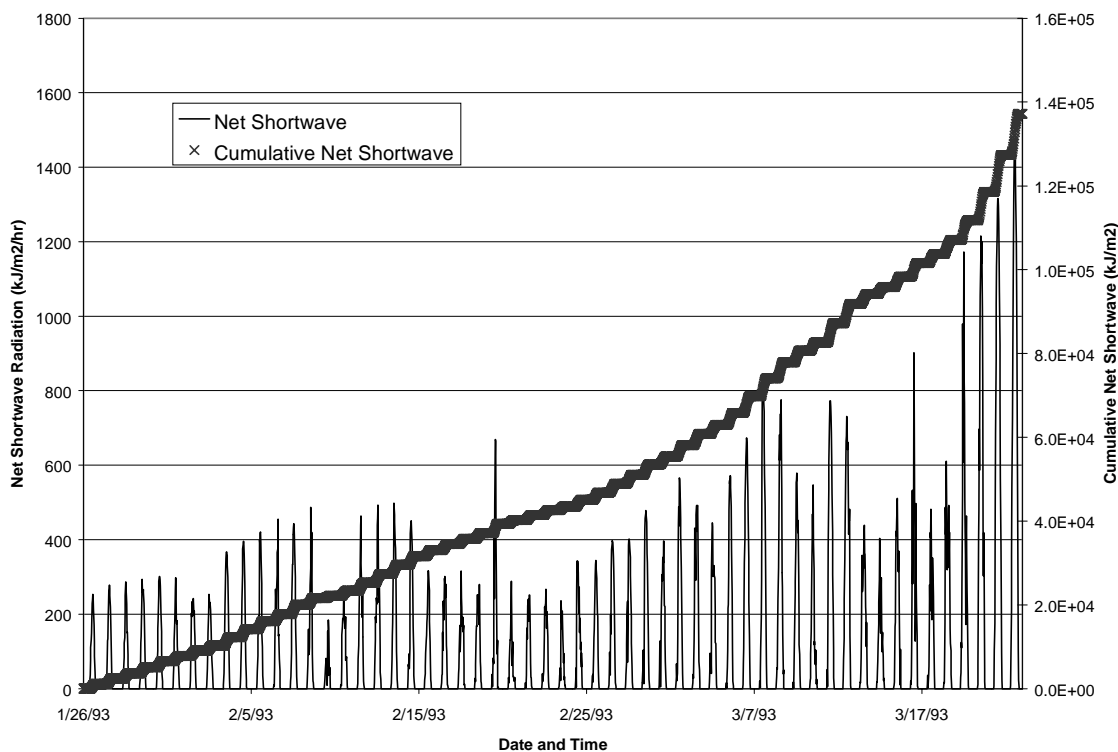
Figure 2-14. Net shortwave fluxes and cumulative net shortwave radiation over time.

4.4. Longwave Radiation

Given temperature changes in the snowpack, the ground heat flux, turbulent fluxes, and net shortwave radiation, we can estimate the longwave radiation during periods when phase changes in the snowpack are not occurring. The outgoing longwave radiation was directly observed and is shown in Figure 2-15. It is unusual to see the longwave radiation balance broken into the incoming and outgoing components, and the net longwave is generally a small number compared to other parts of the energy balance. Individually, the outgoing longwave is a large component of the snowpack energy balance, and it is clear that the incoming longwave must also be fairly large. Incoming longwave radiation can also vary substantially depending on atmospheric conditions.
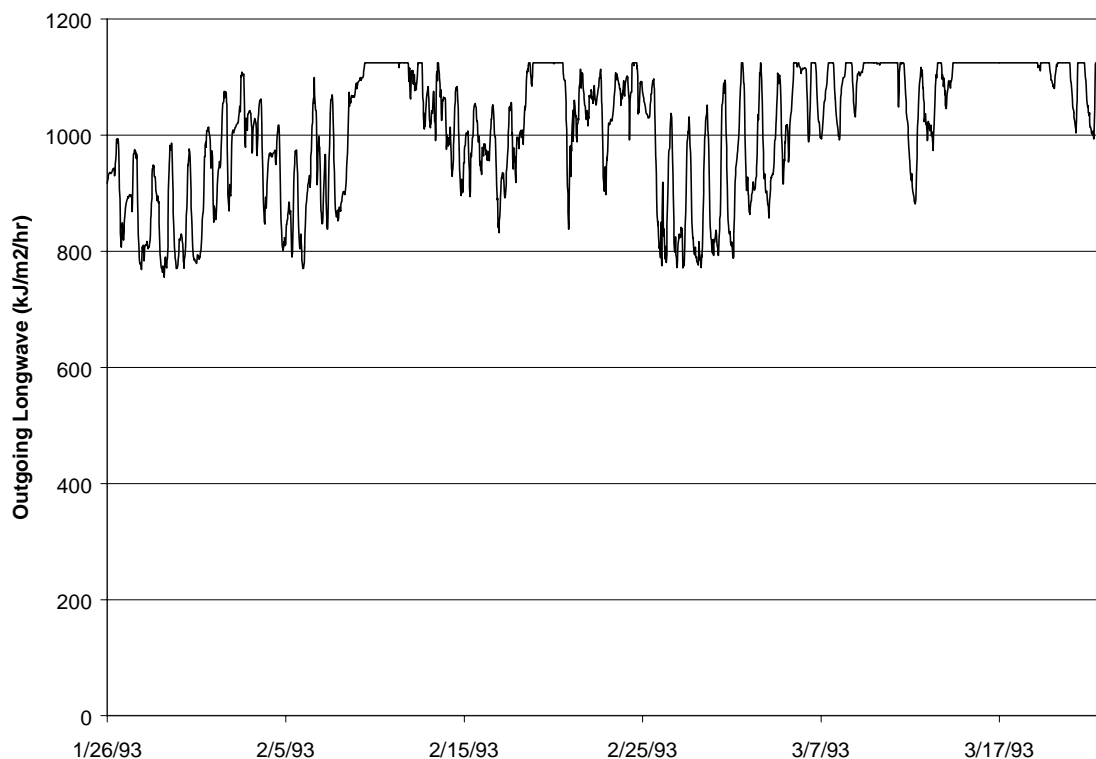
Figure 2-15. Outgoing longwave radiation over the period of study.

Incoming longwave radiation can be approximated with

$$Q_{li} = \varepsilon_a \sigma T_a^4 \tag{40}$$

where ε_a is the effective emissivity of the atmosphere, σ is the Stefan-Boltzman constant, and T_a is the surface air temperature. ε_a is estimated either empirically [e.g., *Satterlund*, 1979] or can be derived from an integration of the emissivity of air and temperature of the air in a column above the site in question [e.g., *Brutsaert*, 1975; *Marks*, 1978]. The cited works estimate Q_{li} under clear skies and non-inversion conditions. Typical values of ε_a from their equations are between 0.71 and 0.76 for winter temperatures and humidity. Under fog or low clouds, ε_a is close to 1. Figure 2-16 shows the clear sky longwave radiation based on the formula of *Satterlund* [1979] and cloudy sky longwave radiation for the period of the study. It also shows the incoming longwave radiation that would be required to cause the temperature changes observed in the snowpack. One important point to note is that the distance between bounding lines representing cloudy and clear sky longwave radiation represents a substantial energy flux relative to any of the other fluxes, so the estimate of the degree of cloudiness in an inversion is an important uncertainty to reduce. In general, the required incoming longwave is between the two bounding lines, suggesting that the reconstructed energy balance is reasonable. We interpret those periods when the incoming longwave radiation required to explain temperature changes is outside of those lines to be when phase changes (melting or freezing) occurred. Excursions above the cloudy longwave would imply freezing of liquid water, and excursions below the clear sky radiation imply melting. If we look at the cumulative energy in freezing and melting (the cumulative excursions)
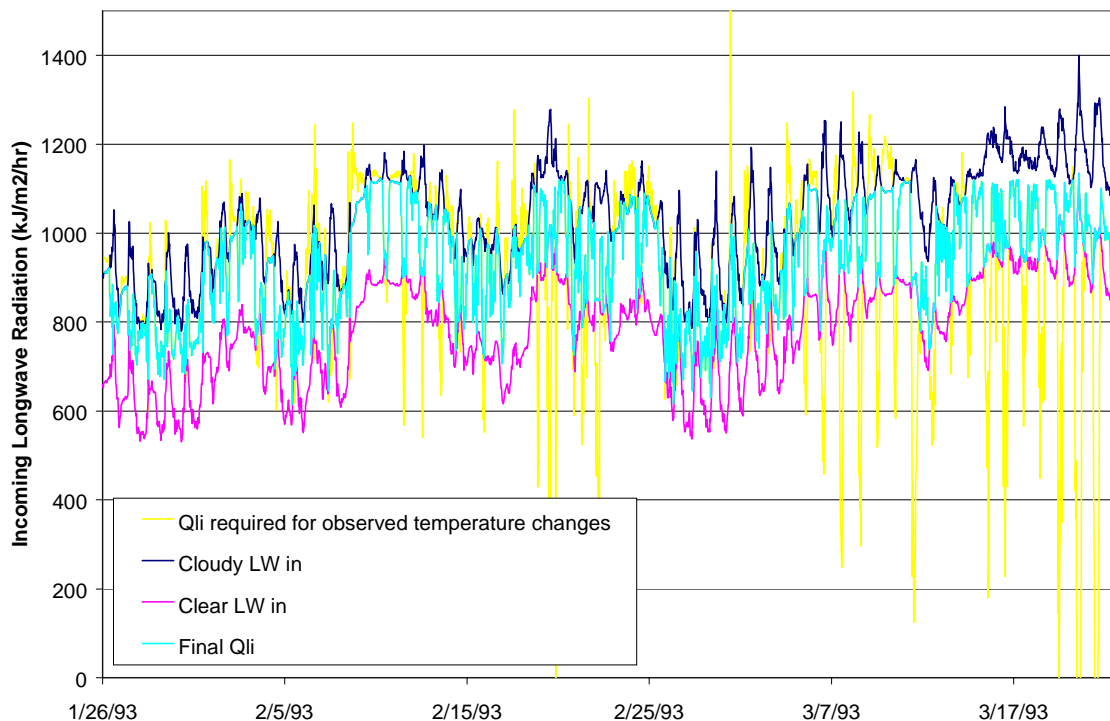
Figure 2-16. Clear sky and cloudy sky incoming longwave radiation plotted with longwave radiation required to satisfy energy balance determined by temperature changes. The light colored lines above and below the cloudy and clear longwave in curves are referred to later as "excursions."

from the point of peak snow accumulation until complete melt, we see a good

correspondence (Figure 2-17) compared to measured reductions in snow water

equivalence. During this period, most of the excursions indicate melt, and the snowpack

temperature changes very little so the figure gives us some indication of how well the

other energy fluxes are estimated. It is important to note in interpreting Figure 2-17 that

there is substantial room for error between the two limiting conditions as depicted in

Figure 2-16, so some of the match may result from compensating errors.

The incoming longwave required for the observed temperature changes in Figure

2-16 moves back and forth between the line for cloudy sky radiation and clear sky
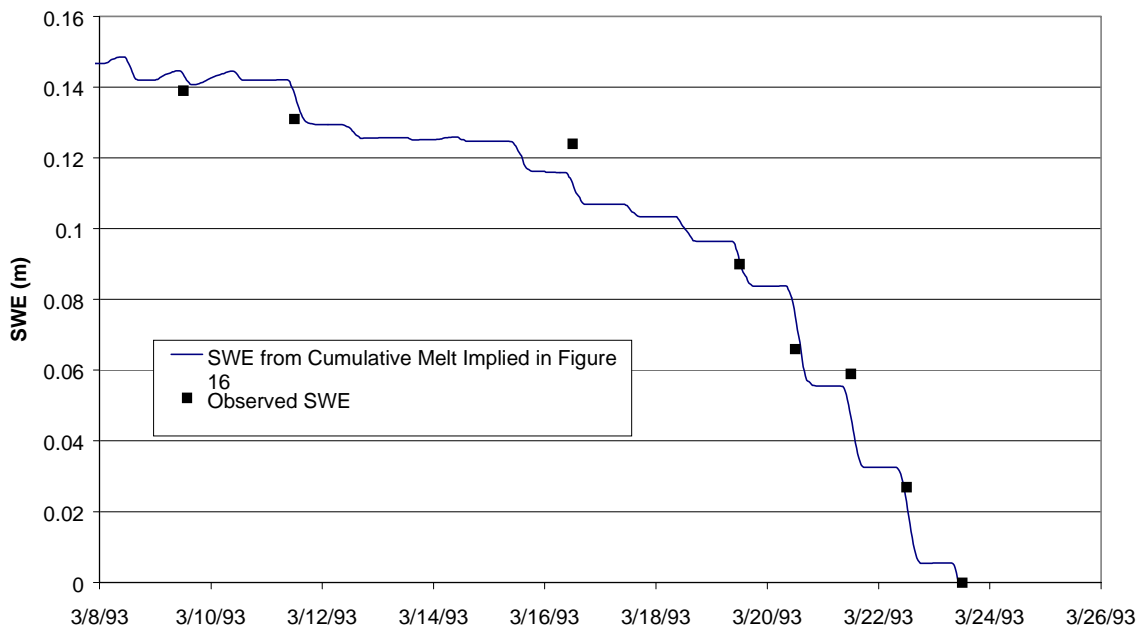
Figure 2-17. Peak snow water equivalence minus melt implied by excursions in Figure 2-16 plotted with measurements of snow water equivalence.

radiation. We described the relative position between the lines as the "inferred cloudiness" to examine how incoming longwave radiation relates to other variables. We examined relative humidity, temperature, deviation of temperature from the 24-hour minimum, time of day, and recorded surface aviation observations (cloud cover and visibility). Inferred cloudiness showed no relationship with temperature. Relative humidity was also a poor predictor because the instrument may read 90 to 95% when the air is saturated, and the degree of cloudiness depends on how much moisture is available beyond saturation. The temperature deviation from the 24-hour minimum showed some relationship to inferred cloudiness, with greater inferred cloudiness generally associated with temperatures closer to the 24-hour minimum. One of the more interesting patterns was how inferred cloudiness varied with time of day (Figure 2-18). The data show a
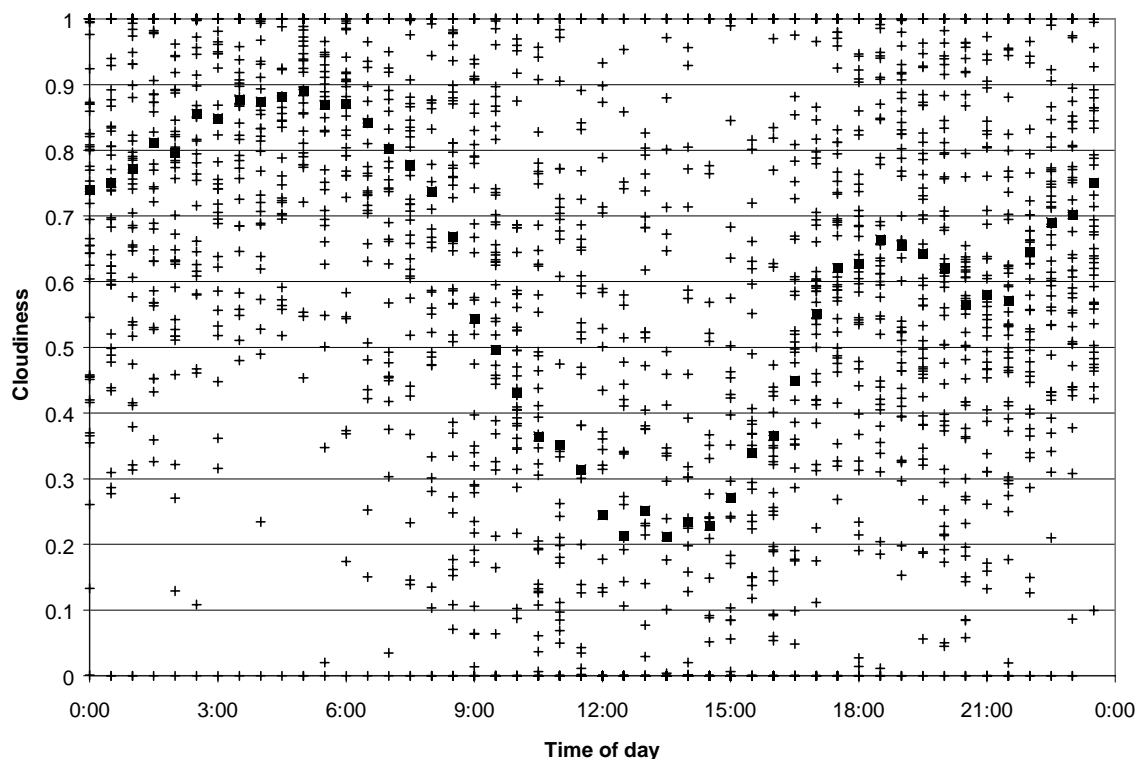
Figure 2-18. Inferred cloudiness versus time of day; crosses are individual observation and large squares are the mean for each half-hour period of the day.

pronounced favoritism for night and early morning fog, corresponding to the general behavior of Cache Valley in the winter and observations we recorded of weather during the 3-month period.

Surface aviation observations (Table 2-3) show that the cloudiness inferred through this procedure has some relationship to actual observations but may not reflect the behavior at a specific time. At the Cache Logan airport, ground observers noted the visibility (fog, haze, clear), and fractional cover of clouds in the sky overhead (Overcast, >90%, Broken Clouds, 50-90%, Scattered Clouds, 10-50%, and Clear, <10%) at several times during most days in the period (about 200 observations). If the inferred cloudiness values relate to the emissivity of the air, there should be some relationship between these

Table 2-3. Cloudiness Inferred from Snowpack Energy Balance Crosstabulated by Ground Visibility and Sky Conditions Recorded at Logan Airport.

Visibility		Overcast	Broken	Clear	Scattered	Obscured	All
				Sky Conditions			
Fog	Avg Cloudiness	0.44	0.42	0.47	0.64	0.41	0.43
	Range	0 - 0.93	0 - 1	0 - 1	0.64 - 0.64	0 - 1	0 - 1
	n	3	10	8	1	17	39
Haze	Avg Cloudiness	0.47	0.42	0.28	0.39	0.45	0.39
	Range	0 - 1	0 - 1	0 - 0.86	0 - 0.90	0 - 1	0 - 1
	n	9	24	18	14	9	74
Clear	Avg Cloudiness	0.24	0.17	0.09	0.12		0.15
	Range	0 - 1	0 - 0.79	0 - 0.60	0 - 1		0 - 1
	n	13	16	15	15		59
All	Avg Cloudiness	0.34	0.34	0.25	0.26	0.42	0.32
	Range	0 - 1	0 - 1	0 - 1	0 - 1	0 - 1	0 - 1
	n	25	50	41	30	26	172

observations and the inferred cloudiness. Table 2-3 shows the relationships at times without precipitation because advected heat fluxes were not considered in the reconstruction of the energy balance. Under snowing conditions, the effect should not be great, but rain can carry significant advected heat because of the latent heat of fusion. In Table 2-3 the average cloudiness is greatest for foggy conditions, next for hazy conditions, and lowest for conditions with no impairment to surface visibility. Under conditions where fog was observed at the airport, inferred cloudiness varies little with upper sky conditions, when they could be observed. Observations of scattered clouds or overcast sky are rare under foggy conditions and may have been selectively categorized as obscured, being difficult to discern under fog. Under foggy conditions, the inferred cloudiness ranged from 0 to 1, indicating that at times, inference about cloudiness and therefore emissivity and incoming longwave radiation based on temperature changes in the snowpack is incorrect. Under hazy conditions, we begin to see more pattern to the

means based on sky conditions, where obscured and overcast skies have the highest

average inferred cloudiness followed by broken clouds, scattered clouds, and clear skies

in that order. Again, the ranges are substantial, but we see that under scattered clouds or

clear skies, we never inferred complete cloudiness. Given clear visibility near the

surface, the pattern between average cloudiness conditions is even more pronounced in

the expected order, overcast, broken, scattered, and clear. Under clear skies, the

maximum inferred cloudiness is 0.6. There are too few observations in snowy weather to

complete a similar analysis, however the average cloudiness under snow is 0.61

compared to the average of 0.32 for non-precipitating conditions.

From this analysis, it is clear that the amount of fog and the cloud cover have a

very strong influence on incoming longwave radiation, and that the uncertainty in

longwave radiation caused by lack of information on cloud or fog cover can be very

large. We now believe that much of the error seen by *Tarboton* [1994] and *Tarboton and*

Luce [1996] during validation of the model with this data was because of poor cloudiness

estimates based on the diurnal temperature range using *Bristow and Campbell* [1984].

Replacing those cloudiness calculations with the cloudiness data reported here results in a

much smaller error. *Cline* [1997] suggests that knowledge of the 500-mb synoptic

pattern may be one method to approach this problem. The time sequence of barometric

pressure may also be useful. Analysis of serial satellite images may be a more direct

approach. Substantial information has been developed for estimating the effects of

clouds and fog on incoming solar and longwave radiation based on direct observation of

sky conditions [*Male and Granger*, 1981].

4.5. Comparison Between Fluxes in a
Mountain Valley

The literature on snow energy balances contains a great deal of emphasis on the subject of relative magnitude of different fluxes [e.g., *Male and Granger*, 1981; *Marks and Dozier*, 1992; *Dingman*, 1994; *Cline*, 1997]. The purpose of such investigations relates to determining which processes are the most important or sensitive in snowmelt models. Figure 2-19 shows the cumulative net radiation, net turbulent exchange, and net ground heat flux. Looking at the final date, one might be tempted to say that the net radiation was the dominant flux. However, when looking at the rest of the season, the answer is not so clear. More specifically, the term "dominant" may not apply to this set of data. The magnitudes of the cumulative fluxes are fairly comparable over much of the time period, and the rate of change in the cumulative fluxes varies over time.
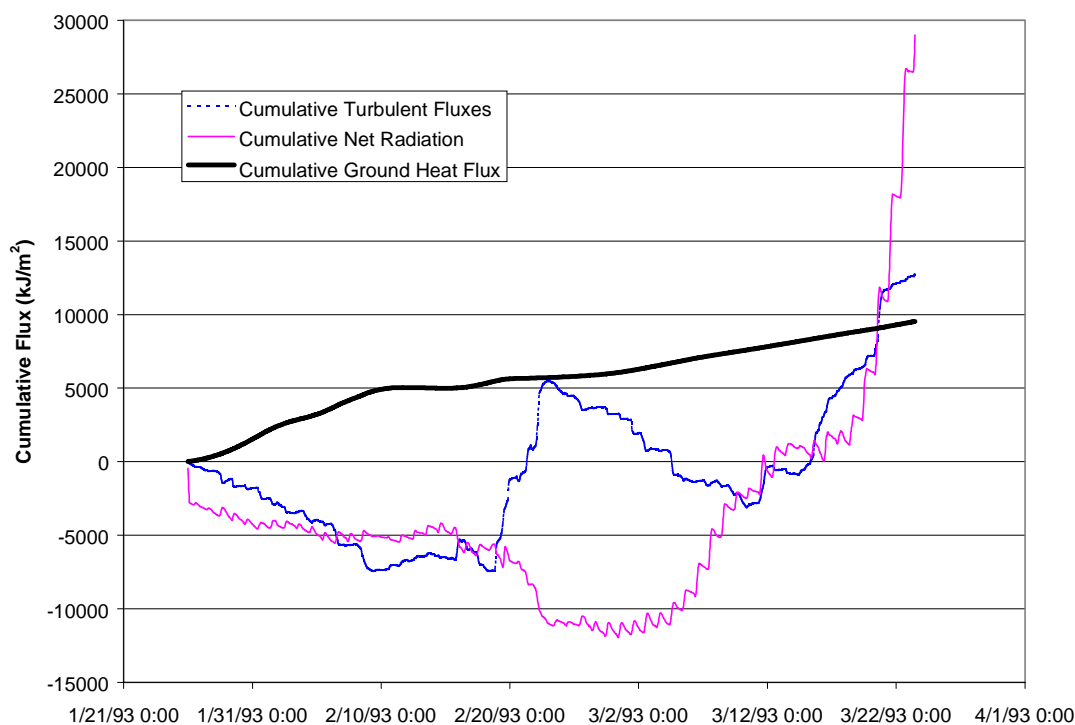
Figure 2-19. Cumulative net radiation, net turbulent transfer, and ground heat flux starting from the beginning of the study period.

The time scale under consideration is important when looking at the question of which flux might be more critical to model correctly. Ground heat flux is relatively constant in time and shows a persistent effect. As noted by others previously, the ground heat flux has small values relative to solar or longwave radiation, yet over a time period, may sum to considerable values. A proper estimate of the ground heat flux may not be critical for estimates during a melt event, but may be important in determining the snowpack temperature and moisture state at the beginning of the event. The net turbulent flux is generally small and slightly negative. It is, however, occasionally interrupted by periods of strong positive turbulent transfer. The values are such that a good understanding of the stability functions is required to estimate the temperature and moisture state of the snowpack during long cold periods, but less influence of the stability functions is seen during fast melt events driven by turbulent exchange.

The significance of one flux over another and the relative effect of error in fluxes is difficult to discern when considering snowpack models that cover the entire winter season. The net effect of the interacting fluxes up to the time of interest gives the state of the snowpack. If the rain and wind of February 19-21 fell on a ripe snowpack, the results could be very different from the same event on a cold snowpack. At this date, the cumulative error of the ground heat flux for a constant average model is -1500 kJ/m^2, or about 4.5 mm of snow water equivalence, a little less than half the snowpack. Without this error, a model might predict substantial melt, and with the error, substantial accumulation as the rain freezes. Even if a compensating error is introduced following the event, the model is working with a very different snowpack after the event, so a fairly unpredictable nonlinearity is introduced. Besides the path dependent behavior

obfuscating the relative importance of errors, interactions between model components may produce interesting interactions between flux errors. For example, if the incoming longwave radiation were underestimated, the snow surface temperature would be underpredicted and consequently the outgoing longwave would be underpredicted and the net turbulent transfer would increase. The effect could be nearly great enough to be greatly compensated if the snow surface conductance is low.

The relative contribution of each process to the energy balance changes over the period of the study according to the weather. This was also an important result of *Cline* [1997]. Cold stable airmasses produced inversions in Cache Valley with calm air and fog. During these periods, incoming longwave radiation increased during the foggy mornings and nights as did the uncertainty in its value. Also during these periods, the ground heat flux increased to values as high as three times its average over the season. Net solar radiation decreased slightly, but was still a large contributor to the energy budget. Turbulent transfer decreased in magnitude and tended to become slightly negative. Uncertainty about the true value of the stability functions increased the uncertainty and potential error for these periods. The stability of the airmass during these periods promotes its persistence and allows errors that accumulate to become potentially large. During these periods, net radiation, turbulent transfer, and ground heat fluxes have similar magnitudes. During stormy periods, the net turbulent transfer is much greater than other fluxes. The only period of warm clear weather was near the end of the study following two storm events. By this time, the albedo was lower, so it is questionable whether the high net radiation relative to other fluxes is a function of the weather or of the snowpack condition at the time, but there was probably influence from both.

4.6. How Conditions Differed Between the Valley and Surrounding Areas

There are differences in temperature and snowpack depth between the site and the USU campus, 150 m higher in elevation (Figure 2-20). The snowpack on campus was shallower and melted sooner, which is not the generally expected result of an increase in elevation. Both sites are level, so the difference is not due to aspect, although the campus site may have received a little more solar radiation (Figure 2-11). Probably much of the explanation comes from the fact that during much of the cold period, temperatures were warmer on campus. For distributed or lumped model representations of the basin, some accounting for the inversion would be needed. Again, it is difficult to discern this type of information from a few climate stations without additional observations and input.
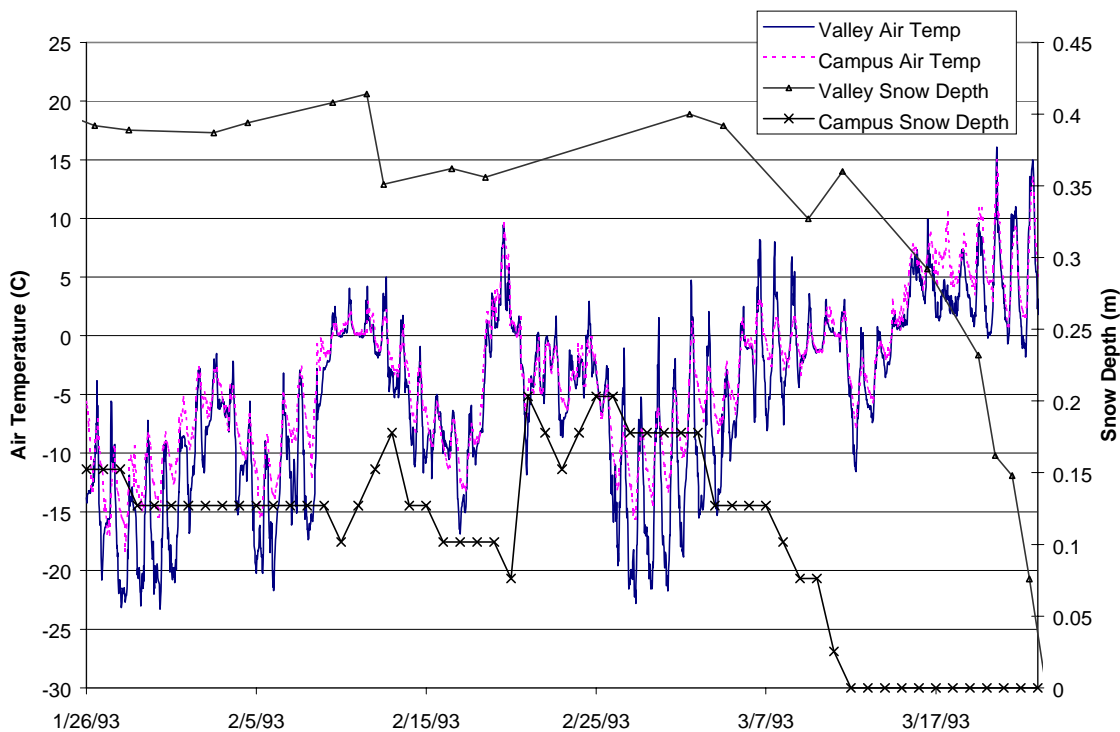
Figure 2-20. Snowpack and temperature at USU campus and Drainage Farm.

5. CONCLUSIONS

During the winter of early 1993, Cache Valley, a long valley at the eastern edge of the basin and range geologic province in Northern Utah, endured a persistent temperature inversion accompanied by fog. The inversion does not occur for long periods every winter, nor does the snow remain on the ground for a long period every winter. However, measurements of the snowpack energy balance taken during this winter hold important lessons about how inversions affect snowpacks and more general lessons about heat conduction within snowpacks. The most interesting feature of the energy balance of the snowpack in this study was how damped the energy fluxes seem to be relative to energy fluxes measured at other sites [e.g., *Male and Granger*, 1981; *Cline*, 1997]. While the ground heat flux is generally considered negligible relative to net turbulent transfer and net radiation, for a long period during the winter of 1993 in Cache Valley, the cumulative ground heat flux was comparable to the magnitude of other cumulative fluxes. In some sense, the layer of cold still air over the snowpack served as insulation from a warmer atmosphere above and resulted in a generally unexpected pattern of complete melt at higher elevations before melt of the valley bottom snowpack had really begun.

The inversion caused unusual conditions not often described or modeled well, and it is important to note features of the energy balance that seem to be affected by the presence of the inversion, in particular turbulent transfer and incoming longwave radiation. Net turbulent transfers were usually a small part of the energy budget but were occasionally very large. Stability corrections suggest that much cooling of the snowpack by turbulent transfer was caused by bouyant instability in the few meters above the

snowpack, e.g., the snowpack surface is warmer than the air 2 m above the snowpack. It

appears contradictory and the instability is very shallow, because at the same time the

valley shows strong atmospheric stability to a depth of at least 150 m. However, slow

cold air drainage may create a shallow unstable layer immediately above the snowpack.

Direct measurement of the sensible heat transfer may assist in better interpreting this

condition. The daily cycle of fog formation and dissipation strongly affected incoming

longwave radiation. This cycle occurs commonly during temperature inversions. If it is

known that an inversion exists, time of day may be a reasonable predictor of whether it is

foggy. This may require additional information. Because the difference between

incoming longwave radiation under foggy conditions generally differs greatly from

incoming longwave radiation under clear sky conditions, there may be great value in

incorporating the additional data.

Heat flow through the snowpack is considered a difficult and complex process to

model. So much so, that it has been generally assumed that single-layer snowpack

models must, of necessity, err in estimates of heat conduction, with their worst

performance during cold periods. By making the assumption that the heating and cooling

of the snowpack is diurnally forced, however, we can substantially improve our

descriptions of heat flow in the snowpack, even a heterogeneous snowpack. By

recognizing further that there are lower frequency forcings, sometimes with greater

power, we can further improve descriptions for extended cold periods. Equation 12,

based on a force-restore model with a superimposed gradient, may be a good candidate to

replace more complex models. In the extreme, we could recognize that the forcing at the

surface could be decomposed into a Fourier series with multiple frequencies. Estimation

of the parameters for that series would use the time series of all previous surface temperatures – essentially the same information used in a finite difference estimation. Hopefully the two numerical schemes would converge on a very similar answer. Within this concept lies the seed for simplification. If we can recognize those few frequencies with the greatest power, we can continue to represent the snowpack as a single-layer, and only use such recent past temperature information as needed. There is an opportunity in the research of temperature records to increase our knowledge of multi-day and multi-week time scale variations in air temperature. Frequency domain representation is a powerful method for compression of images and if it is a useful representation for heat flux calculation, may be an efficient method of storing and using spatio-temporal temperature data.

Water movement through the snowpack has not been addressed in this examination, and may pose a more substantial impediment to creating sound single-layer snowpack models. *Hu and Islam* [1995] report that the force-restore approach does not work as well with soil moisture as with heat flow, noting that moisture flow did not have a strong diurnal forcing. In the case of late season snowmelt, there is a strong diurnal signal, offering hope of greater success. Also the SNAP model [*Albert and Krajewski*, 1998] gives parameterizations for water flow in a single-layer snowpack that have met with some success.

In this piece-wise examination of the energy balance and comparison to models used to estimate some of the components of the energy balance, we noted many potential errors or uncertainties. The magnitude of internal heat fluxes is relatively small compared to incoming, outgoing, or net solar and longwave radiation and turbulent fluxes. The

oversimplification of heat flow in single-layer models makes it easy to assign blame for any discrepancies to the heat flow parameterizations [*Tarboton and Luce*, 1996; *Koivasulo and Heikinheimo*, 1999]. However, it is likely that error estimates for these other fluxes are partially responsible. In the case of *Tarboton* [1994], our examination would suggest that the incoming longwave radiation was underestimated during the initial period because the cloudiness, and therefore, emissivity of the atmosphere was underestimated. In addition, warmer air at higher elevations may have further increased downwelling longwave radiation. The results of *Koivusalo and Heikinheimo* [1999] showing an underestimated snowpack temperature are consistent in magnitude and timing with errors associated with using an average ground heat flux in place of one dynamically determined by heat flow processes in the soil. Our comparisons of the simple albedo model used by *Tarboton* [1994] and *Tarboton and Luce* [1996] show that errors in net shortwave may have been important in that analysis as well. Improved modeling of albedo may also be important when the errors reported here and in *Koivusalo and Heikinheimo* [1999] are noted along with the findings of *Blöschl and Kirnbauer* [1991]. As noted by *Beven* [1989] and others before and since, it is important to validate each part of a physically based model. In the case of complex models with strong interdependence of processes, such as snow energy balance models, where a poorly estimated radiation stream may yield a poor estimate of the turbulent flux, it is all the more important.

REFERENCES

Albert, M. R., and G. N. Krajewski, A fast physically-based point snow melt model for distributed applications, *Hydrol. Process.*, *12*, 1809-1824, 1998.

Anderson, E. A., A point energy and mass balance model of a snow cover, *NOAA Technical Report NWS 19*, U.S. Department of Commerce, Silver Spring, Md., 1976.

Arons, E. M., and S. C. Colbeck, Geometry of heat and mass transfer in dry snow: A review of theory and experiment, *Rev. Geophys.*, *33*, 463-493, 1995.

Barry, R. G., *Mountain Weather and Climate*, 2nd Edition, Routledge, New York, 1992.

Berg, P. W., and J. L. McGregor, *Elementary Partial Differential Equations*, Holden-Day, Oakland, 1966.

Beven, K., Changing ideas in hydrology—the case of physically-based models, *J. Hydrol.*, *105*, 157-172, 1989.

Beven, K., Linking parameters across scales: Subgrid parameterizations and scale dependent hydrological models, *Hydrol. Process.*, *9*, 507-525, 1995.

Blöschl, G., *Scale and Scaling in Hydrology*, Habilitationsschrift, Weiner Mitteilungen Wasser Abwasser Gewasser, Wien, 1996.

Blöschl, G., and R. Kirnbauer, Point snowmelt models with different degrees of complexity - internal processes, *J. Hydrol.*, *129*, 127-147, 1991.

Bristow, K. L., and G. S. Campbell, On the relationship between incoming solar radiation and the daily maximum and minimum temperature, *Agr. Forest Meteorol.*, *31*, 159-166, 1984.

Brutsaert, W., On a deriveable formula for long-wave radiation from clear skies, *Water Resour. Res.*, *11*, 742-744, 1975.

Cline, D., Snow surface energy exchanges and snowmelt at a continental, midlatitude alpine site, *Water Resour. Res.*, *33*, 689-701, 1997.

Colbeck, S. C., An overview of seasonal snow metamorphism, *Reviews of Geophysics and Space Physics*, *20*, 45-61, 1982.

Colbeck, S. C., Air movement in snow due to windpumping, *J. Glaciol.*, *35*, 209-213, 1989.

Deardorff, J. W., Dependence of air-sea transfer coefficients on bulk stability, *J. Geophys. Res.*, *73*, 2549-2557, 1968.

Deardorff, J. W., Efficient prediction of ground surface temperature and moisture with inclusion of a layer of vegetation, *J. Geophys. Res.*, *83*, 1889-1903, 1978.

Dickinson, R. E., A. Henderson-Sellers, and P. J. Kennedy, Biosphere-atmosphere transfer scheme (bats) version 1e as coupled to the ncar community climate model, *NCAR/TN-387+STR*, National Center for Atmospheric Research, Boulder, Colo., 1993.

Dingman, S. L., *Physical Hydrology*, Prentice Hall, Englewood Cliffs, N.J., 1994.

Dooge, J. C. I., Looking for hydrologic laws, *Water Resour. Res.*, *22*, 46S-58S, 1986.

Dunne, T., A. G. Price, and S. C. Colbeck, The generation of runoff from subarctic snowpacks, *Water Resour. Res.*, *12*, 677-685, 1976.

Dyer, A. J., and B. B. Hicks, Flux-gradient relationships in the constant flux layer, *Quart. J. R. Met. Soc. 1970*, *96*, 715-721, 1970.

Eagleson, P. S., The emergence of global-scale hydrology, *Water Resour. Res.*, *22*, 6S-14S, 1986.

Flerchinger, G. N., Simultaneous heat and water model of a snow-residue-soil system, Ph.D. Dissertation, Washington State University, Pullman, Wash., 1987.

Gray, J. M. N. T., L. W. Morland, and S. C. Colbeck, Effect of change in thermal properties on the propagation of a periodic thermal wave: Application to a snow-buried rocky outcrop, *J. Geophys. Res.*, *100*, 15,267-15,279, 1995.

Hanks, R. J., and G. L. Ashcroft, *Applied Soil Physics*, Vol 8, Advanced Series in Agricultural Sciences, Springer-Verlag, Berlin Heidelberg, 1980.

Horne, F. E., and M. L. Kavvas, Physics of the spatially averaged snowmelt process, *J. Hydrol.*, *191*, 179-207, 1997.

Hu, Z., and S. Islam, Prediction of ground surface temperature and soil moisture content by the force-restore method, *Water Resour. Res.*, *31*, 2531-2539, 1995.

Idso, S. B., and R. D. Jackson, Thermal radiation from the atmosphere, *J. Geophys. Res.*, *74*, 5397-5403, 1969.

Jin, J., X. Gao, Z.-L. Yang, R. C. Bales, S. Sorooshian, R. E. Dickinson, S. F. Sun, and G. X. Wu, Comparative analyses of physically based snowmelt models for climate simulations, *J. Climate*, *12*, 2643-2657, 1999.

Jordan, R., A one-dimensional temperature model for a snow cover, technical documentation for SNTHERM.89, *Special Technical Report 91-16*, US Army CRREL, Hanover, N.H., 1991.

Kirnbauer, R., G. Blöschl, and D. Gutknecht, Entering the era of distributed snow models, *Nord. Hydrol.*, *25*, 1-24, 1994.

Koivasulo, H., and M. Heikinheimo, Surface energy exchange over a boreal snowpack, *Hydrol. Process.*, *13*, 2395-2408, 1999.

Male, D. H., and R. J. Granger, Snow surface energy exchange, *Water Resour. Res.*, *17*, 609-627, 1981.

Marks, D., An atmospheric radiation model for general application, in *Proceedings: Modeling of Snow Cover Runoff*, edited by S. C. Colbeck and M. Ray, pp. 167-178, US Army CRREL, Hanover, N.H., 1978.

Marks, D., J. Domingo, D. Susong, T. Link, and D. Garen, A spatially distributed energy-balance snowmelt model for application in mountain basins, *Hydrol. Process.*, *13*, 1935-1959, 1999.

Marks, D., and J. Dozier, Climate and energy exchange at the snow surface in the alpine region of the sierra nevada, 2. Snow cover energy balance, *Water Resour. Res.*, *28*, 3043-3054, 1992.

Morris, E. M., Physics-based models of snow, in *Recent Advances in the Modeling of Hydrologic Systems*, edited by D. S. Bowles and P. E. O'Connell, pp. 85-112, Kluwer Academic, Dordrecht, Netherlands, 1991.

Press, W. H., S. A. Teukolsky, W. T. Vetterling, and B. P. Flannery, *Numerical Recipes in FORTRAN: The Art of Scientific Computing*, Second Edition, Cambridge University Press, New York, 1992.

Price, A. G., and T. Dunne, Energy balance computations of snowmelt in a subarctic area, *Water Resour. Res.*, *12*, 686-694, 1976.

Satterlund, D. R., An improved equation for estimating long-wave radiation from the atmosphere, *Water Resour. Res.*, *15*, 1643-1650, 1979.

Seyfried, M. S., and B. P. Wilcox, Scale and the nature of spatial variability: Field examples having implications for hydrologic modeling, *Water Resour. Res.*, *31*, 173-184, 1995.

Sturm, M., and J. B. Johnson, Thermal conductivity measurements of depth hoar, *J. Geophys. Res.*, *97*, 2129-2139, 1992.

Tarboton, D. G., Measurement and modeling of snow energy balance and sublimation from snow, in *International Snow Science Workshop Proceedings*, pp. 260-279, Snowbird, Utah, 1994.

Tarboton, D. G., T. G. Chowdhury, and T. H. Jackson, A spatially distributed energy balance snowmelt model, in *Biogeochemistry of Seasonally Snow-Covered Catchments, Proceedings of a Boulder Symposium*, edited by K. A. Tonnessen, M. W. Williams and M. Tranter, pp. 141-155, IAHS Publ. no. 228, Boulder, Colo., 1995.

Tarboton, D. G., and C. H. Luce, Utah energy balance snow accumulation and melt model (UEB), computer model technical description and users guide, Utah Water Research Laboratory and USDA Forest Service Intermountain Research Station (http://www.engineering.usu.edu/dtarb/), 1996.

Warren, S. G., Optical properties of snow, *Rev. Geophys.*, *20*, 67-89, 1982.

Yen, Y.-C., The rate of temperature propagation in moist porous mediums with particular reference to snow, *J. Geophys. Res.*, *72*, 1283-1288, 1967.

Zuzel, J. F., and L. M. Cox, Ablation of isolated snowdrifts, in *Proceedings: Modeling of Snow Cover Runoff*, edited by S. C. Colbeck and M. Ray, pp. 135-143, US Army CRREL, Hanover, N.H., 1978.

CHAPTER 3

THE INFLUENCE OF THE SPATIAL DISTRIBUTION OF SNOW ON

BASIN-AVERAGED SNOWMELT[1]

Abstract:

Spatial variability in snow accumulation and melt due to topographic effects on solar radiation, snow drifting, air temperature, and precipitation is important in determining the timing of snowmelt releases. Precipitation and temperature effects related to topography affect snowpack variability at large scales and are generally included in models of hydrology in mountainous terrain. The effects of spatial variability in drifting and solar input are generally included only in distributed models at small scales. Previous research has demonstrated that snowpack patterns are not well reproduced when topography and drifting are ignored, implying that larger scale representations that ignore drifting could be in error. Detailed measurements of the spatial distribution of snow water equivalence within a small, intensively studied 26-ha watershed were used to validate a spatially distributed snowmelt model. These observations and model output were then compared to basin-averaged snowmelt rates from a single-point representation of the basin, a two-region representation that captures some of the variability in drifting and aspect, and a model with distributed terrain but

uniform drift. The model comparisons demonstrate that the lumped single-point representation and distributed terrain with uniform drift both yielded poor simulations of the basin-averaged surface water input rate. The two-point representation was a slight improvement, but the late season melt required for the observed streamflow was not simulated because the deepest drifts were not represented. These results imply that representing the effects of subgrid variability of snow drifting is equally or more important than representing subgrid variability in solar radiation.

INTRODUCTION

The spatial variability of snowmelt processes has received increasing attention in recent years (Blöschl *et al*., 1991; Kirnbauer *et al*., 1994). Varying precipitation input, drifting, and solar radiation intensity on sloping surfaces all relate to topography and contribute to the heterogeneity of surface water input from snowmelt (Seyfried and Wilcox, 1995; Tarboton *et al*., 1995). One of the more marked effects of spatially variable accumulation and melt is the effect on the timing of snowpack releases.

While the importance of topography in determining snow accumulation and melt has been well established, methods to represent the effects of topography on drifting have not been well explored. Several researchers have examined the detailed physics of snow transport under known wind fields (Tabler, 1975; Tabler and Schmidt, 1986; Pomeroy and Gray, 1995). Others have approached the problem through empirical means (Elder *et al*., 1989, 1991; Blöschl and Kirnbauer, 1992). Jackson (1994) and Tarboton *et al*. (1995) estimated drifting for a small watershed by calibrating a drifting parameter in an energy and mass balance snowmelt model at each grid cell. While this calibration

appears to be stable for the years at the site for which it was done, the relationships

between topography and drifting are not easily generalized. If the distributed drifting

cannot be calculated based on readily obtained spatial data, it becomes another of the

unknown or unknowable parameters in distributed models discussed by Beven (1996).

Because precise mapping of a drifting parameter may be difficult, a general

characterization of the effect through a subgrid parameterization for a larger scale model

may be more manageable. At 30-m grid resolution, drifting can be explicitly represented;

for larger model elements, only the net effect of drifting needs to be described. This

study addresses the question of what level of detail is necessary in representing

topography and spatial variability of snow drifting in distributed snowmelt modeling.

METHODS

Study area

The study was carried out using data from the Upper Sheep Creek subbasin of the

Reynolds Creek Experimental Watershed in southwestern Idaho, which enjoys a long and

rich history of hydrologic research (Stephenson and Freeze, 1974; Cooley, 1988; Duffy *et al*., 1991; Flerchinger *et al*., 1992; Flerchinger *et al*., 1994; Jackson, 1994; Seyfried and

Wilcox, 1995; Tarboton *et al*., 1995, among others). Much of the work has focused on

runoff generation mechanisms in the basin, concluding that groundwater flow through

layered basalts is the primary source of streamflow. All of the above studies have noted

the importance of the snowdrift that forms in the southwest portion of the basin in

contributing water during the period of greatest runoff. This background of previous

work measuring snow drifting (Cooley, 1988), a previously developed and calibrated

distributed hydrologic model (Jackson, 1994; Tarboton *et al*., 1995), and an

understanding of the basin's hydrology provide a good foundation from which to explore

the effects of the spatial distribution of snow on basin-averaged snowmelt.

The Upper Sheep Creek watershed has an area of 26 ha, with elevations between

1840 and 2040 m (Figure 3-1). Low sagebrush communities cover the northeast portion

of the basin, and big sagebrush communities cover most of the southwestern half of the

basin. Aspen grow in a narrow strip along the northeast-facing slope where the drifts

form (Figure 3-2). Severe winter weather and winds keep the aspen dwarfed to heights

between 4 and 7 m. Average annual precipitation is 508 mm, and the first-order stream

exiting the basin is ephemeral.

Study outline

We used distributed and lumped snowpack models to examine the ability of

simplified representations of spatial variability in topography and drifting to estimate

surface water input. Each of four simulations was considered as a hypothesis and

compared with distributed snow water equivalent measurements, such as those described

by Cooley (1988), and the timing of basin outflow through a weir. First, the fully

distributed snowmelt model was run with the distributed topography and distributed drift

factors reported in Jackson (1994) and Tarboton *et al*. (1995). This simulation was used

to check the validity of the snowmelt model and calculate the basin-averaged snowmelt
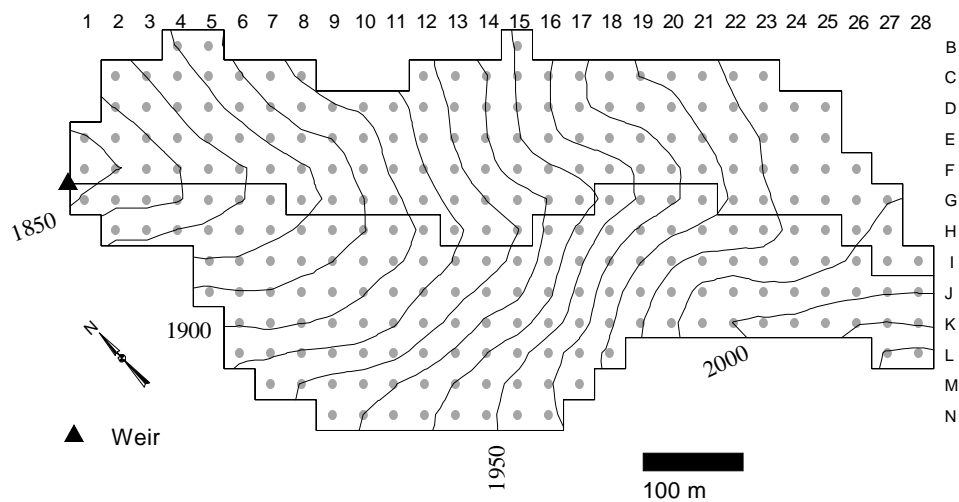
Figure 3-1. Map of Upper Sheep Creek with snow survey grid. Contour interval is 10 m. The area above the line separating the two halves of the watershed will be referred to as the northeast side later in the paper. The area below the line will be referred to as the southwest side
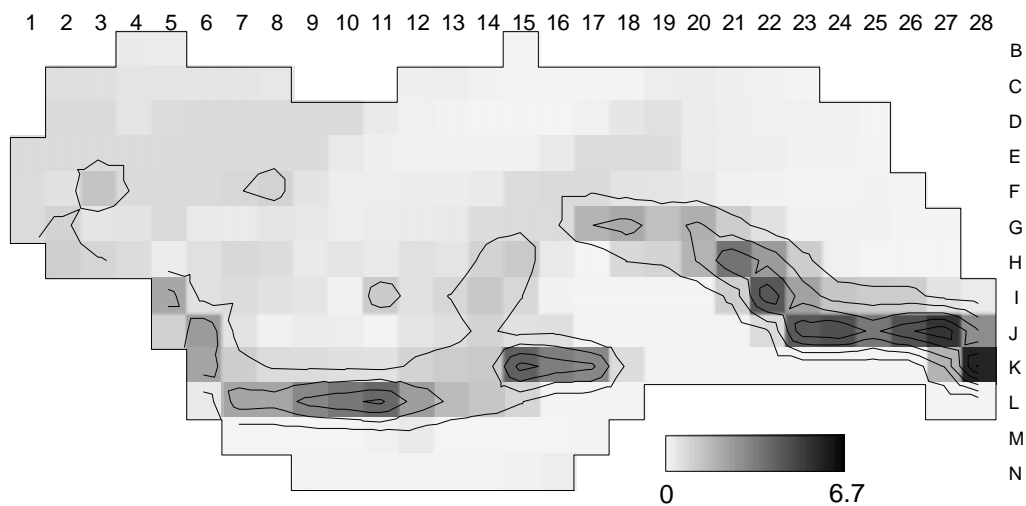
Figure 3-2. Map of drift multipliers used at Upper Sheep Creek (after Jackson, 1994)

flux for conditions approximating the actual conditions. The next two simulations were simplifications of that representation. From aerial photography and field observations, it is clear that drifting occurs primarily on shadowed, northeast-facing slopes, while sunnier, southwest-facing slopes are scoured by prevailing winds. This strong covariance in processes yields a shallow snowpack over time on southwest-facing slopes versus a deep snowpack over time on northeast-facing slopes and suggests that a division of the basin into a north basin and a south basin may yield some of the observed basin-wide behavior in snowpack distribution. This single division into two regions is a substantial simplification compared to the 255 cells used in the fully distributed model.

The second simplification treated the basin as a single unit with a single aspect, slope, and drift factor. This simulation was run to confirm that it gave a poor approximation to the data and to see where the two-region simplification fit between the fully lumped and fully distributed representations.

A final simulation examined the importance of the drift factor. In this simulation, the spatial variation in topography was preserved, but the drift factor was set to unity everywhere, removing the spatial variability due to drifting, but modeling the control that topography has over incident radiation.

Data collection

Measurements of snow water equivalent were taken on nine dates in 1993 with a snow tube and scale. A grid guided distributed sampling over the watershed (Figure 3-1). The spacing on the grid is 30.48 m (100 ft), and the long axis is oriented 48 degrees west of north. Precipitation, temperature, relative humidity, and incoming solar radiation were

measured for water year 1993 at a weather station near location J 10. Wind speed was

measured at D 3. Flow was measured at a weir at location F 0.

Model description

The snowmelt model is an energy and mass balance model with a vertically

lumped representation of the snowpack. It is more completely described in Tarboton and

Luce (1997). Two primary state variables are maintained in the model, snow water

equivalent, W [m], and internal energy of the snowpack and top 40 cm of soil, U [kJ m^{-2}].

U is zero when the snowpack is at 0°C and contains no liquid water. These two state

variables are updated according to

$$dU/dt = Q_{sn}+Q_{li}-Q_{le}+Q_p+Q_g+Q_h+Q_e-Q_m \tag{1}$$

$$dW/dt = P_r+P_s-M_r-E \tag{2}$$

where Q_{sn} is net solar radiation; Q_{li} is incoming longwave radiation; Q_{le} is outgoing

longwave radiation; Q_p is advected heat from precipitation; Q_g is ground heat flux; Q_h is

the sensible heat flux; Q_e is the latent heat flux; Q_m is heat advected with melt water; P_r is

the rate of precipitation as rain; P_s is the rate of precipitation as snow; M_r is the melt rate;

and E is the sublimation rate. The model is driven by inputs of precipitation, air

temperature, humidity, wind speed and incoming solar radiation. Snow surface

temperature, a key variable in calculating latent and sensible heat fluxes and outgoing

longwave radiation, is calculated from the snow surface energy balance, where incoming

and outgoing fluxes must match. These simulations were run on a 6-hour time step.

The effect of plant canopy on snowmelt is parameterized by decreasing the albedo of the snow surface as the snow depth decreases below the canopy height. This parameterization is most appropriate for short vegetation, such as sagebrush. Because the aspens are free of leaves until the soil warms slightly, errors introduced by not considering the taller canopy are minimal.

The distributed model runs the point model (described in the preceding two paragraphs) at each cell in the grid (Figure 3-1). The model uses a drift multiplier to estimate enhancement of local incoming snow through wind transport. The fraction of precipitation falling as rain or snow is a function of temperature. The fraction falling as snow is multiplied by the drift multiplier to estimate grid cell precipitation. The drift multiplier was calibrated from 1986 snow survey data from Upper Sheep Creek. Drift multipliers were adjusted at each grid cell to match the snow water equivalent on February 25 and March 26, 1986 (Jackson, 1994; Tarboton *et al*., 1995). Values of the multiplier over the basin are shown in Figure 3-2 (Jackson, 1994) and ranged from 0.2 to 6.8, with an average of 0.975. A value less than one indicates that the basin loses more snow to neighboring basins than it gains.

Distributed solar radiation was estimated based on pyranometer data at the weather station, which was used to calculate an effective atmospheric transmission factor. Local horizons, slope, and azimuth were used to find local sunrise and sunset times and to integrate solar radiation received on the slope during each time step. The calculated atmospheric transmission factor characterized cloudiness for incoming longwave radiation calculations.

Site characteristics used for the single-point and two-point representations of the basin are summarized in Table 3-1. For the single-point model, the average basin elevation and drift factor were used. Slope and aspect were calculated along the long axis of the basin to estimate the lumped basin behavior. For the two-point model, representative cells were picked for the northeast and southwest sides of the basin to set slope, aspect, and elevation. Each point was assigned an average drift factor for the region it represented.

RESULTS

Maps of observed snow water equivalent over Upper Sheep Creek watershed are shown in Figure 3-3a. The effect of drifting in concentrating snow, and, consequently, late season snow water equivalent along the southwest side of the basin is evident. Maps of modeled snow water equivalent with the fully distributed snowmelt model (Figure 3-3b) show a generally similar pattern. Table 3-2 lists the basin-averaged snow water equivalent from the observations and the model, showing that the fully distributed model tends to overestimate snow water equivalent in the early melt season and slightly underestimate snow water equivalent in the late melt. Plotting observed against modeled data for each date (Figure 3-4) shows that the fully distributed model overestimates snow water equivalent for locations with moderate to high snow water equivalents, but underestimates snow cover where there is little snow, with systematic overestimation most apparent in the early melt season. The correlation coefficient (Pearson's r) and a measure of fit to the 1:1 line (Wilmott, 1981;Wilmott *et al.*, 1985) are given in Table 3-3.

Table 3-1. Effective site characteristics for single-point and two-point

representations of the basin

	Single-point representation	Northeast side	Southwest side
Slope	0.159	0.286	0.345
Aspect	312°	299°	357°
Drift Factor	0.975	0.62	1.29
Elevation	1925 m	1912 m	1939 m
Relative Area	100%	47%	53%

Table 3-2. Basin-averaged snow water equivalent (m) from observations and models

Date	Observed	Model with drift	Model no drift
Feb 10	0.22	0.28	0.28
Mar 3	0.28	0.38	0.39
Mar 23	0.23	0.23	0.10
Apr 8	0.18	0.16	0.00
Apr 15	0.17	0.16	0.00
Apr 29	0.13	0.13	0.00
May 12	0.09	0.07	0.00
May 19	0.04	0.03	0.00
May 25	0.02	0.01	0.00

Table 3-3. Agreement between modeled and measured images

Date	Pearson's r	Willmott's d
Feb 10	0.83	0.90
Mar 3	0.84	0.90
Mar 23	0.90	0.94
Apr 8	0.88	0.93
Apr 15	0.89	0.94
Apr 29	0.89	0.94
May 12	0.90	0.94
May 19	0.87	0.92
May 25	0.65	0.76
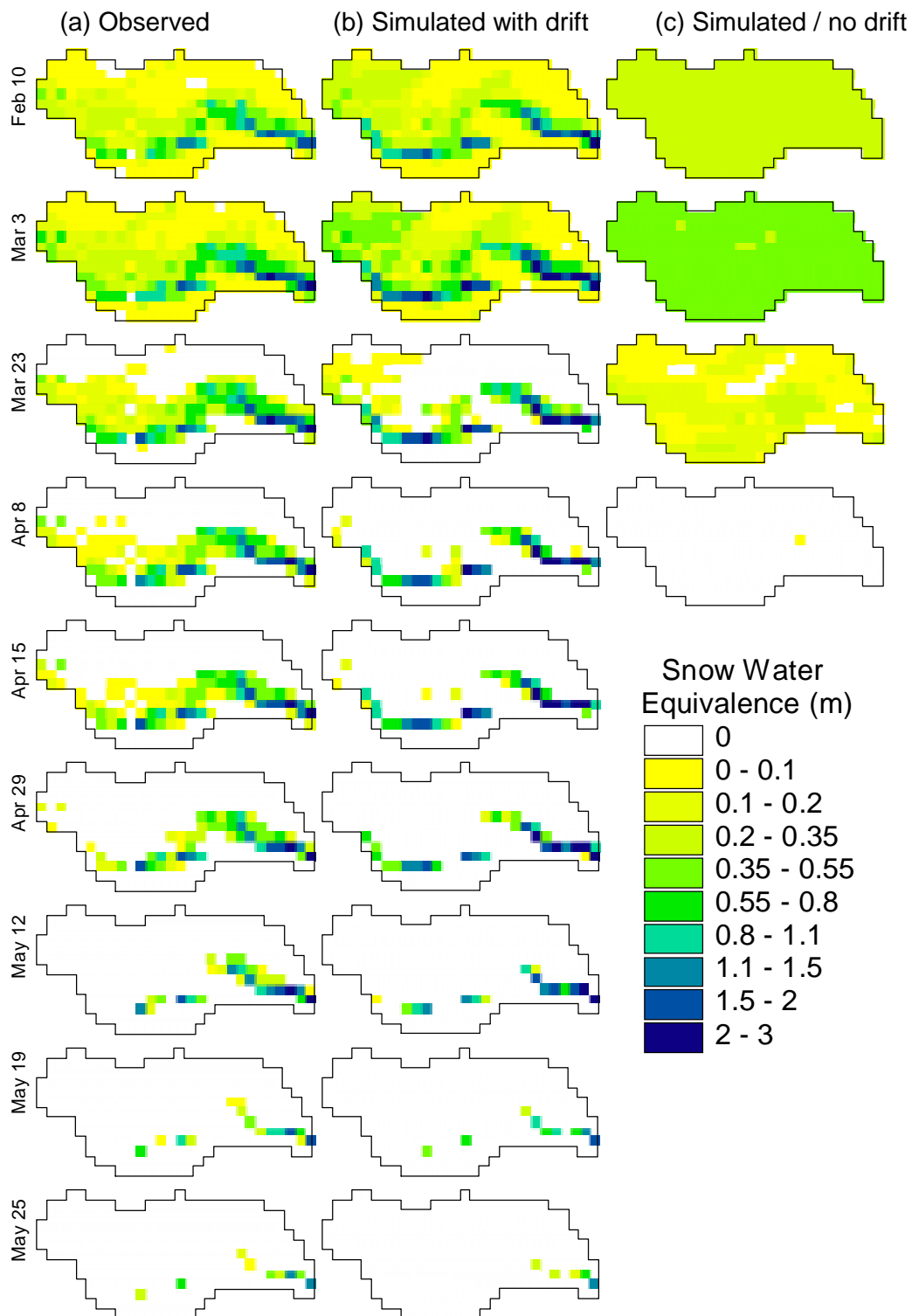
Figure 3-3. Snow water equivalence mapped over the basin on nine dates of snow survey in 1993 for: (a) observed, (b) modeled with spatially varying drift factor, and (c) modeled with uniform drift factor. No snow modeled after April 8 with uniform drift factor
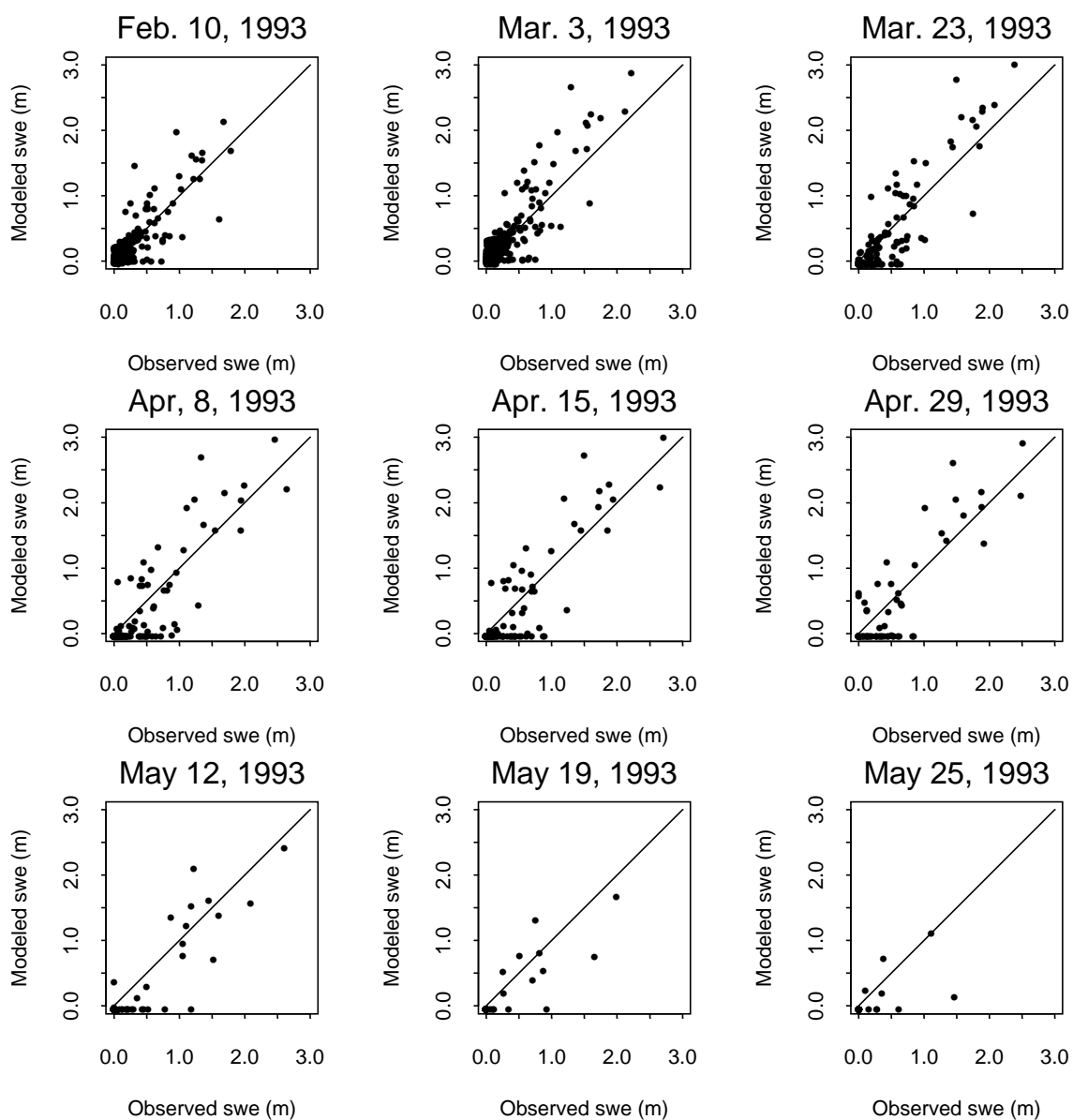
Figure 3-4. Comparison of observed and modeled snow water equivalent for each snow survey date. The line through each plot is the 1:1 line

It should be noted that there is a degree of spatial autocorrelation, the structure of which

is not exactly known. The goodness of fit implied by the r values may therefore be

somewhat overstated. These results, obtained with multipliers calibrated using 1986

measurements (Jackson, 1994), show drifting patterns that compare favorably with 1993

observations, suggesting consistency in drifting from year to year.

A comparison of the predictions of the distributed model using a uniform drift

factor over the basin (Figure 3-3c) to the observed data (Figure 3-3a), shows that drifting

is an important process in creating variability in snow water equivalence across the basin

and in determining the timing of melt outflows. Differences in melt caused by

differences in solar radiation and temperature across the basin are not great enough to

explain the spatial patterns of snow water equivalent values over the basin. The snow

water equivalent modeled in this manner shows considerably less variability than that

measured or modeled with spatially varying drift factor. Consequently, all cells in the

basin become snow-free almost simultaneously, and the persistence of the snowpack in

the basin is dramatically reduced relative to observations. This result implies that spatial

variability in snow drifting has a greater effect on the behavior of Upper Sheep Creek

than spatial variability in solar radiation and temperature.

As an additional check on the behavior of the fully distributed model, we also

compared modeled and measured surface water inputs (snowmelt plus rain) averaged

over the period between snow water equivalent measurements. Cumulative surface water

input and sublimation from the snowpack (loss) can be calculated as the measured

cumulative precipitation less the measured snow water equivalent on a particular date.

The average loss rate for the periods between measurements was then calculated from the

cumulative values. Figure 3-5 shows the average snow loss rate based on the

measurements and on the fully distributed model plotted over time. Before the melt
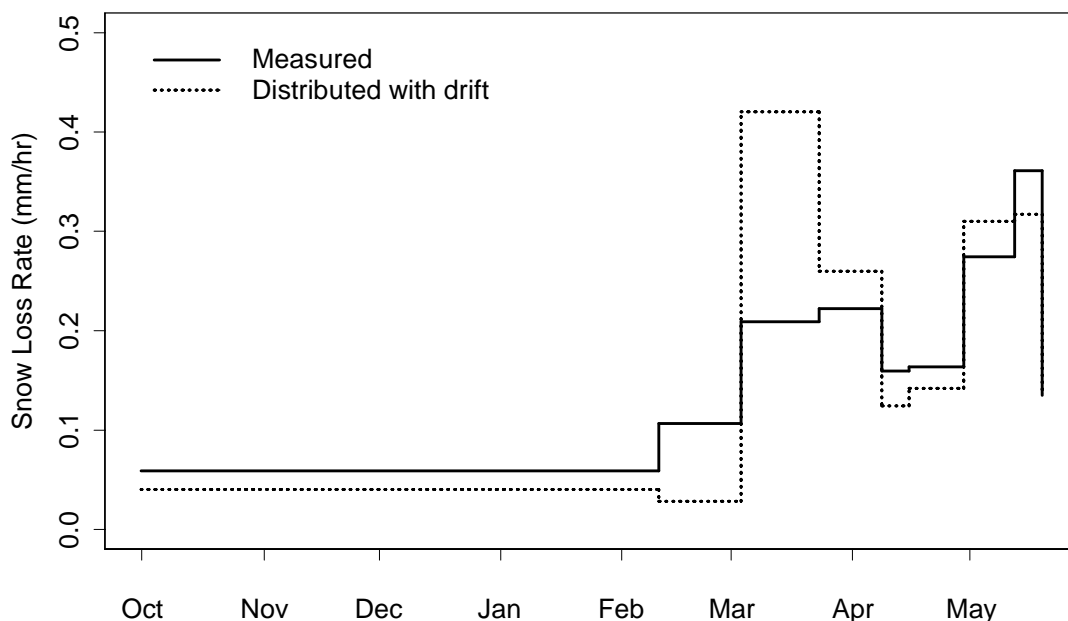
Figure 3-5. Measured average loss rate and modeled loss rate over time. Losses are the sum of melt and sublimation

season begins, the measured rates are slightly greater. During the second measurement interval (February 10 to March 3), the fully distributed model lost less snow, which increased the error in snow water equivalent seen on March 3 in Table 3-2. During the next measurement interval, the model overpredicted losses, mostly as melt. From Figure 3-3, it appears that much of the difference is in the south facing part of the basin, which has low snow water equivalents. The model shows buildup and loss of snow in this area, while the measurements indicate that perhaps no accumulation occurred.

Figure 3-6 shows the calculated basin-averaged surface water input rate versus modeled basin-averaged surface water input rate for the four models (fully distributed, single-point, two-regions, distributed without drifting). To prepare Figure 3-6, we subtracted the modeled sublimation from the measured loss rate to estimate the

Distributed with Drift

Two Regions

Single Point

Distributed No Drift
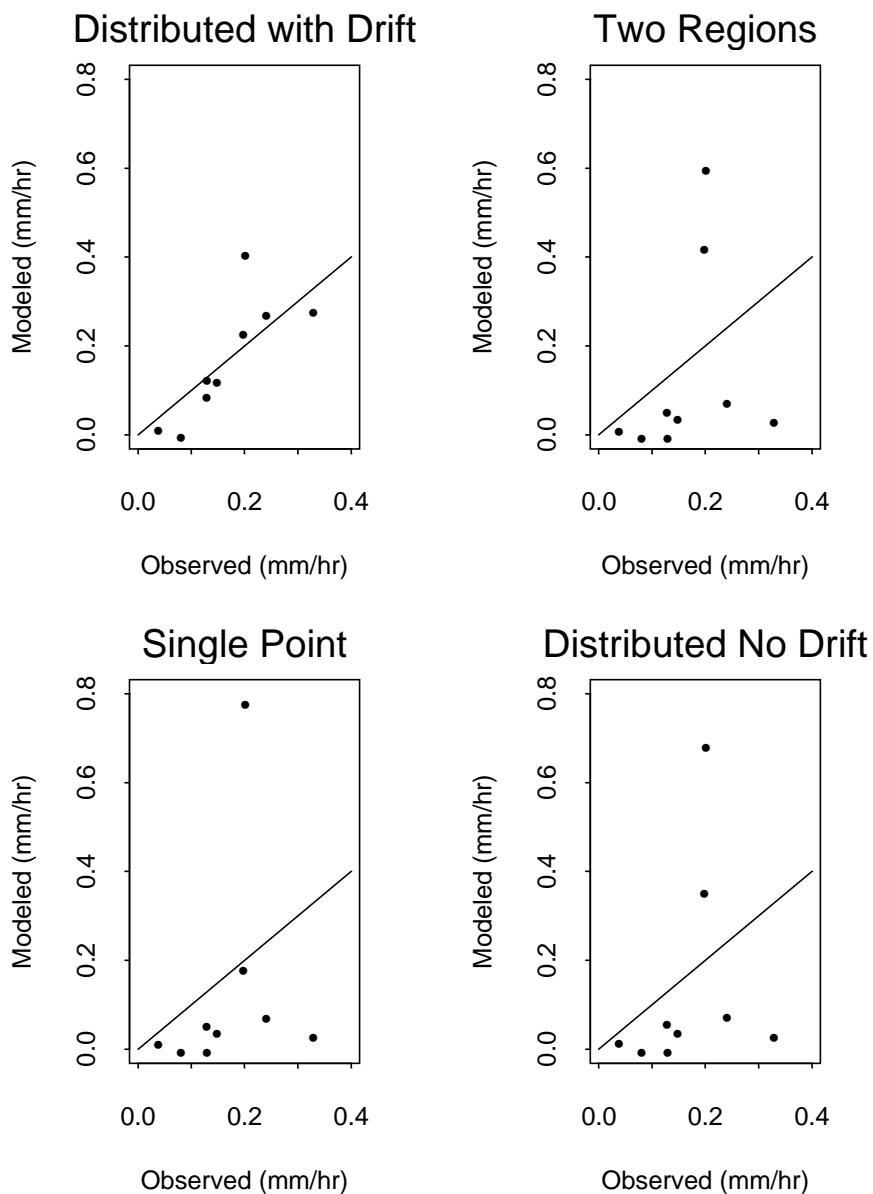
Figure 3-6. Observed and modeled average surface water input rate for the nine periods defined by the nine snow water equivalent measurements and the beginning of the water year (no snow)

"measured" surface water input rate. Because sublimation is small relative to melt during the melt season, this is a very small correction. A striking feature of Figure 3-6 is how well the distributed model with drifting performs except for one measurement period

(March 3 to 23), where the surface water input is substantially overpredicted. The other

models show poor comparisons between measured and modeled surface water input rates.

These results suggest that the basin-averaged surface water input rates from the fully

distributed model, which includes snow drifting, are reasonably representative of the

actual surface water input rates experienced by the basin during the late melt season.

They also show that the alternative models considered in this study give poor predictions

of melt outflow rates.

Streamflow is a second source of evidence that can be used qualitatively to come

to the same conclusion that of the four models examined, only the fully distributed model

gives reasonable estimates of snowpack outflow. Flerchinger *et al.* (1992) provide a

conceptual model of runoff generation in the basin, suggesting that early melt primarily

serves to recharge the groundwater while later melt generates streamflow through a

groundwater response. During average snow years (such as 1993), they found response

times through a confined aquifer on the order of 3-5 days. From the cumulative modeled

surface water inputs over water year 1993 and the cumulative streamflow (Figure 3-7), it

can be seen that the timing of basin-averaged surface water input rates for the three

simplified models differs from that of the fully distributed model. Very little surface

water input (flat line) is predicted by the simplified models during the period of greatest

streamflow (steep line), while the fully distributed model is still predicting substantial

outflow during that time period (steep line). Timing is a little easier to compare precisely

in Figure 3-8, from which the same conclusion may be drawn. Comparison to Figure 3-7

shows that the brief spikes in surface water input predicted by the three simplified models
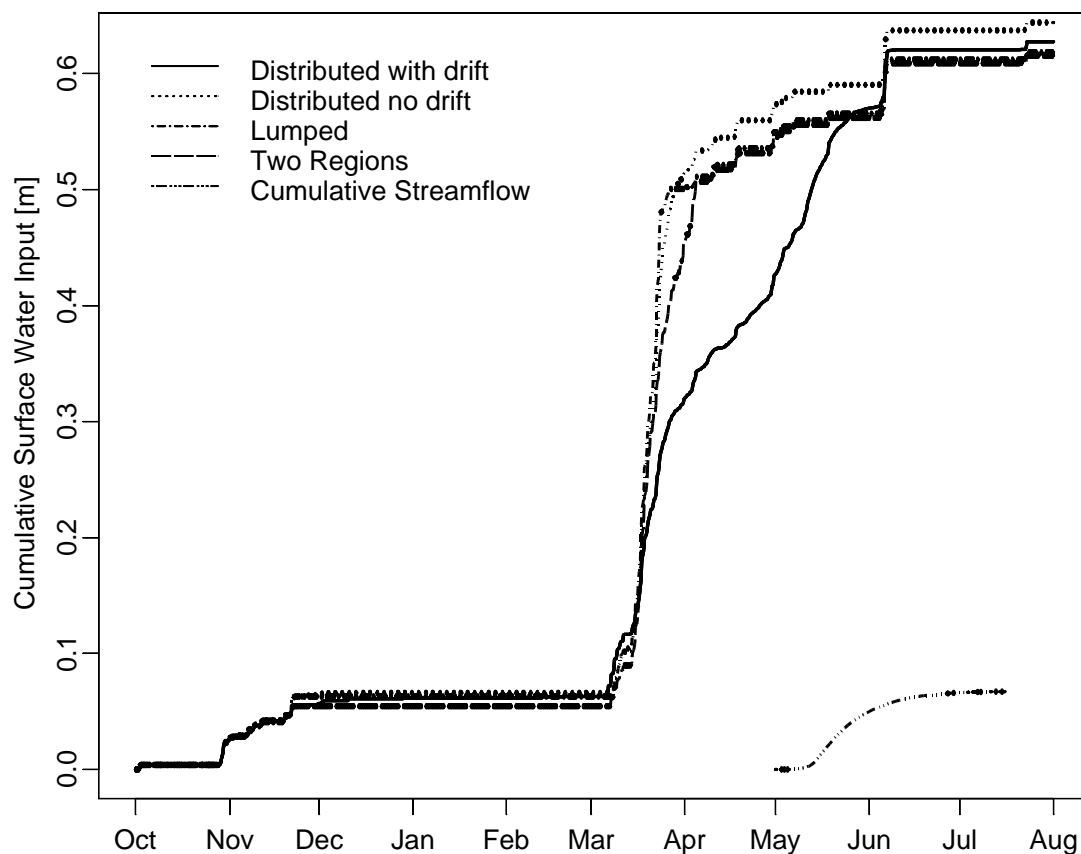
Figure 3-7. Cumulative surface water input for each of the four models and cumulative streamflow for the period October 1992 to July 1993

after mid-April (rainfall) represent little water. The fully distributed model is the only

model that predicts significant melt late in the season, coinciding in timing with the

observed rise of the streamflow hydrograph. The other models show surface water inputs

concentrated almost entirely in the month of March, which is an unlikely source of water

for peak streamflow in May.
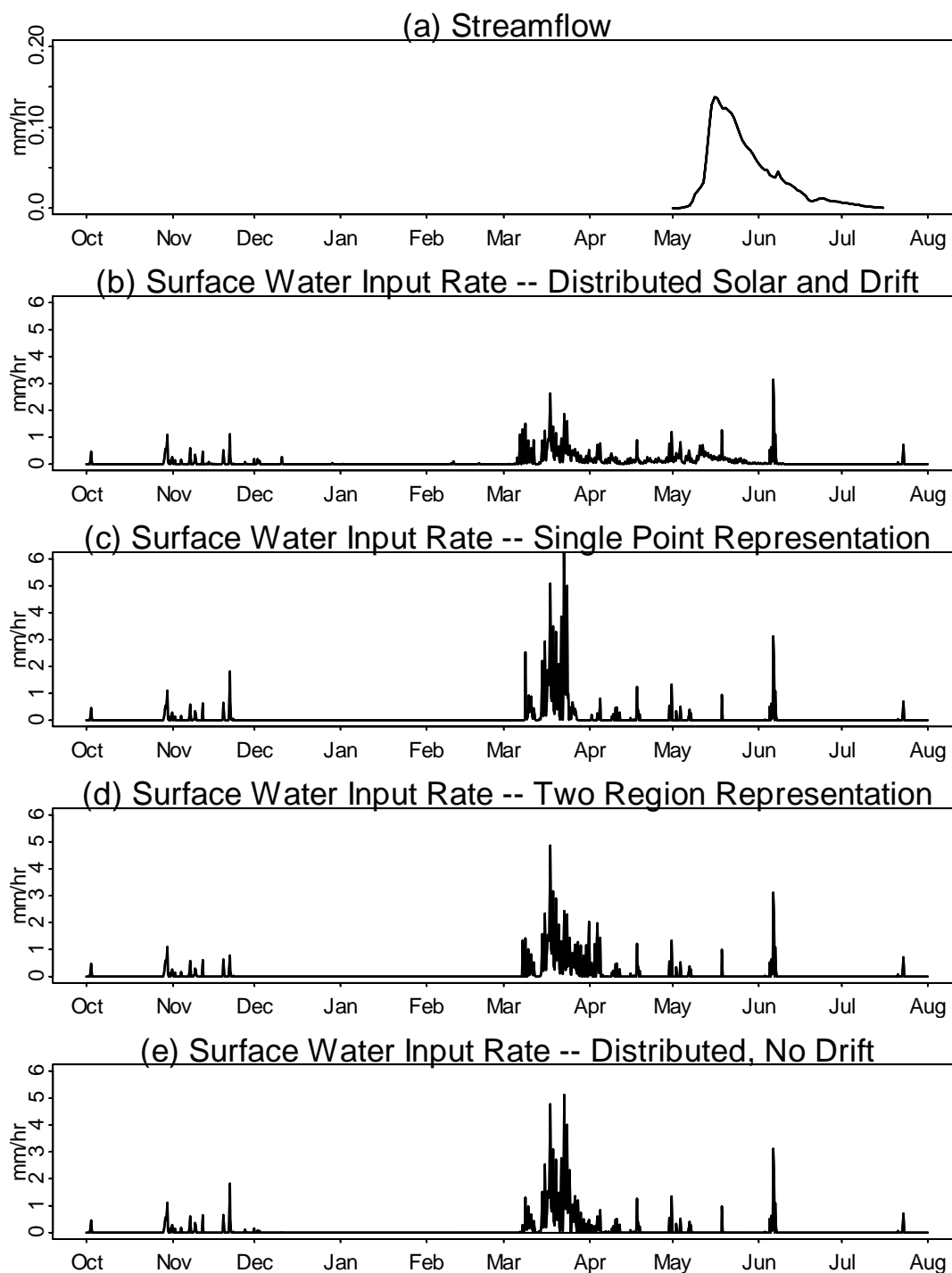
Figure 3-8. Surface water inputs from snowmelt and basin outflow for the period October 1992 to July 1993. (a) Observed streamflow, (b) Distributed model with drift multipliers. (c)Lumped model, (d) Two-region model, and (e) Distributed model with no drift multipliers

DISCUSSION AND CONCLUSIONS

In semi-arid mountainous watersheds such as Upper Sheep Creek, wind plays a large role in redistributing snow, and the spatial variability and pattern of snow water equivalent is highly dependent on wind-induced drifting. Deep snowdrifts provide melt water into late spring. Using detailed snow water equivalent measurements and distributed snowpack modeling, we examined the effects of spatial variability of snow accumulations on snowmelt processes at the scale of a small watershed (~ 400 m across). We found that representing basin snowmelt as a single point yields inaccurate results. Using two regions with contrasting drifting and solar input to represent the basin improves the simulations little. We also examined the relative contribution of solar input and drifting to the observed spatial patterns of snow water equivalent and the temporal patterns of surface water input. Our results show that detailed snow drifting information, which may be difficult to obtain, is equally or perhaps more important than modeling the effects of local topography on radiation.

This examination relied heavily on a distributed snowpack model for reference, and some effort has been made to test how appropriate the model is for this basin. Comparisons of measured and modeled patterns of snow water equivalent on each measurement date showed reasonable agreement. The model showed some bias towards overestimation of snow water equivalent in the early melt season with better agreement in the middle and late melt season. Surface water input was slightly underestimated throughout the accumulation season, and overestimated in the early melt season. By mid to late melt season, there is generally better agreement in surface water input rates. From

the maps in Figure 3-3, it appears that much of the discrepancy centers on the southwest-facing slope. Because of the generally low snow water equivalents on these slopes, it is likely that the calibration using 1986 data resulted in poor estimates of the drift factor. Alternatively, the drifting here may have been inconsistent between the 1986 and 1993 snow seasons. This source of error demonstrates how sensitive timing of basin snowmelt is to estimates of distributed drifting and how difficult those estimates are to obtain. Between the time the snow on the southwest-facing slope melted and the end of May, distributed model snow water equivalent and melt rates compared favorably to measurements. During this time period, melt from the much deeper drifts on the northeast-facing slopes contributed most of the surface water inputs. These deeper drifts are caused by prevailing winds and are probably much more consistent from year to year as indicated by the noted correlation between vegetation patterns and drift patterns in Upper Sheep Creek (Flerchinger *et al.*, 1994).

Snowmelt modeling at the catchment scale is generally done as a part of water balance modeling. There is some question as to whether potential errors in drifting, such as those found in the distributed snowmelt model, would propagate through to runoff generation estimates. In Figure 3-8, the fully distributed model shows a peak basin-wide surface water input rate during March. From Figure 3-5, we know that the surface water input rates predicted by the fully distributed model in Figure 3-8 are about twice what they should be during March. Because runoff in this basin occurs from sustained input to the small portion of the basin under the largest drifts (Stephenson and Freeze, 1974), it is unlikely that the relatively small depth of melt modeled on the southwest-facing slope,

where the errors appeared to be the greatest, would appear as runoff. Errors in this area

of the basin would most likely be manifested as errors in evapotranspiration. The

concentrated surface input under the drifts, up to 3 m over the melt season, yields most of

the runoff through subsurface flow (Flerchinger *et al*., 1992) and saturation overland

flow, suggesting that errors in the amount of snow drifting over the area of the deep drifts

could be translated directly into errors in runoff.

Accurate estimates of snow drifting in a basin are difficult to obtain, but they are

important to the prediction of basin snowmelt. Errors in estimates of both basin-wide

evapotranspiration and basin runoff may occur from errors in estimates of snow drifting

when using a distributed hydrology model. An integrated or "lumped" representation of

the basin snowpack is one way to avoid this problem when only basin-averaged

information is desired. None of the lumped representations used in this study included a

subgrid parameterization that adequately represented the effects of drifting, and

consequently none provided a reasonable simulation of melt water inputs to the basin.

An important challenge lies in finding a subgrid parameterization that addresses this

important source of spatial variability in snow water equivalent. A bigger challenge may

lie in relating the basin-wide surface water input rate to runoff generation processes that

are spatially dependent on drifting.

REFERENCES

Beven, K. J. 1996. 'A discussion of distributed hydrological modelling', in Abbott, M. B.
  and . Refsgaard, J. C. (eds), *Distributed Hydrological Modelling*. Kluwer Academic
  Publishers, Netherlands, pp. 255-278.

Blöschl, G., Gutknecht, D., and Kirnbauer, R. 1991. 'Distributed snowmelt simulations in an alpine catchment. 2. Parameter study and model predictions', *Wat. Resour. Res.,* **27**, 3181-3188.

Blöschl, G., and Kirnbauer, R. 1992. 'An analysis of snow cover patterns in a small alpine catchment', *Hydrol. Process.*, **6**, 99-109.

Cooley, K. R. 1988. 'Snowpack variability on western rangelands', *Western Snow Conference Proceedings*, *Kalispell, Montana, April 18-20, 1988*. pp. 1-12.

Duffy, C. J., Cooley, K. R., Mock, N., and Lee, D. 1991. 'Self-affine scaling and subsurface response to snowmelt in steep terrain', *J. Hydrol.*, **123**, 395-414.

Elder, K., Dozier, J., and Michaelsen, J. 1989. 'Spatial and temporal variation of net snow accumulationn in a small alpine watershed, Emerald Lake basin, Sierra Nevada, California, U.S.A.', *Ann. Glaciol.,* **13,** 56-63.

Elder, K., Dozier, J., and Michaelsen, J. 1991. 'Snow accumulation and distribution in an alpine watershed', *Wat. Resour. Res.* **27**, 1541-1552.

Flerchinger, G. N., Cooley, K. R., Hanson, C. L., Seyfried, M. S., and Wight, J. R. 1994. 'A lumped parameter water balance of a semi-arid watershed', *American Society of Agricultural Engineering Paper No. 94-2133*, International Summer Meeting of the ASAE, June 19-22, Kansas City, Missouri. American Society of Agricultural Engineering, St. Joseph.

Flerchinger, G. N., K. R. Cooley, and D.R. Ralston. 1992. Groundwater response to snowmelt in a mountainous watershed. *Journal of Hydrology*, **133**, 293-311.

Jackson, T.H.R. 1994. 'A spatially distributed snowmelt-driven hydrologic model applied to Upper Sheep Creek', *Ph.D. Thesis*, Utah State University, Logan, Utah.

Kirnbauer, R., Blöschl, G., and Gutknecht, D. 1994. 'Entering the era of distributed snow models', *Nord. Hydrol.*, **25**, 1-24.

Pomeroy, J. W. and Gray, D. M. 1995. '*Snowcover: Accumulation, Relocation and Management*'. National Hydrology Research Institute Science Report No. 7. NHRI, Saskatoon, Saskatchewan, Canada. 144 p.

Seyfried, M. S. and Wilcox, B. P. 1995. 'Scale and the nature of spatial variability: Field examples having implications for hydrologic modeling', *Wat. Resour. Res.*, **31**, 173-184.

Stephenson, G. R. and Freeze, R. A. 1974. 'Mathematical simulation of subsurface flow contributions to snowmelt runoff, Reynolds Creek watershed, Idaho', *Wat. Resour. Res.*, **10**, 284-294.

Tabler, R. D. 1975. 'Estimating the transport and evaporation of blowing snow', In: *Snow Management on Great Plains Symposium, Bismark North Dakota, July 1975*. Great Plains Agricultural Council, University of Nebraska, Lincoln, Nebraska. pp. 85-104.

Tabler, R. D. and Schmidt, R. A. 1986. 'Snow erosion, transport and deposition, in relation to Agriculture.' In: *Snow Management on Great Plains Symposium, Saskatchewan, July 1985*. Great Plains Agricultural Council, University of Nebraska, Lincoln, Nebraska. pp. 12-58.

Tarboton, D. G. and Luce, C. H. 1997. *Utah Energy Balance Snow Accumulation and Melt Model (UEB), Computer Model Technical Description and Users Guide*. Utah Water Research Laboratory, Logan, Utah.

Tarboton, D.G., Chowdhury, T. G., and Jackson, T. H. 1995. 'A spatially distributed energy balance snowmelt model', in: Tonnessen, K. A., Williams, M. W., and Tranter, M. (eds), *Biogeochemistry of Seasonally Snow-Covered Catchments, Proceedings of a Boulder Symposium, July 3-13*, IAHS Publ., **228**, 141-155.

Wilmott, C. J. 1981. 'On the evaluation of model performance in physical geography', in Gaile, G. L. and Willmott, C. J. (eds), *Spatial Statistics and Models*, D. Reidel Publishing Company, pp. 443-460.

Wilmott, C. J., Ackleson, S. G., Davis, R. E., Feddema, J.J., Klink, K. M., Legates, D. R., O'Donnel, J., and Rowe, C. M. 1985. 'Statistics for the evaluation and comparison of models', *J. Geophys. Res.,* **90**, 8995-9005.

CHAPTER 4

SUBGRID PARAMETERIZATION OF SNOW DISTRIBUTION FOR AN ENERGY AND MASS BALANCE SNOW COVER MODEL[1]

Abstract:

Representation of sub-element scale variability in snow accumulation and ablation is increasingly recognized as important in distributed hydrologic modeling. Representing subgrid scale variability may be accomplished through numerical integration of a nested grid or through a lumped modeling approach. We present a physically based model of the lumped snowpack mass and energy balance applied to a 26-ha rangeland catchment with high spatial variability in snow accumulation and melt. Model state variables are snow-covered area average snow energy content (U), the basin-average snow water equivalence (W_a), and snow-covered area fraction (A_f). The energy state variable is evolved through an energy balance. The snow water equivalence state variable is evolved through a mass balance, and the area state variable is updated according to an empirically derived relationship, $A_f(W_a)$, that is similar in nature to depletion curves used in existing empirical basin snowmelt models. As snow accumulates, the snow-covered area increases rapidly. As the snowpack ablates, A_f decreases as W_a decreases. This paper shows how the relationship $A_f(W_a)$ for the melt

season can be estimated from the distribution of snow water equivalence at peak accumulation in the area being modeled. We show that the depletion curve estimated from the snow distribution at peak accumulation in the Upper Sheep Creek subbasin of Reynolds Creek Experimental Watershed compares well against the observed depletion data as well as modeled depletion data from an explicit spatially distributed energy balance model. Comparisons of basin average snow water equivalence between the lumped model and spatially distributed model show good agreement. Comparisons to observed snow water equivalence show poorer but still reasonable agreement. The subgrid parameterization is easily portable to other physically based point snowmelt models. It has potential application for use in hydrologic and climate models covering large areas with large model elements, where a computationally inexpensive parameterization of subgrid snow processes may be important.

INTRODUCTION

Within the last 20 years, interest in scaling has increased within the hydrologic research community. The increase in interest has been driven in part by a desire to apply physically based hydrologic models to catchments and global circulation model (GCM) grid cells. Snowmelt has been an important hydrologic process examined with respect to scaling. In mountainous regions, snowmelt is one of the largest surface water inputs controlling runoff. Snow cover affects the atmosphere through its strong influence on the surface radiation and energy balance.

At the catchment and GCM scale, interest lies in determining the effects of changing land use. Some of the interest of atmospheric modelers relates to the effects of

changing climate. Therefore, empirical hydrologic models may not be useful at these larger scales (Seyfried and Wilcox, 1995). Empirical models require calibration under particular conditions. If land use or general climate conditions change, the correlations may not necessarily be the same. Physically based models use parameters that are, at least in principle, related to physical conditions and can sometimes be measured.

Physically based models tend to have a foundation in point-scale research. Much research of snowmelt processes has been conducted at the plot or point scale (Hathaway *et al*., 1956; Anderson, 1976; Morris, 1986, 1990; Jordan, 1991; Tarboton *et al*., 1995; Tarboton and Luce, 1996). Point scale models are often not applicable for larger areas even using effective parameters calibrated for the catchment (Arola and Lettenmaier, 1996; Luce *et al*., 1997, 1998). Snowmelt shares this characteristic with other hydrologic processes (Beven, 1995; Kalma and Sivapalan, 1995). Generalized solutions available to solve the problem are numerical integration (Abbott and Refsgaard, 1996), spatial distribution functions (Moore, 1985), and parameterizations (Beven, 1995; Blöschl, 1996).

For snowmelt, several solutions have been applied. Numerical integration has been and continues to be a popular method through use of distributed hydrologic models (Blöschl *et al*., 1991; Wigmosta *et al*., 1994; Kirnbauer *et al*., 1994; Liston, 1997). The distribution function approach has also been applied to create lumped models (Horne and Kavvas, 1997; Anderson, 1973; Rango and Van Katwijk, 1990; Martinec *et al*., 1994). The areal depletion curve concept, which amounts to a distribution function approach, has been applied to empirical models including the National Weather Service River Forecasting System (NWSRFS) and the Snowmelt Runoff Model (Martinec *et al*., 1994).

This approach can be adopted into a physically based modeling framework by

developing a relationship between the state variable of interest, snow water equivalence

over the basin, and the areal extent of snowcover. This is similar to the approach of

TOPMODEL (Beven and Kirkby, 1979) where saturated area is estimated as a function

of the basin-averaged stored water. In TOPMODEL, the parameterization relating the

stored water state variable to the saturated area is derived based on an analysis of the

topography. With the lumped snowmelt model, the parameterization relating the basin-

averaged snow water equivalence state variable to the fractional snow coverage is derived

based on a probability distribution/density function (pdf) of peak snow water

equivalence. Other remote sensing and modeling tools (Elder *et al*., 1989, 1991, 1995,

1998; Elder, 1995; Rosenthal and Dozier, 1996) may be used to relate topography to the

pdf of peak snow water equivalence.

The objectives of this paper are to present and test a physically based lumped

model of snowpack evolution for a small watershed (26 ha) that uses a depletion curve

parameterization to relate the basin-averaged snow water equivalence to snow-covered

area. A secondary purpose is to present a method for deriving the depletion curve from

snowpack measurements at peak accumulation. This is part of an ongoing effort to

extend physically based modeling methodology to larger scales where it is impractical to

apply a point model over a grid of model elements small enough to ignore subgrid

variability.

METHODS

The basic approach of this study compared the outputs of the lumped model to outputs from a distributed snowmelt model and a series of distributed snow water equivalence observations. The lumped model treats the study area (26 ha) as a single model element with subgrid variability parameterized through a depletion curve. The distributed model was applied at a 30-m grid scale ignoring only subgrid variability smaller than this scale and amounts to a numerical integration of the spatially distributed processes that are parameterized in the lumped model. The depletion curve parameterization used for the lumped simulation was derived from observations of the snow water equivalence pattern near the time of peak accumulation. This depletion curve was compared to that derived from the series of distributed observations and from the output of the distributed model.

Study area and observations

Snow survey and climatological data from the Upper Sheep Creek subbasin of the Reynolds Creek Experimental Watershed in southwestern Idaho (Figure 4-1) form the observational basis of this study. The Upper Sheep Creek watershed has an area of 26 ha and ranges between 1840 and 2040 m elevation (Figure 4-2). Low sagebrush (*Artemisia arbuscula* Nutt.) communities cover the northeast portion of the basin, and big sagebrush (*Artemisia tridentata* Nutt.) communities cover much of the southwestern half of the basin. Aspen (*Populus tremuloides* Michx.) grow in a narrow strip along the northeast-facing slope where snow drifts typically form (Figure 4-3). Severe winter weather and

Figure 4-1. Map of northwestern United States showing approximate region of study watershed
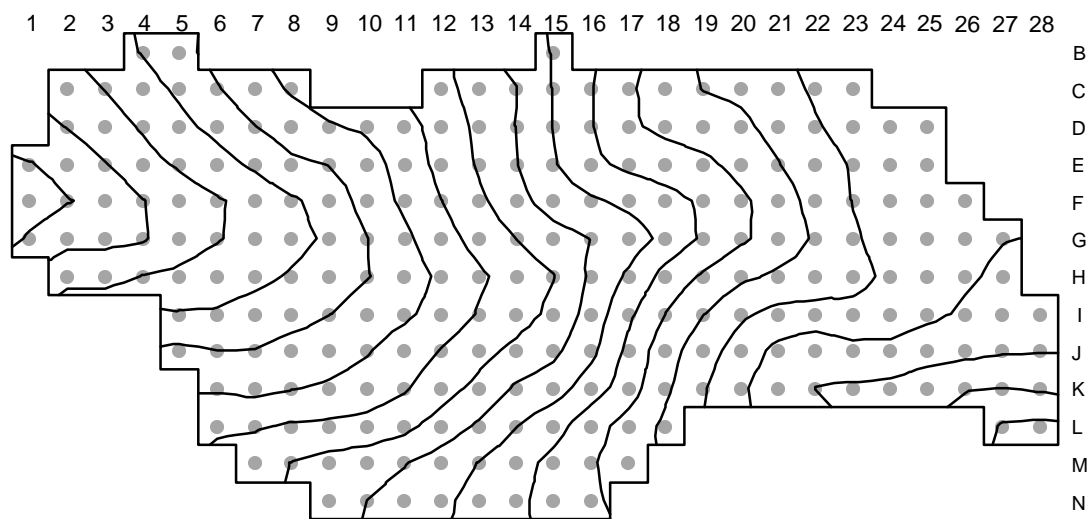
Figure 4-2. Map of Upper Sheep Creek snow survey grid with 10-m elevation contours
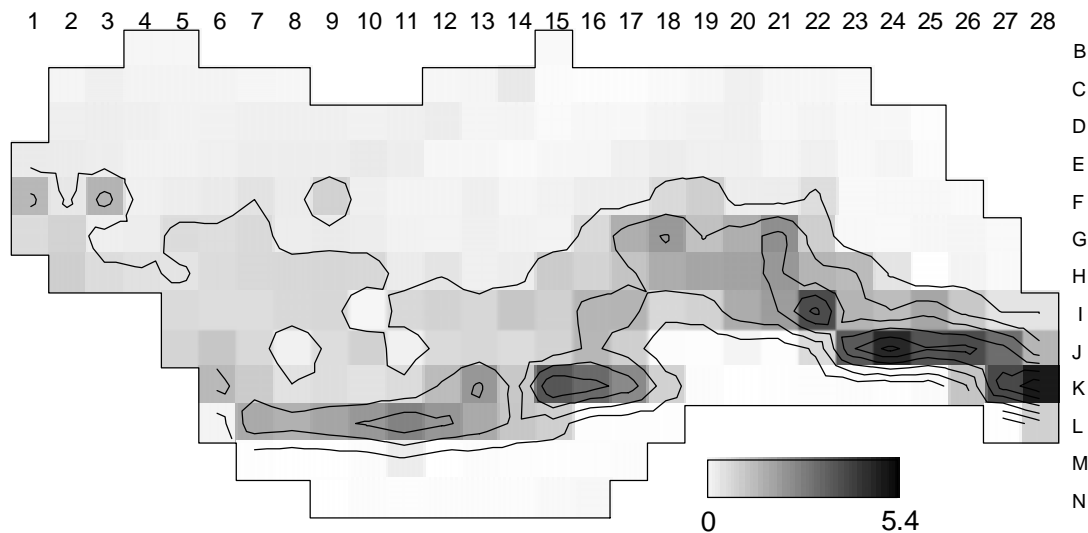
Figure 4-3. Map of drift factors calibrated at Upper Sheep Creek based on 1993 observations. Darker areas are areas of greater snow accumulation and greater drift factor values. Contour interval is 0.8

winds prevent the aspen from growing to heights greater than 4-7 m. Average annual precipitation is 508 mm, and the first-order stream exiting the basin is ephemeral.

Upper Sheep Creek has been the site of many previous hydrologic investigations (Stephenson and Freeze, 1974; Cooley, 1988; Duffy *et al.*, 1991; Flerchinger *et al.*, 1992, 1994; Jackson, 1994; Seyfried and Wilcox, 1995; Tarboton *et al.*, 1995; Luce *et al.*, 1997, 1998; among others). Runoff generation has been the focus of much of the work, and all of the studies have noted the importance of the wind-induced snowdrift in the southwest portion of the basin to the basin hydrology. Previous work (Luce *et al.*, 1997, 1998) has shown that snow drifting is the primary determinant of spatial variability of snow in this watershed, more important than topographically induced variations of radiation. Previous work measuring snow drifting (Cooley, 1988) and distributed snowmelt modeling (Jackson, 1994; Tarboton *et al.*, 1995; Luce *et al.*, 1997, 1998) has provided both foundation and incentive for development of a lumped snowmelt model of the basin that

parameterizes the subgrid variability due to snow drifting and spatially variable

radiation processes.

The data used in this paper comprise measurements of snow water equivalence

taken on nine dates in 1993 with a snow tube and scale. A systematic grid sampling

strategy was used throughout the watershed (Figure 4-2). The grid spacing was 30.48 m

(100 ft), and the long axis was oriented 48 degrees west of north. Precipitation,

temperature, relative humidity, and incoming solar radiation were measured for water

year 1993 at a weather station near location J 10. Wind speed was measured at D 3.

Distributed point model

The distributed model is a cell-by-cell execution of the Utah Energy Balance

(UEB) snowpack energy and mass balance model (Tarboton *et al*., 1995; Tarboton and

Luce, 1996). In order to run the model in a distributed fashion, climatic inputs (radiation

and precipitation) were calculated individually for each cell based on measurements from

the weather station, topography, and a calibrated drift factor.

UEB is an energy and mass balance model with a vertically lumped representation

of the snowpack. A schematic is shown in Figure 4-4a. Two primary state variables are

maintained in the model, snow water equivalence, W [m], and internal energy of the

snowpack and top 40 cm of soil, U [kJ m^{-2}]. U is zero when the snowpack is at 0°C and

contains no liquid water. These two state variables are updated according to

$$dU/dt = Q_{sn}+Q_{li}-Q_{le}+Q_p+Q_g+Q_h+Q_e-Q_m \qquad (1)$$

$$dW/dt = P_r+P_s-M_r-E \qquad (2)$$

a)

b)
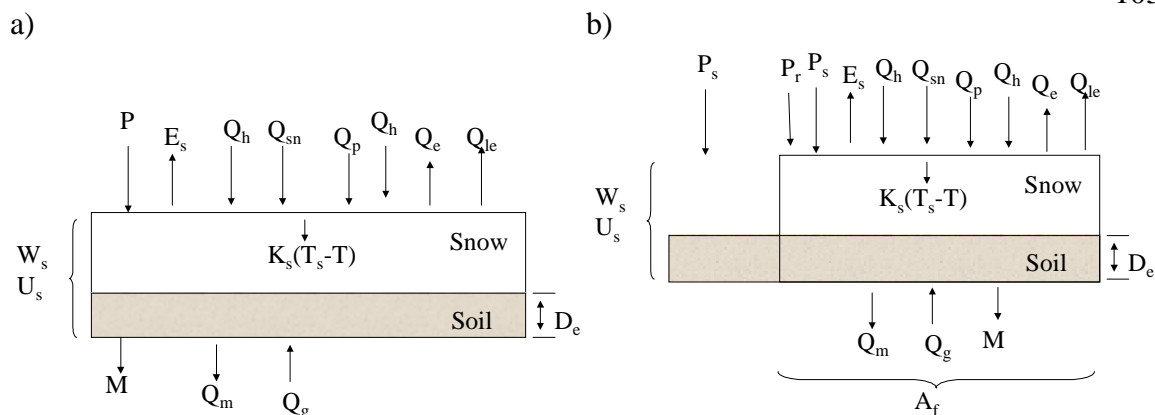
Figure 4-4. Schematic diagrams of a) Utah Energy Balance point scale snowmelt model and b) the lumped snowmelt model

where Q_{sn} is net solar radiation; Q_{li} is incoming longwave radiation; Q_{le} is outgoing longwave radiation; Q_p is advected heat from precipitation; Q_g is ground heat flux; Q_h is the sensible heat flux; Q_e is the latent heat flux; Q_m is heat advected with melt water; P_r is the rate of precipitation as rain; P_s is the rate of precipitation as snow; M_r is the melt rate; and E is the sublimation rate. The model is driven by inputs of precipitation, air temperature, humidity, wind speed and incoming solar radiation. Snow surface temperature, a key variable in calculating latent and sensible heat fluxes and outgoing longwave radiation, is calculated from the energy balance at the surface of the snowpack, where incoming and outgoing fluxes must match. These simulations were run on a 6-hour time step.

The effect of plant canopy on snowmelt is parameterized by decreasing the albedo of the snow surface as the snow depth decreases below the canopy height. This parameterization is most appropriate for short vegetation, such as sagebrush. Because the aspens are free of leaves until the soil warms slightly, errors introduced by not considering the taller canopy are minimal.

The distributed model uses a drift multiplier to estimate enhancement of local incoming snow at each cell through wind transport. The fraction of precipitation falling as rain or snow is a function of temperature. The fraction of the gage catch falling as snow is multiplied by the drift multiplier to estimate grid cell precipitation. The drift multiplier was calibrated at each grid cell to minimize the mean square error of the point model relative to observations on February 10, March 3, and March 23, 1993. Values of the multiplier over the basin are shown in Figure 4-3 and ranged from 0.16 to 5.36, with an average of 0.928.

Temporal variations in solar radiation were estimated based on an average atmospheric transmission factor calculated from pyranometer data at the weather station. Local horizons, slope, and azimuth were used to find local sunrise and sunset times and to integrate solar radiation received on the slope of each grid cell during each time step. The calculated atmospheric transmission factor characterized cloudiness for incoming longwave radiation calculations.

Lumped model with depletion curve
parameterization

Figure 4-4b depicts schematically the lumped model with subgrid parameterization using depletion curves. This is a modification of the UEB point-model (Figure 4-4a) described above. The snow-covered area fraction, A_f, is introduced as a new state variable, and the basin or element average snow water equivalent, $W_a = W_s * A_f$, is used as the mass state variable. The point snowmelt model is driven by basin averaged climate inputs to calculate fluxes to and from this fractional area. Because there is only one meteorological station at Upper Sheep Creek, basin average inputs were

calculated from a single meteorological station and topographic information. A_f is adjusted after each time step, based on changes in W_a. During accumulation A_f increases to full cover quickly with initial snowfall, and stays at full cover until melt begins. During melt, as W_a decreases, A_f is decreased following a depletion curve (Figure 4-5), $A_f(W_a)$, starting from a point of maximum accumulation, A towards B.

When there is new snowfall part of the way along, for example at point B, W_a is incremented by the new snowfall water equivalence $\square W$ (taken over the whole area) and A_f goes to one (point C in Figure 4-5). The new snowfall (covering the whole element) will be subjected to the same processes that led to spatial variability in the old snow, and the new snow will melt first. Therefore, we assume the system returns along a rescaled depletion curve to the point of original departure, B. In this fashion multiple accumulation and ablation periods can be accommodated. In principle there could be multiple rescalings and multiple points B, reminiscent of hysteresis loops in soil wetting and drying characteristic curves. However, our code kept track of only one departure (point B) at any given time.

Snow accumulation may vary between years, theoretically requiring a different depletion curve for each year dependent on the peak accumulation of the year. The spatial pattern, however, is relatively consistent. Therefore, we used a single dimensionless depletion curve, scaled by the maximum snow water equivalence (W_{amax}) since W_a was last 0 (generally the beginning of the snow season). This provides scaling of the depletion curve, letting the onset of melt be determined naturally from the modeling of physical processes, rather than using parameters determining the "beginning" of the melt season. It allows for melt episodes during the accumulation

New snowfall

ΔW_a

C **A**

1

A_f
or
A_f^*

Rescaled

Depletion
curve

B

0

W_a W_{amax}

0     $W^* = W_a/W_{amax}$ 1
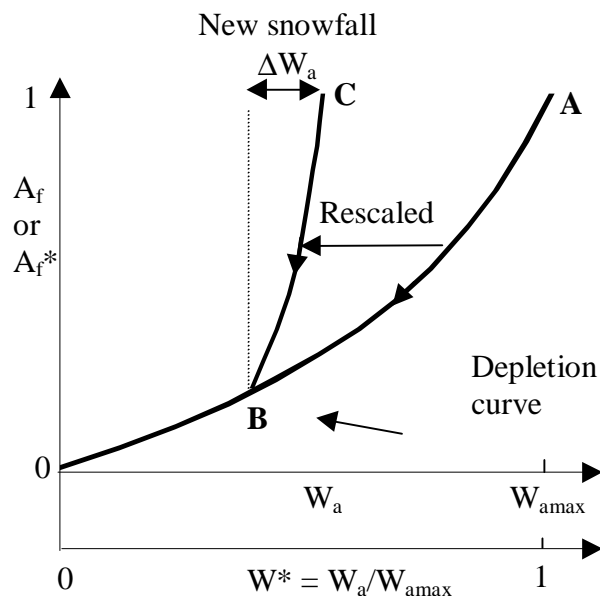
Figure 4-5. Schematic of depletion curve in lumped snowmelt model

season and accumulation episodes during the melt season. The following equation gives a

particular depletion curve, $A_f(W_a)$, in terms of the dimensionless depletion curve.

$$A_f(W_a) = A_f^*(W_a/W_{amax}) \tag{3}$$

Snowfall inputs to the lumped model are adjusted by an element (basin) average

drift factor to account for the fact that even at the larger lumped model element scale,

drifting and differences between the basin average precipitation and gage precipitation

may affect the net snow accumulation. In the results reported here the basin average drift

factor, 0.928, was used.

Depletion curves

The depletion curve represents the functional decrease of snow-covered area

fraction, A_f, with decreasing basin-average snow water equivalence, W_a, through the melt

season. This can be viewed as a parameterization of the distribution of snow over the

basin. Note that this definition of a depletion curve differs somewhat with the classical definition of A_f as a function of melt, so requires some description on how such curves may be estimated.

Spatial heterogeneity in snowpack water equivalence is linked to spatial variability in topography and vegetation, which control relative accumulation and melt. Topography controls relative accumulation through elevational temperature effects (precipitation as rain or snow) and drifting and controls melt through elevational temperature effects and exposure to sunlight (Dozier, 1979; Dozier and Frew, 1990). Vegetation controls accumulation through effects on drifting and interception and controls melt through effects on solar radiation, wind, and temperature. The primary drivers in variability change with scale (Seyfried and Wilcox, 1995). Luce *et al.* (1997, 1998) found that the primary control on the spatial distribution of snow water equivalence in Upper Sheep Creek was drifting. In larger basins, variations in wind, temperature, or solar exposure could be important sources of variability in melt. Drifting exerts its influence during the accumulation season. This suggests that the depletion curve for Upper Sheep Creek would be related to the distribution of snow water equivalence during the peak accumulation.

To formally develop this relationship, assume a generic probability distribution (pdf) for snow water equivalence, $f_g(w)$, that retains a consistent shape through the melt season. The implication is spatially uniform melt. This pdf gives the probability for point snow water equivalence areally sampled, offset by an additive constant. As the snow accumulates and ablates this function shifts to the right or left. This procedure is shown in Figure 4-6, and is conceptually similar to a procedure suggested in Dunne and Leopold
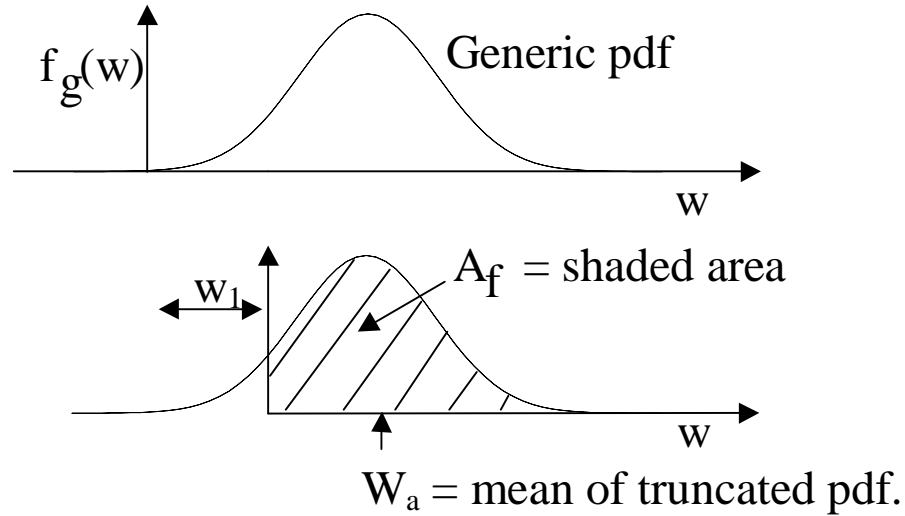
Figure 4-6. Schematic of generic snow water equivalence probability distribution

(1978) but generalized to non-Gaussian pdfs. The positioning of the generic pdf is controlled by the parameter w_1, which represents the amount of melt that has occurred. The tail to the left of the y-axis represents snow free area, for any particular melt depth, w_1. The snow-covered area fraction in terms of this pdf is defined as:

$$A_f\left(w_1\right)= \int\limits_{0}^{\infty} f_g\left(w+w_1\right)dw = \int\limits_{w_1}^{\infty} f_g\left(w\right)dw = 1 - F_g\left(w_1\right) \tag{4}$$

where $F_g(w_1)$ is the cumulative density function evaluated at w_1. For any arbitrary w_1, $A_f(w_1)$ is the fraction of the basin with swe at peak accumulation greater than w_1. Practically, the function, $A_f(w)$, may be numerically evaluated directly from a sample of snow water equivalence values across the area of interest. (Note: This function, $A_f(w)$ is not the same as the depletion curve, $A_f(W_a)$, the difference being indicated through a lower case dummy argument, w or w_1.)

The probability distribution of snow water equivalence for any particular w_1 has a nugget at zero because a negative swe has no physical interpretation. This nugget can be represented mathematically with a Dirac delta function, so that the finite probability of the areally sampled snow water equivalence being zero is $1 - A_f(w_1)$. The part of the pdf to the right of the axis represents the snow water equivalence pdf for non-zero snow water equivalence (all of the snow-covered points in the areal sampling). Consequently, the basin-average snow water equivalence is defined (from the usual definition of a mean) as:

$$W_a(w_1) = \int_{w_1}^{\infty}(w - w_1)f_g(w)dw = \int_{w_1}^{\infty}(w)f_g(w)dw - w_1 A_f(w_1) \tag{5}$$

Now recognize from (4) that

$$f_g(w) = -\frac{dA_f}{dw} \tag{6}$$

Therefore,

$$W_a(w_1) = -\int_{w_1}^{\infty}(w)\frac{dA_f}{dw}dw - w_1 A_f(w_1) \tag{7}$$

Integrating by parts,

$$W_a(w_1) = -[wA_f(w)]_{w_1}^{\infty} + \int_{w_1}^{\infty}A_f(w)dw - w_1 A_f(w_1) \tag{8}$$

Because $A_f(w) = 0$ for w greater than the maximum point SWE in the basin,

$$\lim_{w\to\infty} wA_f(w) = 0 \tag{9}$$

and the first and third terms of equation (8) cancel leaving us with

$$W_a(w_1) = \int_{w_1}^{\infty} A_f(w)dw \tag{10}$$

Equation (10) may be thought of as a layer-cake integration (i.e., a layer-by-layer

integration of the areal extent of each layer) of the amount of snow in the basin after melt

of depth w_1. This form is useful, because $A_f(w)$ can be obtained easily from data.

Numerical integration of $A_f(w)$ can be used to obtain $W_a(w)$. W_{amax} is $W_a(w=0)$. The

depletion curve, $A_f^*(W_a/W_{amax})$, may be approximated by calculating $A_f(w)$ and

$W_a(w)/W_{amax}$ for several values of w.

The pdf of snow water equivalence values sampled at peak snow accumulation

define the pdf for all $w_1 \geq 0$. Using the 254 sampled values of snow water equivalence

from Upper Sheep Creek on March 3, 1993, $A_f(w_1)$ was calculated using equation 4 for

w_1 between 0 and the maximum observed snow water equivalence in steps of 0.05 m.

$W_a(w_1)$ was calculated for the same w_1 values using equation 10. A_f is plotted against

W_a/W_{amax} in Figure 4-7. A three-part curve was used to numerically encode this

function.

$$A_f = \begin{cases} 0.18\sqrt{W_a/W_{a\,max}} & \text{if } 0 \leq W_a/W_{a\,max} \leq 0.13 \\ 0.42\sqrt{W_a/W_{a\,max}} - 0.11 & \text{if } 0.13 \leq W_a/W_{a\,max} \leq 0.34 \\ (W_a/W_{a\,max})^{1.5} & \text{if } 0.34 \leq W_a/W_{a\,max} \leq 1.0 \end{cases} \tag{11}$$

$A_f(W_a)$ was also found from the series of nine measurements and from the distributed

model run for comparison to the curve estimated from the peak accumulation pdf.
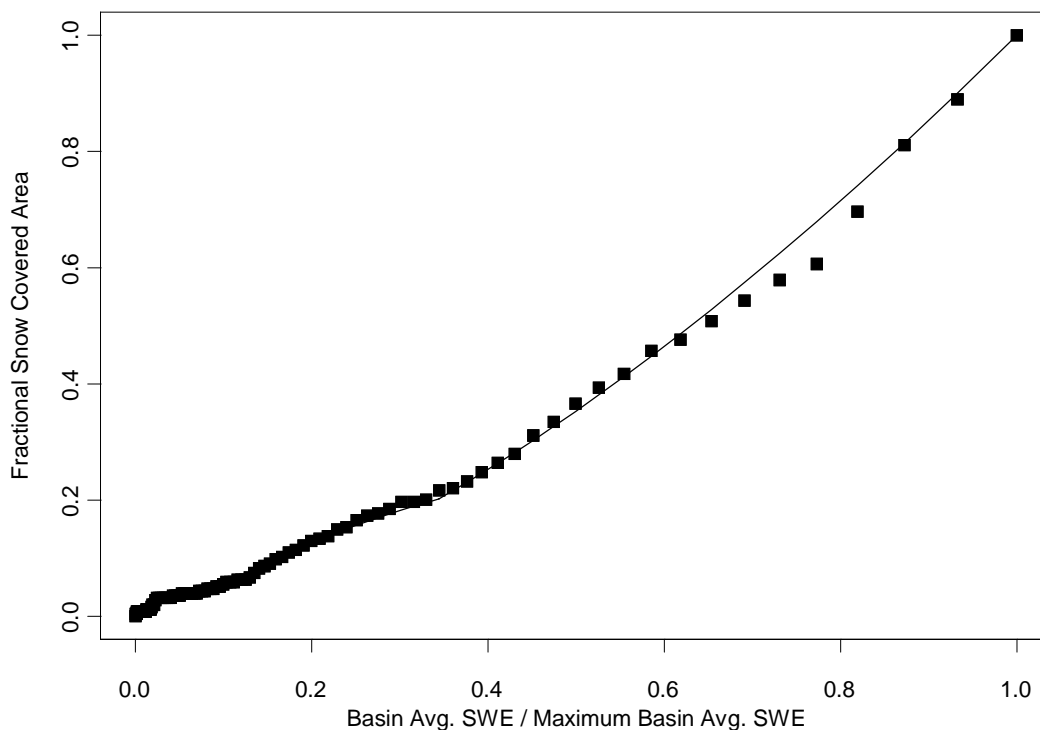
Figure 4-7. Depletion curve derived from pdf of March 3, 1993 snow water equivalence measurements and fitted curve

RESULTS AND DISCUSSION

A comparison between snow water equivalence predicted by the lumped and distributed models and measured in the snow survey is presented in Figure 4-8. The lumped model matched the distributed model very well, but both models overestimated the peak accumulation and showed a slightly early melt compared to observations.

The cell-by-cell calibration of the drift factor done using the February 10, March 3, and March 23 observations gives some insight into the source of the error for the two models. Figure 4-9 shows an example of the fit for two adjacent cells. One curve is a better fit to the data than the other and are typical of calibrations obtained at other cells. Both modeled curves have a similar shape, dictated by the model physics and driving
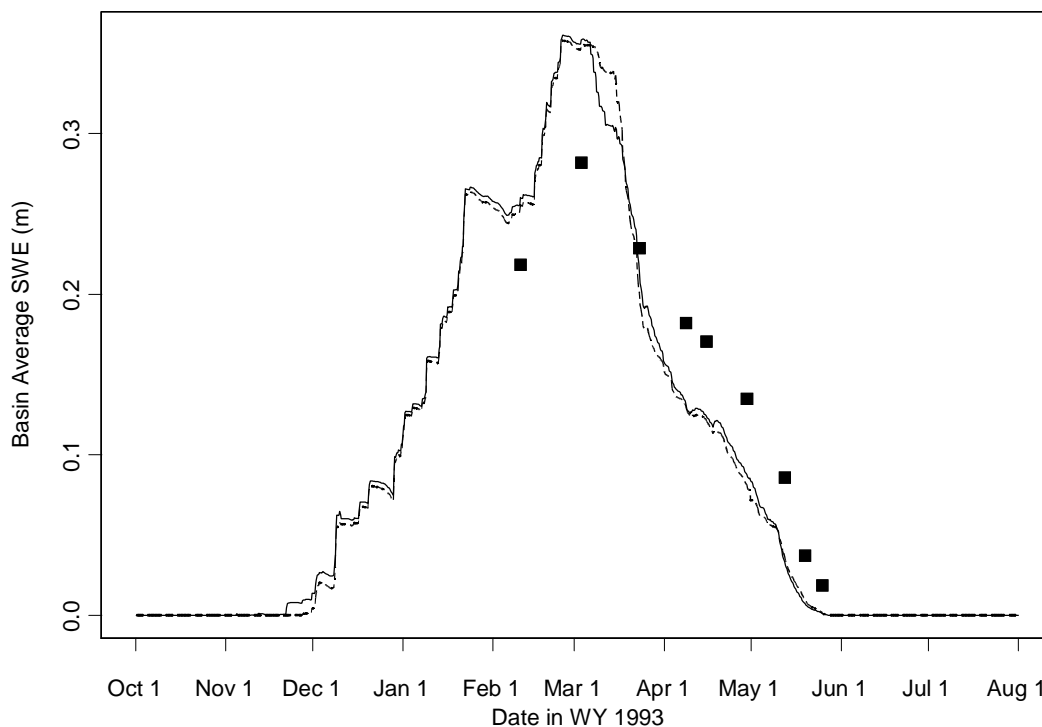
Figure 4-8. Modeled and observed basin averaged snow water equivalence for water year 1993. Solid line is the distributed model; dashed line is the lumped model. Points are observations

climatic inputs. The differences between the model curves are based on one cell receiving greater modeled snow precipitation than the other, as determined by the value of the drift multiplier, the only parameter adjusted in the calibration. At some cells, the fit to the calibration period was good (e.g., L14) and at others, it was poor (e.g., K14). In almost all cells with a poor fit, the pattern was similar to that at K14 (i.e., overprediction of the peak accumulation). Both modeled curves predict early melt. The sum of many cells with this pattern of overprediction and underprediction is an identical pattern of overprediction and underprediction of the average (Figure 4-8).

In this study we used the UEB model with the intent of having only the drift factor as an adjustable parameter. All other parameters were set based on literature or
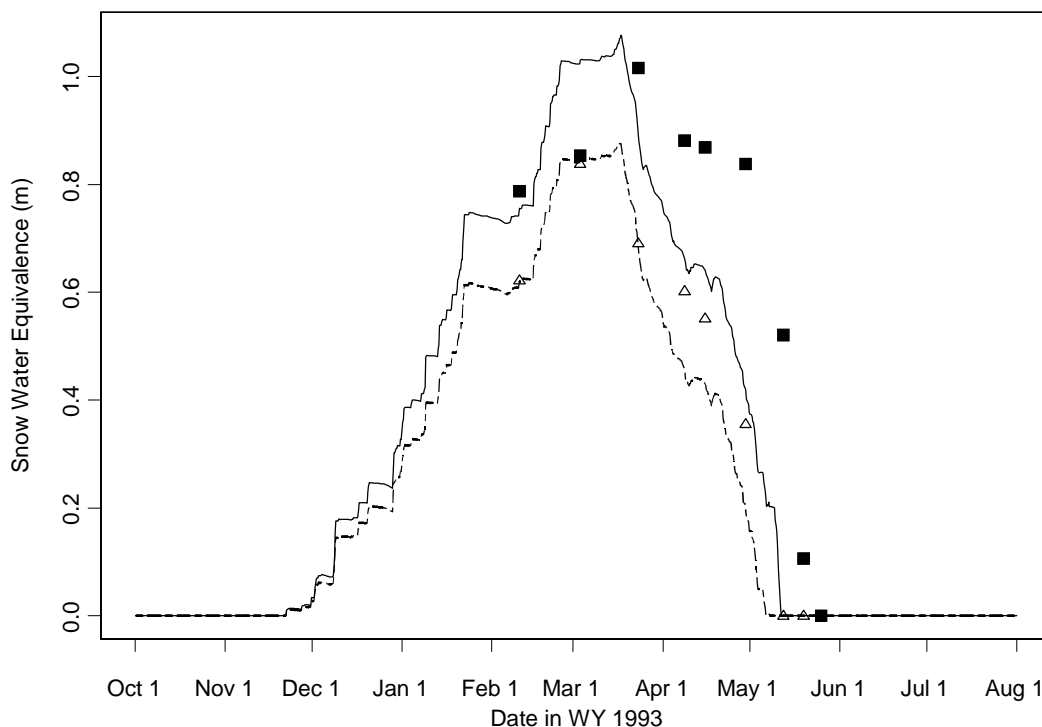
Figure 4-9. Plots of observed and modeled snow water equivalence at cells K14 (solid line and solid squares) and L14 (dashed line and open triangles). Model was calibrated by minimizing mean square error for the first three measurements of the year. The drift factor estimated for K14 is 2.55 and for L14 is 2.09. The solid line is representative of locations where poor calibrations were obtained and the dashed line is representative of locations where good calibrations were obtained

calibration to a few sites (Tarboton and Luce, 1996). From this basis, it could be said that the remaining differences between the observation and point model estimates indicate problems with the point model. It is possible that these errors could be rectified by making changes to the point model, but the emphasis of this paper is not incrementally improving point models; rather it is the development of the distribution function approach which could be used with any point model (e.g., Anderson, 1976; Jordan, 1991).

With one adjustable parameter in the point model, there are theoretically 255 adjustable parameters for the basin, corresponding to each grid cell. However, our experience shows that the fundamental shape of the snow water equivalence graph over

time is affected little by the drift factor. This means that for the aggregated

distributed simulation there is really only one adjustable parameter, the average drift

factor. Simulating over 255 cells provides a pdf of snow water equivalence over the

basin, and distributed solar inputs. Luce *et al*. (1997, 1998) showed that the distributed

solar information is of lesser value for this basin. Thus the fundamental information used

by the distributed model is the same information used by the lumped model, a mean "drift

factor" and a pdf of relative snow accumulation. When seen in this light, the close

agreement between the two models is not surprising.

Beven (1996) suggests that distributed models have too many degrees of freedom

to be properly calibrated. Indeed, it may be possible that the 255 values of drift factor

could have been manipulated together to provide a much better fit of the basin averaged

snow water equivalence. However, when the distributed model is constrained to match

the values at each cell, the aggregated distributed model results are the same as a lumped

model using the probability density function information. This supports the idea that

processes that can be modeled in a distributed fashion with independence from cell to cell

may also be efficiently modeled using a lumped model that relates a probability density

function of important site characteristics to important lumped state variables.

A comparison of the depletion curves derived from the pdf of peak snowpack

accumulation, the distributed model run, and the nine observations is shown in Figure 4-

10. This figure shows that the depletion curve derived from the pdf of snow water

equivalence at the date of maximum accumulation (March 3) is a good approximation to

the observed and distributed model estimates of the actual depletion curve.
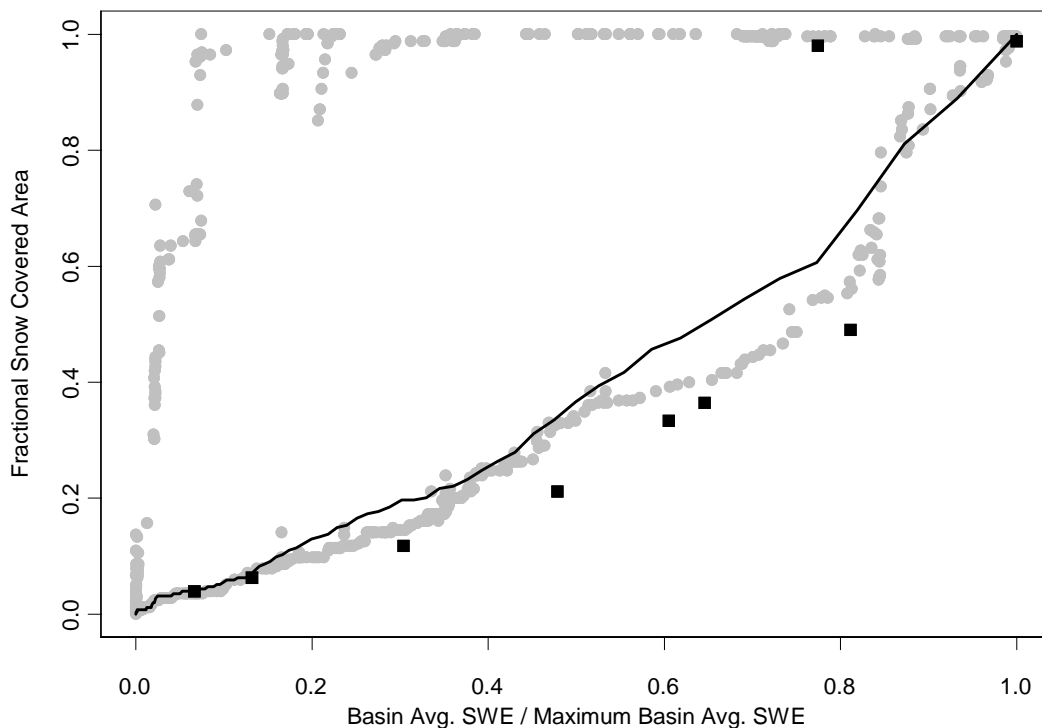
Figure 4-10. Comparison of depletion curves derived from 1) pdf of March 3, 1993 snow survey (line), 2) distributed model output (gray circles), and 3) snow surveys taken on nine dates (solid squares)

This finding improves the utility of the depletion curve concept because detailed observations of snow water equivalence over a basin at multiple times are unusual. Such observations would be necessary to either directly estimate the depletion curve or calibrate a distributed model. One may protest that gridded observations of snow water equivalence over a basin during peak accumulation are also rare. Tools have been developed (Elder *et al*., 1989, 1991, 1995, 1998; Elder, 1995; Rosenthal and Dozier, 1996) to use remote sensing and modeling to estimate the distribution of peak snowpacks. These tools and data are comparatively inexpensive and provide a practical means to generate a depletion curve for the lumped model.

CONCLUSIONS

Through the use of an areal depletion curve it is possible to obtain lumped snowmelt model simulations that agree well with distributed model results and observed data. We have also presented a new method for the derivation of areal depletion curves from the distribution of peak snow water equivalence, and shown that the areal depletion curve obtained using this method compares well with the actual and modeled (using a detailed distributed model) areal depletion of snow. The finding suggests that the lumped model formulation applied here is a good substitute for the distributed model when detailed spatial patterns are not required. The distributed model required 255 simulations using the UEB model for each time step where the lumped model required only one, demonstrating considerable savings in computational effort. Effort in determining distributed parameters is likewise reduced.

The reasoning behind the model should work with any point energy balance model. From the point-by-point calibration work, it was clear that the UEB model (Tarboton and Luce, 1996) did not always match the point scale data well. It is possible that both the distributed results and basin average results could be improved with a more detailed energy balance model.

Comparison of the depletion curve derived from the probability density function of peak snow accumulation to the observed depletion curve and that produced by the distributed model are encouraging. This finding combined with tools to quantify the distribution of snow over basins based on topography or remote sensing gives the lumped modeling approach presented here potential practical utility. This finding may also be useful for lumped empirical models that use the depletion curve concept.

REFERENCES

Abbott MB, Refsgaard JC (eds). 1996. *Distributed Hydrological Modeling*. Kluwer Academic Publishers: Dordrecht, Netherlands.

Anderson EA. 1973. *National Weather Service River Forecast System – Snow Accumulation and Ablation Model*. NOAA Technical Memorandum NWS HYDRO-17, US Dept. of Commerce: Silver Spring, MD.

Anderson EA. 1976. *A Point Energy and Mass Balance Model of a Snow Cover*. NOAA Technical Report NWS 19, US Dept. of Commerce: Silver Spring, MD.

Arola A, Lettenmaier DP. 1996. Effects of subgrid spatial heterogeneity on GCM-Scale land surface energy and moisture fluxes, *Journal of Climate* **9**: 1339-1349.

Beven KJ. 1995. Linking parameters across scales: subgrid parameterizations and scale dependent hydrological models. In *Scale Issues in Hydrological Modelling*, Kalma JD, Sivapalan M (eds), John Wiley & Sons, Ltd.: Chichester, pp. 263-281.

Beven KJ. 1996. A discussion of distributed hydrological modelling. In *Distributed Hydrological Modelling*, Abbott MB, Refsgaard JC. (eds), Kluwer Academic Publishers: Dordrecht, Netherlands, 255-278.

Beven KJ, Kirkby MJ. 1979. A physically based contributing area model of basin hydrology, *Hydrological Sciences Bulletin* **24**(1): 43-69.

Blöschl G. 1996. *Scale and Scaling in Hydrology*. Wiener Mitteilungen: Vienna, Austria.

Blöschl G, Gutknecht D, Kirnbauer R. 1991. Distributed snowmelt simulations in an alpine catchment. 2. Parameter study and model predictions. *Water Resources Research* **27**: 3181-3188.

Cooley KR. 1988. Snowpack variability on western rangelands. In *Proceedings of the 56th Western Snow Conference,* Kalispell, MT; 1-12.

Dozier J. 1979. A solar radiation model for a snow surface in mountainous terrain. In *Proceedings, Modeling Snow Cover Runoff*, Colbeck SC, Ray M (eds); US Army Cold Regions Research and Engineering Laboratory, Hanover, NH; 144-153.

Dozier J, Frew J. 1990. Rapid calculation of terrain parameters for radiation modeling from digital elevation data. *IEEE Transactions on Geoscience and Remote Sensing* **28**(5): 963-969.

Duffy CJ, Cooley KR, Mock N, Lee D. 1991. Self-affine scaling and subsurface response to snowmelt in steep terrain. *Journal of Hydrology* **123**: 395-414.

Dunne T, Leopold LB. 1978. *Water in Environmental Planning*. W.H. Freeman and Company: New York.

Elder K. 1995. *Snow distribution in alpine watersheds*. Ph.D. thesis, Department of Geography, University of California, Santa Barbara, CA.

Elder KJ, Dozier J, Michaelsen J. 1989. Spatial and temporal variation of net snow accumulation in a small alpine watershed, Emerald Lake basin, Sierra Nevada, California, U.S.A. *Annals of Glaciology* **13**: 56-63.

Elder KJ, Dozier J, Michaelsen J. 1991. Snow accumulation and distribution in an alpine watershed. *Water Resources Research* **27**: 1541-1552.

Elder K, Michaelsen J, Dozier J. 1995. Small basin modeling of snow water equivalence using binary regression tree methods. In *Biogeochemistry of Seasonally Snow-Covered Catchments*, *Proceedings of a Boulder Symposium*, Tonnessen KA, Williams MW, Tranter M. (eds); IAHS Publ. no. 228; 129-139.

Elder K, Rosenthal W, Davis R. 1998. Estimating the spatial distribution of snow water equivalence in a montane watershed. *Hydrological Processes* **12**: 1793-1809.

Flerchinger GN, Cooley KR, Ralston DR. 1992. Groundwater response to snowmelt in a mountainous watershed. *Journal of Hydrology* **133**: 293-311.

Flerchinger GN, Cooley KR, Hanson CL, Seyfried MS, Wight JR. 1994. A lumped parameter water balance of a semi-arid watershed. *International Summer Meeting of the American Society of Agricultural Engineering, Kansas City, Missouri.* American Society of Agricultural Engineering; St. Joseph, MI.; Paper No. 94-2133.

Hathaway GA, et al. 1956. *Snow Hydrology, Summary Report of the Snow Investigations*. US Army Corps of Engineers, North Pacific Division: Portland, OR.

Horne FE, Kavvas ML. 1997. Physics of the spatially averaged snowmelt process. *Journal of Hydrology* **191**: 179-207.

Jackson THR. 1994. *A spatially distributed snowmelt-driven hydrologic model applied to Upper Sheep Creek*. Ph.D. thesis, Department of Civil and Environmental Engineering, Utah State University, Logan, Utah.

Jordan R. 1991. *A One-Dimensional Temperature Model for a Snow Cover, Technical Documentation for SNTHERM.89*. Special Technical Report 91-16, US Army CRREL: Hanover, NH.

Kalma JD, Sivapalan M (eds) 1995. *Scale Issues in Hydrological Modeling*. John Wiley & Sons, Ltd: Chichester.

Kirnbauer R, Blöschl G, Gutknecht D. 1994. Entering the era of distributed snow models. *Nordic Hydrology* **25**: 1-24.

Liston GE. 1997. Modeling subgrid-scale snow distributions in regional atmospheric and hydrologic models. *Eos, Transactions, American Geophysical Union* **78**(46): F204, AGU Fall Meeting Suppl.

Luce CH, Tarboton DG, Cooley KR. 1997. Spatially distributed snowmelt inputs to a semi-arid mountain watershed. In *Proceedings of the 65th Western Snow Conference*, Banff, Alberta; 344-353.

Luce CH, Tarboton DG, Cooley KR. 1998. The influence of the spatial distribution of snow on basin-averaged snowmelt. *Hydrological Processes* **12**: 1671-1684.

Martinec J, Rango A, Roberts R. 1994. *The Snowmelt-Runoff Model (SRM) Users Manual, Updated Edition 1994, Version 3.2*. Department of Geography — University of Bern: Bern, Switzerland.

Moore RJ. 1985. The probability-distributed principle and runoff production at point and basin scales, *Hydrological Sciences Journal* **30**(2): 273-297.

Morris EM. (ed.) 1986. *Modelling Snowmelt-Induced Processes*. IAHS Publication No. 155. Institute of Hydrology: Wallingford.

Morris EM. 1990. Physics-based models of snow. In *Recent Advances in the Modeling of Hydrologic Systems*, Bowles DS, O'Connell PE (eds), Kluwer Academic Publishers: Dordrecht, The Netherlands, 85-112.

Rango A, Van Katwijk V. 1990. Development and testing of a snowmelt-runoff forecasting technique. *Water Resources Bulletin* **25**(1): 135-144.

Rosenthal W, Dozier J. 1996. Automated mapping of montane snow cover at subpixel resolution from the Landsat Thematic Mapper, *Water Resources Research* **32**(1): 115-130.

Seyfried MS, Wilcox BP. 1995. Scale and the nature of spatial variability: Field examples having implications for hydrologic modeling. *Water Resources Research* **31**(1): 173-184.

Stephenson GR, Freeze RA. 1974. Mathematical simulation of subsurface flow contributions to snowmelt runoff, Reynolds Creek watershed, Idaho. *Water Resources Research* **10**(2): 284-294.

Tarboton DG, Chowdhury TG, Jackson TH. 1995. A spatially distributed energy balance snowmelt model. In *Biogeochemistry of Seasonally Snow-Covered Catchments*, *Proceedings of a Boulder Symposium*, Tonnessen KA, Williams MW, Tranter M. (eds); IAHS Publ. no. 228; 141-155.

Tarboton DG, Luce CH, 1997. *Utah Energy Balance Snow Accumulation and Melt Model (UEB). Computer Model Technical Description and Users Guide*. Utah Water Research Laboratory: Logan, UT.

Wigmosta MS, Vail LW, Lettenmaier DP. 1994. A distributed hydrology-vegetation model for complex terrain. *Water Resources Research* **30**(6): 1665-1679.

CHAPTER 5

SCALING UP SNOWPACK ACCUMULATION AND MELT MODELS[1]

Abstract. In this paper we discuss purpose and means for increasing the support or integration scale of a model element for physically based snow accumulation and melt models. It is sometimes desirable to use relatively large model elements in a distributed snowpack model. Generally the purpose is to better match the scale of observations or to match the support scale of calculations in an atmospheric model. The motivation to increase the support scale of snowmelt models is to take up the opportunities for simplification inherent in using a statistical description of the system as opposed to spatially explicit descriptions of the process throughout the unit of interest. When scaling-up models, different processes or state information may become important in the description of a model element. At scales where spatial variability in snow water equivalence can be substantial, some measure of the variability of the snowpack must be included as a state variable or observable. Covariance between snow water equivalence and the accumulation rate or melt rate at each point is the source of temporal changes in spatial variance of snow water equivalence. Areal depletion curves relating snow-covered area to basin average snow water equivalence have been shown to be an effective parameterization of subgrid variability caused by differential accumulation. We present further theory to improve estimation of depletion curves through more thorough examination of the relationship between snow-covered area, average snow water

---

[1] Coauthored by Charles H. Luce and David G. Tarboton.

equivalence in the snow-covered area, and average snow water equivalence in the model element. Information on radiation can be added to depletion curves, thus accounting for information in the joint probability density function of drifting and exposure to direct-beam solar radiation. The "hiding function" approach introduced here further corrects for the fact that snowpack evolution does not depend on element average energy inputs, but on energy inputs to that portion of the model element that is covered by snow. If drifting occurs on north-facing slopes, the difference between fractional area coverage and fractional solar exposure can be substantial. The relative role of sources of variability as the support scale increases is discussed and provides a basis for discussion of optimal element size.

1. INTRODUCTION

1.1. Purpose of Scaling Up Snowmelt Models

Patches of snow during the melt season exist because of differential accumulation and melt. Patches have varying size and the definition of a "patch" in part depends on the extent of the view or analysis. Satellite photographs of part of a continent reveal "patches" many square kilometers in extent, where a person wandering through a catchment may only recognize the small piles of snow huddled behind bushes as "patches." This reminds us that heterogeneity in snow accumulation and melt, which leads to a patchy appearance of snow cover during the melt season, exists at continental scales and scales of a less than a square meter.

Distributed snowmelt models (DSM) have been adopted as the tool of choice to describe heterogeneity in accumulation and melt. *Theoretically* DSM allow simulation of
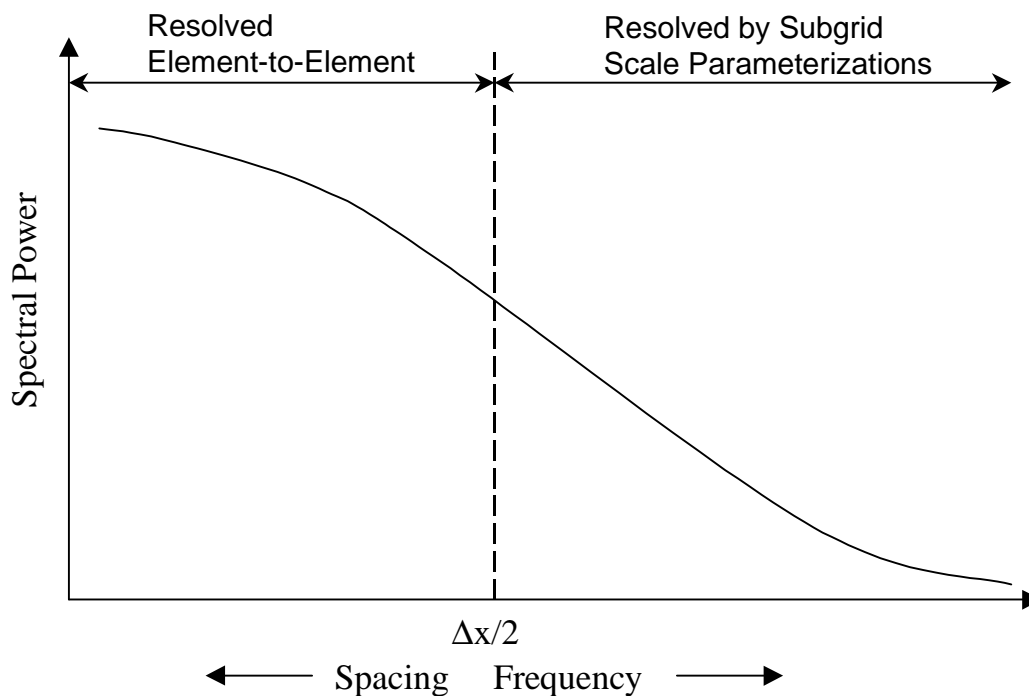
Figure 5-1. Conceptual power spectrum depicting a process important in snow accumulation or melt. Δx is the grid spacing. Variability with a characteristic length greater than the grid size must be represented explicitly by different parameters in each element. Variability with shorter characteristic lengths must be represented by parameterizations. [After *Kirnbauer and Blöschl*, 1994]

patches of any size depending on the choice of element size any the model. Patches composed of one or more elements can be resolved, but smaller patches may not be resolved (Figure 5-1) [*Kirnbauer et al.*, 1994; *Blöschl*, 1996]. The fact that smaller patches cannot be resolved is not necessarily a drawback, so much as a design choice. If there is a need to explicitly model the location of patches down to a particular size, the model elements must be smaller. The potential difficulty is that many DSM treat each element as a uniform block for energy and mass balance [*Leavesley et al.*, 1983; *Wigmosta et al.*, 1994; *Tarboton et al.*, 1995, among others]. This practice effectively truncates the power spectrum in Figure 5-1 to the right of the element size. Although there may not be a need to explicitly locate patches below a certain size, the fact that they

exist can still be important in describing the snowmelt within a model element [*Arola and Lettenmaier*, 1996; *Bathurst and Cooley*, 1996; *Luce et al.*, 1998; *Blöschl*, 1999; *Liston*, 1999; *Luce et al.*, 1999].

In practice, there are many difficulties in taking distributed models down to finer and finer scales. Computational speed limitations for large simulations are a real and practical consideration. In addition, at smaller scales more and sometimes different information is needed to describe site conditions. While vegetation within a 30-m grid cell may be described with a vegetation type and density, 1-m grid cells either have or do not have a plant, which may be an individual with specific characteristics – not average characteristics. At smaller scales, recognition of processes generally assumed to be unimportant for larger scales may become important. Lateral transport of liquid water in the snowpack over distances of 2-3 m to fingers conducting vertically through the snowpack has been observed by the authors in the field and by others [*Kattleman*, 1989; *Conway and Benedict*, 1994; *Williams et al.*, 1999]. The net effect of this process can be parameterized for a 30-m element, but at scales where transfers between elements are likely, the process must be modeled explicitly with two-dimensional water flow, because these processes can have profound influences on snowpack surface temperature and albedo [*Williams et al.*, 1999].

Distributed hydrologic and snowmelt models can also suffer from a mismatch between the scale of observation of driving weather conditions and the scale of the model elements or state variables. Precipitation, for example, is measured at widely spaced points, typically with fine temporal resolution. Even at an experimental watershed, spacing between gages may be on the order of 5 to 10 km [*Hanson and Johnson*, 1993].

In order to capture the effects of the diurnal pattern of heating and cooling on the surface temperature, which can be a strongly nonlinear process, climate information is needed on time scales of at least one to a few hours. Even though precipitation measurements at gages may have 10- or 15-minute resolution in time, interpolated precipitation is probably inaccurate for short time periods. Interpolation of monthly precipitation appears reasonable in some studies, but hourly or even daily precipitation cannot be reasonably interpolated from widely spaced precipitation gages [*Obled*, 1990; *Daly et al.*, 1994; *Johnson and Hanson*, 1995]. Similar problems almost certainly exist for temperature and longwave radiation, particularly in places where temperature inversions are likely. Wind data, so critical to lateral snow transport and convection of sensible and latent heat, is even rarer than precipitation data and interpolation of the wind field in mountainous terrain is difficult [*Barry*, 1992] and in practice seldom done. Given that turbulent heat transfers are often the second most important heat flux at a point in a snowpack over a season [*Male and Granger*, 1981; *Marks and Dozier*, 1992; *Dingman*, 1994], there is a strong suggestion that the energy balance at each point in a basin cannot be well modeled.

If information from an atmospheric model is used to drive the snowpack model (so as to provide boundary conditions for the atmospheric model), the scale mismatch can be equally severe. Atmospheric models are generally run with large elements ranging from about 1 km for detailed modeling exercises over a small area for a few storms to many 10's of km for continental scale examinations. Computational resources in part determine the element size for these models. Element size also reflects the degree to which the modelers would rather integrate or average the effects of turbulence over an area and time period as opposed to explicitly accounting for individual gusts. Output

from the atmospheric models to the snowpack models is areally averaged precipitation, temperature, wind, etc. What a point in a basin experiences is different than the spatial average, and differences increase with the atmospheric model size. Nesting a fine scale snow model below a large scale atmospheric model opens one to this type of problem.

Finally, there is the issue of model validation or calibration. Without some ability to demonstrate that a model matches a measurement it cannot be calibrated, and any acceptance of the calculations is based on belief. It is not uncommon to match basin runoff data to a distributed snowmelt and runoff model run over the basin [e.g., *Beven and Binley*, 1992; *Bathurst and Cooley*, 1996]. This process can lead to unusual, and non-unique, parameter estimates during calibration [*Beven*, 1989; *Kirnbauer et al.*, 1994; *Bathurst and Cooley*, 1996; *Blöschl*, 1996]. Also, this process does not confirm that the point scale modeling of the snowpack is correct. *Blöschl and Kirnbauer* [1992], *Leavesley and Stannard* [1990], and *Kirnbauer et al.* [1994] recommend that spatial patterns of snow cover be used to evaluate spatial accuracy of DSM. Where available, detailed measurements of the snow water equivalence may be useful [*Cooley*, 1988; *Tarboton et al.*, 1995; *Luce et al.*, 1998].

In short, the reason to scale up snowmelt models is to take up the opportunities for simplification inherent in using a statistical description of the system as opposed to explicit descriptions of the process throughout the unit of interest. *Brutsaert* [1986] gives a good definition of parameterization that also hints at its purpose:

> Parameterization is the mathematical means of describing the subresolution or microscale processes of the phenomenon, in terms of resolvable scale variables; these macroscale variables are the ones which can be treated explicitly in the analysis or for which records are obtainable. (p. 40S).

The concept is old in hydrology; for example, it is the basis of Darcy's law. Using larger

elements creates challenges in building new descriptions of processes [*Brutsaert*, 1986;

Dooge, 1986; *Klemeš*, 1986; *Wood et al.*, 1990; *Beven*, 1995]. Using larger elements can

also create great opportunities for simplification. The goal is to discover relationships

based on physical reasoning that are valid for larger model elements. When observations

are available, there exists a tremendous capacity to fit data for predictive purposes (e.g.,

neural nets or data mining), and *Dooge* [1986] warns that this is not the same as deriving

expressions for behavior that can be generalized between basins. What is needed is a

method to parameterize the effects of heterogeneity within elements, the size of which is

determined by understanding of processes and availability of data.

1.2. The Means for Scaling Up

There are many difficult issues to be faced in scaling up snowmelt models. Many

of the problems are active research areas for land surface parameterization in climate

models, including estimating spatially aggregated radiative and convective fluxes [e.g.,

Brutsaert, 1986; *Shuttleworth*, 1988; *Stewart et al.*, 1996]. Among the difficulties faced

with these research topics are adequate descriptions of the ground surface in terms of soil

moisture, vegetation, and snow distribution. It is almost universally recognized that if

these processes are linear, the spatially averaged flux would be the flux calculated based

on the average state variable. With regards to energy exchanges over a snow surface,

there is a pronounced nonlinearity described by the presence or absence of snow.

Consequently, the fractional snow-covered area is an important state variable or

observable when scaling up snowpack models.

In scaling up these models, the goal is to relate observable inputs and outputs, not in a strictly empirical manner, but through physical reasoning. This increases the transferability of the concept to other locations, times, and conditions and makes the concept useful in higher level abstractions. For example, our interest here is in modeling the fluxes to the snowpack, which may cover a fraction of the area; however, a climate modeler would be interested in the complete exchange of energy between the model element and the atmosphere. One test of concepts and parameterizations presented here is whether or not they are useful beyond predictions of snowpack outflow.

There are a few examples of scaling up hydrologic processes in the literature [e.g., *Beven and Kirkby*, 1979; *Bresler and Dagan*, 1983; *Dagan and Bresler*, 1983]. *Blöschl* [1996] provides a brief general review, citing four primary methods used in scaling up. The first is to do nothing and continue to treat larger elements (Blöschl terms this the model support scale or integration scale) as points. The second is to use effective parameters, an acceptable process for linear processes. The third is development of parameterizations from an intuitive reframing of the problem (similar to suggestions by *Dooge* [1986]), and the fourth suggestion by *Blöschl* [1996] is to use perturbation theory to develop larger scale descriptions. *Blöschl* [1999] describes advances in this area for snowpack modeling, and cites few examples of successful upscaling for snowmelt processes. The foundation of many examples in hydrology use physical reasoning to discover the net effect of spatial heterogeneity in processes.

1.3. A Description of Snow Accumulation
and Melt over an Area

When discussing snow accumulation and melt in an area, there are two fundamental parts to the description, the average behavior or mass balance, and variability of the mass balance. At a point scale, homogeneity is implicit, and variability is unimportant in the description. At larger scales, heterogeneity in mass balance leads to periodically bare areas, which impose a substantial nonlinearity and prevent reasonable use of methods like "effective parameters." In the hierarchy of information needs discussed by *Blöschl* [1996], the need for spatial information (statistics) in describing a snow-covered area may be greater than mean and variance. Information about the spatial autocovariance, connectivity, and anisotropy are arguably important if lateral transport (blowing snow) is important in the net mass exchange, because there may be feedback between the variability in snow cover and the degree of redistribution [*Liston and Sturm*, 1998; *Prasad et al.*, 2000]. For the sake of simplicity, in this paper we will limit the discussion to a slightly simpler system where only the probability density function is relevant information. Implicit in this description is the concept that the snowpack does not move, and that the proximity of locations with different depths makes little difference in the net behavior. We are adopting the concept of *Tarboton et al*. [1995] and *Tarboton and Luce* [1996] where drifting can be considered an enhancement to local precipitation. In this slightly simplified view, the two observable variables are the mean and variance of snow water equivalence.

Variability in snow water equivalence in an area is derived from differential accumulation and differential melt. Conceptually, during accumulation the areal mean snow water equivalence increases as snow accumulates, and the variability increases

a) Differential Accumulation   b) Differential Melt
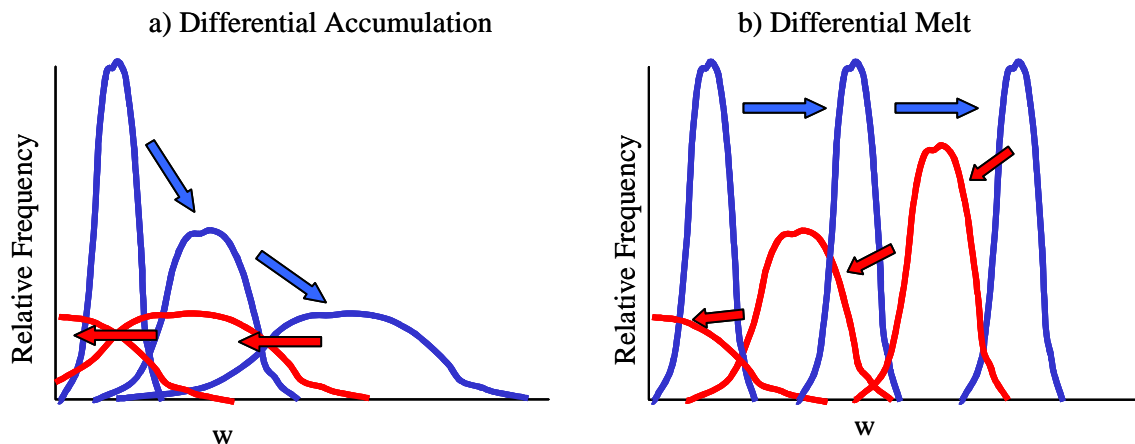
Figure 5-2. Schematic of changes in the distribution of snow in an area during a) snowpack accumulation and b) snowmelt. In (a) the variance increases with accumulation, but the distribution is not changed by melt, except as it is truncated by melting to bare areas. Such a situation might occur in low gradient rolling terrain with high winds and lots of drifting, but little variation in solar radiation. In (b) we show relatively uniform accumulation (only slight variance increase) and an increase in variance with melt. This situation might occur where there is slight preference for accumulation on north-facing slopes.

because some places receive more snow than others do on a consistent basis. Figure 5-2 shows a conceptual evolution of the snowpack over a basin during accumulation and during melt. Starting from a uniform snowpack (no snow) at the beginning of the season (represented by a Dirac delta function at 0 swe), as snow accumulates, the mean and variance increase until peak accumulation is reached. In Figure 5-2b, we show differential melt that increases the variability of snow water equivalence, until such time as some of the area becomes snow free. This would occur if areas with shallow accumulation melted faster than areas with deeper accumulation. Such a circumstance is not unusual in the mountainous western United States, where drifts form on northeast-facing slopes, and southwest-facing slopes tend to have more wind scour. Wind patterns during passage of synoptic cyclones from the Pacific Ocean create this general pattern.

For such a basin (e.g., that shown in Figure 5-2b) the shallow scoured areas are also the

areas receiving greatest insolation, and the deep drifts receive less insolation. In a

circumstance where locations with greater accumulation receive more sunlight (e.g.,

clearings in forests), a reduction in variance during melt may occur. During melt,

variability may increase or decrease depending on whether locations with large

accumulation or small accumulation melt preferentially.

We can describe this effect mathematically using a perturbation approach. Begin

with mass conservation

$$\frac{\partial W}{\partial t} = P - E - M$$

(1)

where W is the snow water equivalence (m), t is time (hr), P is precipitation (m/hr), E is

evaporation or sublimation (m/hr), and M is melt (m/hr). For simplicity, consider M to

be the result of energy inputs, e.g.

$$M = \max\left[0, \frac{1}{\lambda_h \rho_w}\left(Q_{sn} + Q_{li} - Q_{le} + Q_e + Q_h + Q_g + Q_p - \frac{\partial U}{\partial t} \right) \right]$$

(2)

where λ_h is the latent heat of fusion (kJ/kg), ρ_w is the density of water (kg/m^3), Q_{sn} is net

solar radiation (kJ/m^2/hr), Q_{li} is incoming longwave radiation (kJ/m^2/hr), Q_{le} is longwave

radiation emitted from the snowpack (kJ/m^2/hr), Q_e is latent heat of vaporization

(kJ/m^2/hr), Q_h is sensible heat (kJ/m^2/hr), Q_g is ground heat flux (kJ/m^2/hr), Q_p is the heat

advected with precipitation (kJ/m^2/hr), and $\partial U/\partial t$ is the change in snowpack energy

content with time (kJ/m^2/hr). From equation (1),

$$\frac{\partial \langle W \rangle}{\partial t} = \langle P \rangle - \langle E \rangle - \langle M \rangle \tag{3}$$

where the angular brackets denote the spatial average. We can decompose the snow water equivalence at a point into the spatial average W and the residual snow water equivalence at the point.

$$W(x, y) = \langle W \rangle + W'(x, y) \tag{4}$$

and the same decomposition can be made for P,E, and M. Therefore, we can also write

$$\frac{\partial W'}{\partial t} = P' - E' - M' \tag{5}$$

Our ultimate goal is to examine the evolution of the distribution of the snow water equivalence in an area with time. Equation (3) describes how the mean changes with time. To examine how the spread changes with time, we will start with an identity for derivative of a square and substitute equation (5) into the result.

$$\frac{\partial W'^2}{\partial t} = 2W'\frac{\partial W'}{\partial t} = 2W'(P' - E' - M') \tag{6}$$

Averaging over an area,

$$\frac{\partial \langle W'^2 \rangle}{\partial t} = 2\langle W'P' \rangle - 2\langle W'E' \rangle - 2\langle W'M' \rangle \tag{7}$$

we can further note that $\langle W'^2 \rangle$ is the variance in snow water equivalence, $\langle W'P' \rangle$ is the covariance of snow water equivalence and precipitation, $\langle W'E' \rangle$ is the covariance of

snow water equivalence and evaporation or condensation, $\langle W'M'\rangle$ is the covariance of

snow water equivalence and melt. Equation (7) mathematically describes what was

verbally stated above, that correlation between accumulated snow and changes in the

snowpack leads to both increases and decreases in variance.

2. EXAMPLES OF PARAMETERIZATION

2.1. First Approximation: Parameterizing
Differential Accumulation

Luce et al. [1999] describe and test a spatially lumped model of snow

accumulation and melt. The model is fairly simple and assumes that all of the variance in

the snowpack is created by differential accumulation (although some small amount of

differential melt during the accumulation season is integral to the calibration) and that

melt during the melt season is essentially uniform over snow-covered areas. In terms of

equation 7 the last two terms are essentially ignored and the integrated variance at the

peak of accumulation is assumed captured in the probability density function of snow

water equivalence in the basin as assessed by sampling [e.g., *Cooley*, 1988] or modeling

[e.g., *Elder et al.*, 1998]. It is useful to review the work of *Luce et al.* [1999] briefly and

note additional features of the area-averaged snowmelt problem not detailed there.

Their approach uses a parameterization relating the snow-covered area fraction,

A_f, to the area-average snow water equivalence, W_a, during the melt season. Examples of

the relationship are shown in Figure 5-3, the observed relationship, the relationship

calculated by the distributed snowpack model, UEB [*Tarboton et al.*, 1995; *Tarboton and*

Luce, 1996], and calculated based on the snow distribution [*Luce et al.*, 1999]. The

classical depletion curve relates area to cumulative snowmelt [*Anderson*, 1973], however,
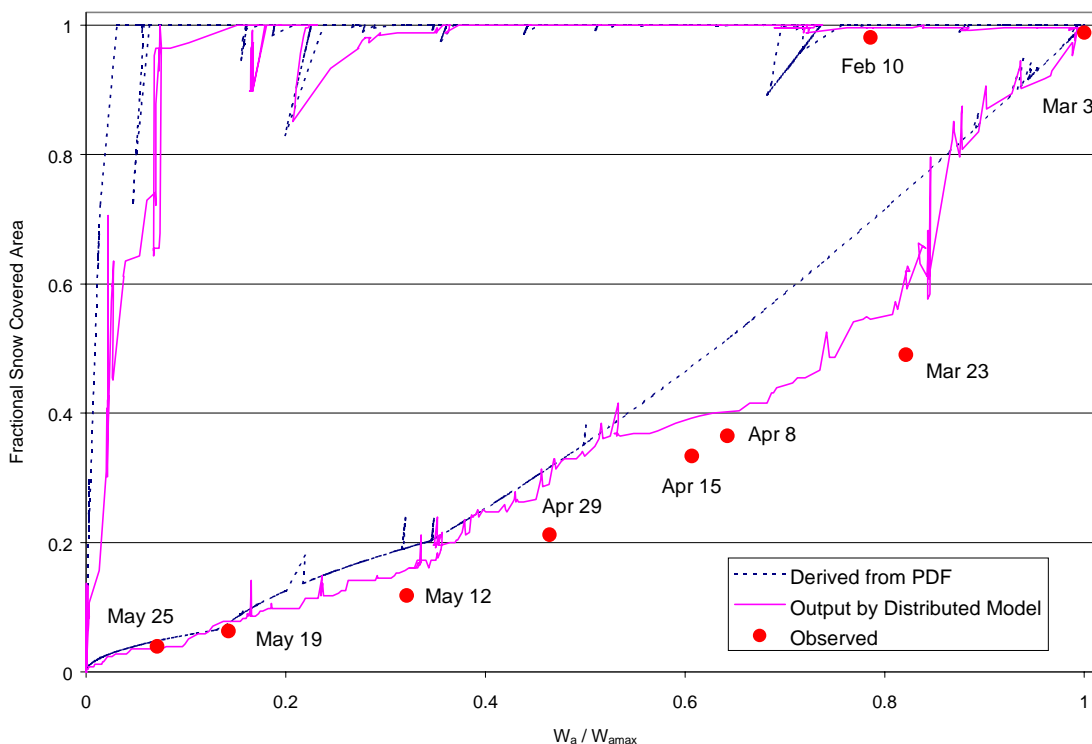
Figure 5-3. Depletion curve for Upper Sheep Creek derived by three methods: 1) from PDF of snow water equivalence on March 3, 1993, 2) from distributed model outputs, and 3) from observations. Note hysteresis in relationship as snow covers entire area with only slight accumulation in early season (on left), while melt uncovers areas gradually.

because of similarities with reference to the decline in snow-covered area, the curves in Figure 5-3 have also acquired the name "depletion curve." Given similarities in data requirements, the distinction is academic, but clarification now may help prevent later confusion. In the literature, we now see depletion curves of three forms each with the fractional snow-covered area on the y-axis and one of three variables on the x-axis, cumulative melt, date, and snow water equivalence.

Figure 5-4 depicts schematically the lumped model with subgrid parameterization using depletion curves compared to a schematic of a point scale model (UEB). The primary difference in the schematics is that in the lumped model, the snow-covered area

A) Point Model
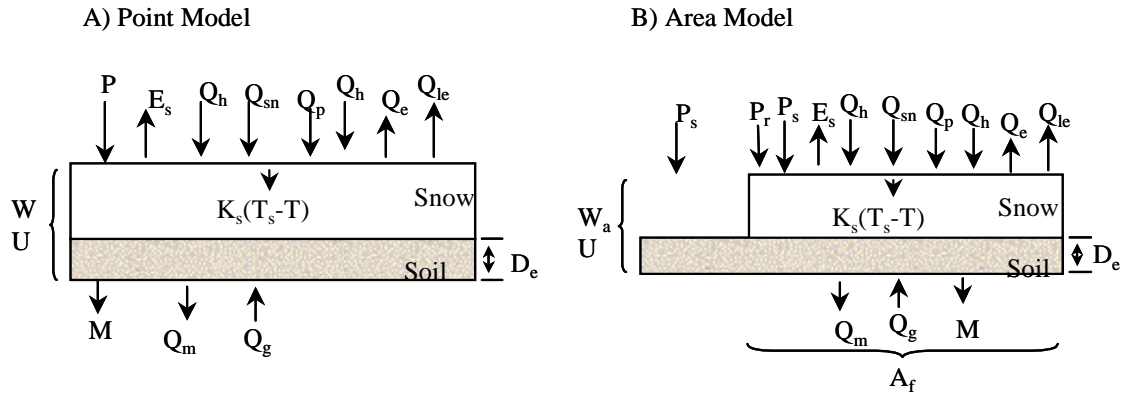
B) Area Model

Figure 5-4. Schematics of point and area models.

fraction, A_f, is introduced as a new state variable. The model evolves three state

variables: 1) W, the snow water equivalence of the snow-covered area, 2) U, the

snowpack energy content of the snow-covered area, and 3) the fractional snow-covered

area, A_f. Note that the basin average snow water equivalence is given by

$$W_a = W \cdot A_f \tag{8}$$

The three state variables are evolved according to

$$\frac{\partial U}{\partial t} = Q_{sn} + Q_{li} - Q_{le} + Q_e + Q_h + Q_g + Q_p - Q_m \tag{9}$$

$$\frac{\partial W}{\partial t} = P_r + P_s - M_r - E \tag{10}$$

and

$$A_f = A_{dc}(W_a) \tag{11}$$

where Q_{sn} is net solar radiation; Q_{li} is incoming longwave radiation; Q_{le} is outgoing

longwave radiation; Q_p is advected heat from precipitation; Q_g is ground heat flux; Q_h is

the sensible heat flux; Q_e is the latent heat flux; Q_m is heat advected with melt water; P_r is

the rate of precipitation as rain; P_s is the rate of precipitation as snow; M_r is the melt rate;

and E is the sublimation rate, and A_{dc} represents the functional relationship of the areal

depletion curve. The model is driven by inputs of precipitation, air temperature, humidity,

wind speed and incoming solar radiation. Snow surface temperature, a key variable in

calculating latent and sensible heat fluxes and outgoing longwave radiation, is calculated

from the energy balance at the surface of the snowpack, where incoming and outgoing

fluxes must match. Specifics of the calculations describing the terms in equations 9 and

10 are found in *Tarboton and Luce* [1996].

A_f is adjusted after each time step, based on changes in W_a. Overall, the depletion

curve is hysteretic in nature. During accumulation A_f increases to full cover quickly with

initial snowfall, and stays at full cover until melt begins. During melt, as W_a decreases, A_f

is decreased following the depletion curve, $A_{dc}(W_a)$, starting from a point of maximum

accumulation, A towards B (Figure 5-5). When there is new snowfall part of the way

along, for example at point B, W_a is incremented by the new snowfall water equivalence

ΔW (taken over the entire area) and A_f goes to one (point C in Figure 5-5). The new

snowfall (covering the whole element) will be subjected to the same processes that led to

spatial variability in the old snow, and the new snow will melt first. Therefore, we

assume the system returns along a rescaled depletion curve to the point of original

departure, B. In this fashion multiple accumulation and ablation periods can be

accommodated. In principle there could be multiple rescalings and multiple points B,

New snowfall

ΔW

C

A

1

Rescaled

A_f

Depletion
curve

B

0

W

W_{max}

0

$W^* = W/W_{max}$

1
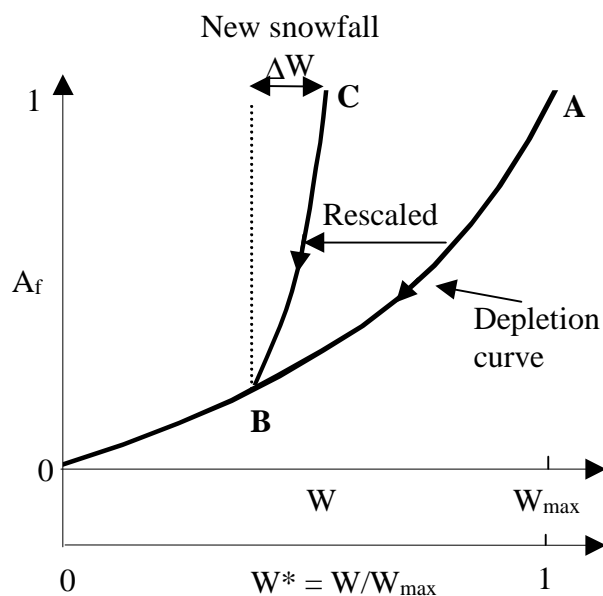
Figure 5-5. Schematic of depletion curve.

reminiscent of hysteresis loops in soil wetting and drying characteristic curves. However,

our code currently tracks only one departure (point B) at any given time.

Snow accumulation may vary between years, theoretically requiring a different

depletion curve, $A_{dc}(W_a)$, for each year dependent on the peak accumulation of the year.

The spatial pattern, however, is relatively consistent because topography and general

climatic conditions remain consistent from year to year [*Kirnbauer and Blöschl*, 1994;

Sturm et al., 1995]. Therefore, we used a single dimensionless depletion curve, scaled by

the maximum snow water equivalence (W_{amax}) since W_a was last 0 (generally the

beginning of the snow season). This provides scaling of the depletion curve, letting the

onset of melt be determined naturally from the modeling of physical processes, rather

than using parameters determining the "beginning" of the melt season. It allows for melt

episodes during the accumulation season and accumulation episodes during the melt

season. The following equation gives a particular depletion curve, $A_{dc}(W_a)$, in terms of the dimensionless depletion curve.

$$A_{dc}(W_a) = A_{dc}^* (W_a/W_{amax}) \qquad\qquad (12)$$

where A_{dc}^* is the dimensionless depletion curve operating on the seasonally rescaled basin average snow water equivalence (ranges from 0-1). The consistency of pattern from year to year is sometimes questioned, however, when the dimensionless depletion curves for several years are plotted together, there is a surprising degree of consistency for years with substantially different snowfall totals (Figure 5-6).

Comparison of the lumped model to a distributed model and distributed observations for water year 1993 at Upper Sheep Creek in the Reynolds Creek Experimental Watershed showed strong agreement between the lumped model and the distributed model and reasonable agreement of both to observations (Figure 5-7) [*Luce et al.*, 1999]. From the description of the model above, there are some expected shortcomings relative to fully distributed models. For example, in a point model, melt outflow cannot begin until the cold content has been satisfied and some liquid water has been generated. In a shallow snowpack, there is much less cold content to satisfy than in a deep snowpack by virtue of the fact that there is much less mass per unit area. The deeper snowpack also requires more melt water to be generated before melt outflow can begin. For a given energy input at the surface, melt outflow should start much earlier in shallower snowpacks than in deep drifts. In the lumped model, melt outflow is assumed uniform. This explains the delay in melt in the lumped model at the beginning of the melt season (Figure 5-7) because it assumes a uniform snowpack at any particular instant,
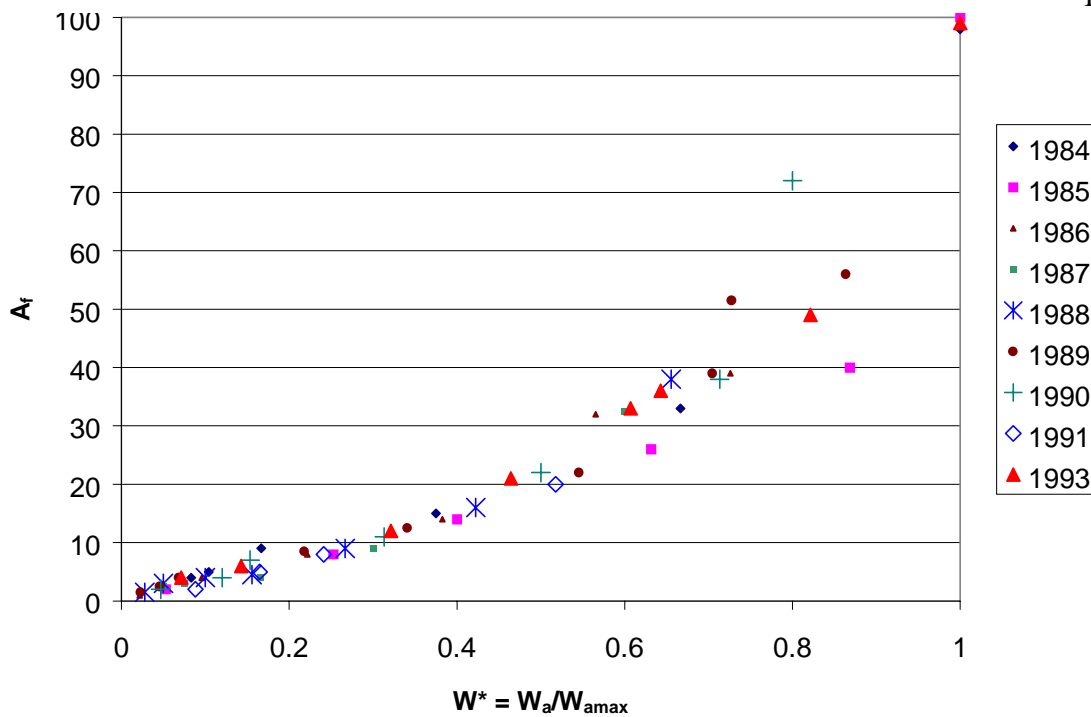
Figure 5-6. Depletion curves from several years of data at Upper Sheep Creek (Data provided by K. Cooley).
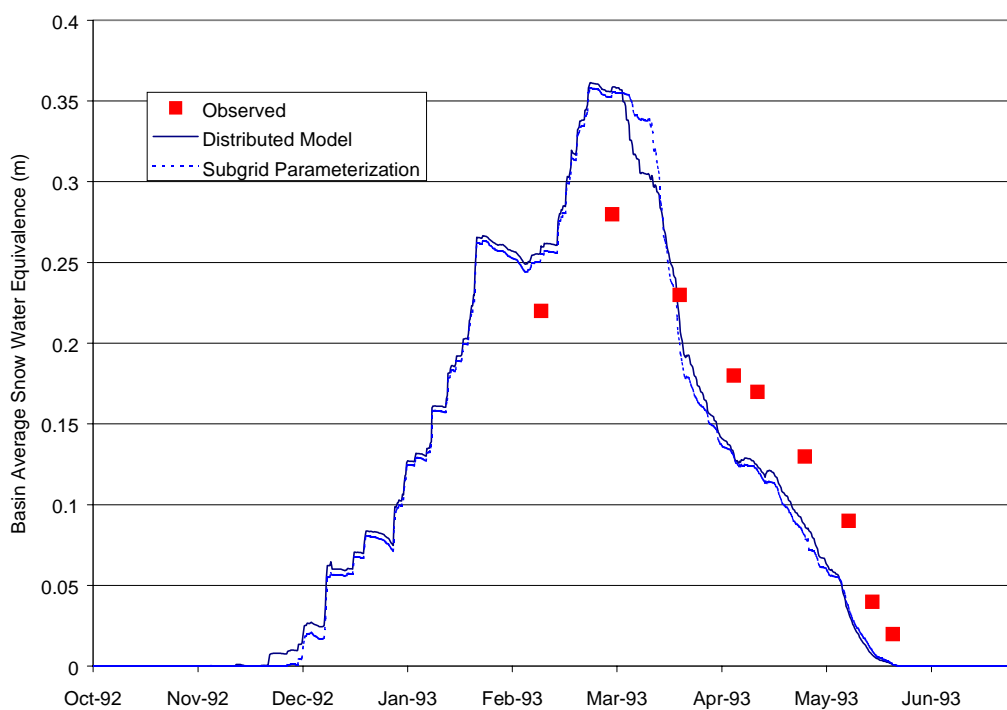
Figure 5-7. SWE over time observations, distributed model, and lumped model.

whereas the distributed model showed melt outflow from locations with a snowpack shallower than the average. The reason that the error appears small is that satisfying the cold content of a column of snow requires very little energy compared to the total energy required to melt a column of snow. The reason that the difference is large enough to be visible is because the difference in melt required before outflow occurs represents a fairly substantial energy input difference, but again much smaller than the amount of energy required to melt the entire column of snow.

2.2. Derivation of Areal Depletion Curves
for Differential Accumulation

The depletion curve, $A_{dc}(W_a)$, may be estimated from the probability density function (pdf) of snow water equivalence sampled spatially. Implicit in this derivation is the assumption that spatial variability is created primarily by differential accumulation, and melt is uniform. Figure 5-8 shows a map of snow water equivalence in Upper Sheep Creek on March 3, 1993, close to the maximum accumulation for the basin. Imagine a cross section through this snowpack and that this snowpack experiences a spatially uniform cumulative melt depth, M (Figure 5-9). We can convert the spatially explicit representation of the snowpack water equivalence in Figures 5-8 and 5-9 to a generic probability density function (pdf) of snow water equivalence, $f_g(w)$, that retains a consistent shape through the melt season (spatially uniform melt), so that the parameter, M, represents a shift of the $w = 0$ axis over the pdf to the right as the snow ablates (Figure 5-10). This procedure is conceptually similar to a procedure suggested in *Dunne and Leopold* [1978] but generalized to non-Gaussian pdfs. The tail to the left of the y-axis represents snow-free area, for any particular melt depth, M. The snow-covered area
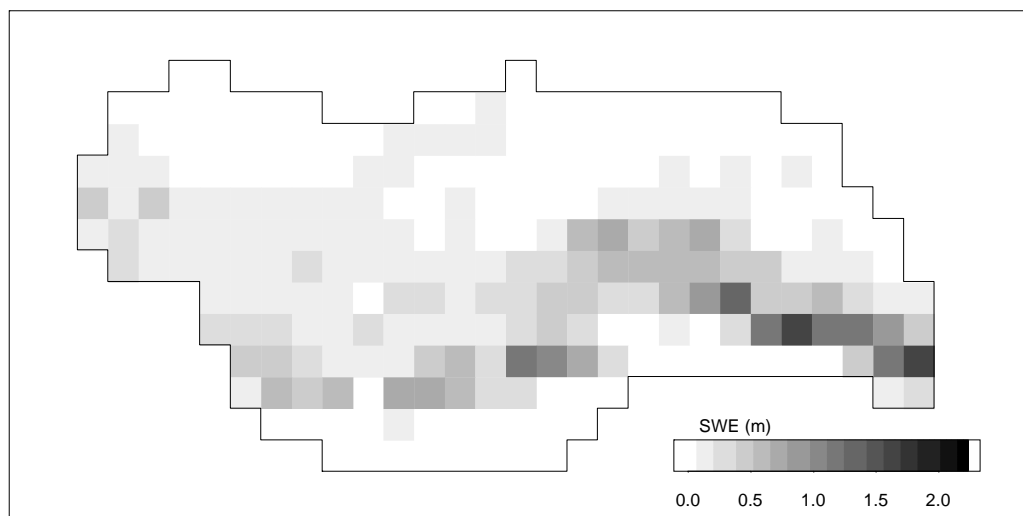
Figure 5-8. Map of snow water equivalence over Upper Sheep Creek on 3/3/93.
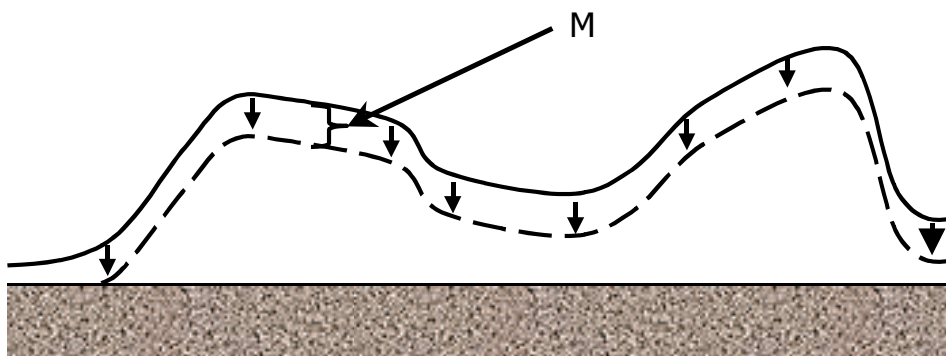
Figure 5-9. Conceptual cross section of a snowpack showing the effect of a uniform melt depth, M, over the snowpack.
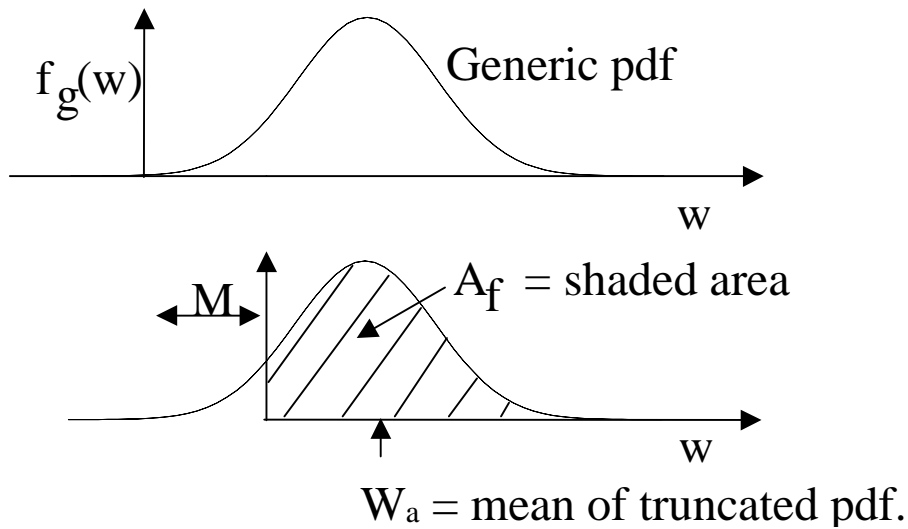
Figure 5-10. Schematic of PDF of snowpack in Figure 5-9, showing effect of uniform melt depth M on PDF.

fraction in terms of this pdf is defined as:

$$A_f(M) = \int_0^\infty f_g(w+M)\,dw = \int_M^\infty f_g(w)\,dw = 1 - F_g(M) \tag{13}$$

where $F_g(M)$ is the cumulative density function evaluated at M. For any arbitrary M, $A_f(M)$ is the fraction of the basin with swe at peak accumulation greater than M. Practically, the function $A_f(M)$ may be numerically evaluated directly from a sample of snow water equivalence values across the area of interest. The function $A_f(M)$ is the classical depletion curve expressed as fractional snow-covered area as a function of average melt depth.

The probability distribution of snow water equivalence for any particular M has a nugget at zero because a negative swe has no physical interpretation. This nugget can be represented mathematically with a Dirac delta function, so that the finite probability of

the areally sampled snow water equivalence being zero is 1-A_f(M). The part of the pdf to

the right of the axis represents the snow water equivalence pdf for non-zero snow water

equivalence (all of the snow-covered points in the areal sampling). Consequently, the

basin-average snow water equivalence is defined (from the usual definition of a mean) as:

$$W_a(M) = \int_M^\infty (w - M)f_g(w)dw = \int_M^\infty wf_g(w)dw - MA_f(M) \tag{14}$$

where equation 13 has been used to obtain the last term. Now recognize from (13) that

$$f_g(w) = -\frac{dA_f(w)}{dw} \tag{15}$$

Therefore,

$$W_a(M) = -\int_M^\infty w\frac{dA_f(w)}{dw}dw - MA_f(M) \tag{16}$$

Integrating by parts,

$$W_a(M) = -[wA_f(w)]_M^\infty + \int_M^\infty A_f(w)dw - MA_f(M) \tag{17}$$

Because A_f(w) = 0 for w greater than the maximum point snow water equivalence in the

basin.

$$\lim_{w\to\infty} wA_f(w) = 0 \tag{18}$$

and the first and third terms of equation (8) cancel, leaving us with

$$W_a(M) = \int_M^\infty A_f(w)dw \tag{19}$$

Equation (19) may be thought of as a layer-cake integration (i.e., a layer-by-layer integration of the areal extent of each layer) of the amount of snow in the basin after melt of depth M (Figure 5-11). This form is useful, because the function $A_f(M)$ is the number of samples with snow water equivalence greater than M divided by the total number of samples. Numerical integration of $A_f(M)$ can be used to obtain $W_a(M)$ and

$$W_{amax} = W_a(M=0). \tag{20}$$

The depletion curve may be found from

$$A_{dc}{}^*(W_a(M)/W_{amax}) = A_f(M) \tag{21}$$

which can be evaluated for many values of M.

In the absence of observations at the peak snow water equivalence, simulation may be useful to estimate the distribution of snow water equivalence in an area of interest. Empirical approaches [e.g., *Elder et al.*, 1998; *Winstral et al.*, 1999] can be used to extrapolate data from one area to another similar area. This carries with it the risk that the regression is spurious or overfit. Physically based approaches [e.g., *Liston and Sturm*, 1998] would seemingly reduce this risk. *Prasad et al*. [2000] noted that the drifting model of *Liston and Sturm* [1998] did not match exact locations of drifts on the landscape, but that the modeled pdf of snow water equivalence over an area was close to the observed pdf. This is another reminder that the finer the scale of model we attempt, the less likely it is that the information at each model element will be correct.
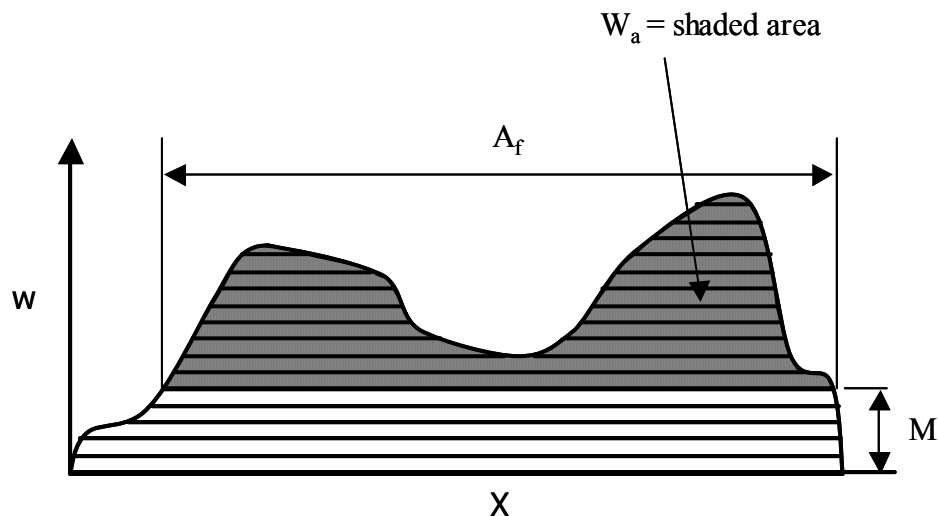
Figure 5-11. Schematic of snowpack showing how W_a can be estimated as an integral of $A_f(w)$.

We can also attempt to directly model cumulative density functions using the concepts presented in equation 7. Given a correlation between the snow water equivalence on the ground and the incremental change in snow water equivalence, we can estimate the change of each percentile in snow water equivalence. In some cases it is necessary to consider additional variables that affect both past accumulation and present rates of change. For example, there generally exists some degree of correlation between elevation and precipitation depth and some degree of correlation of temperature with elevation. We can also posit a simple relationship specifying the fraction of precipitation that will be snow or rain as a function of temperature, e.g.,

$$
P_s = \begin{cases} 0 & \text{for } T_a \geq T_r \\ P\dfrac{T_r - T_a}{T_r - T_b} & \text{for } T_b < T_a < T_r \\ P & \text{for } T_a \leq T_b \end{cases} \tag{22}
$$

where P_s is the precipitation as snow, P is total precipitation, T_a is the air temperature (C),

T_r is the air temperature above which all precipitation is rain (e.g., 3 °C), and T_b is the

temperature below which all precipitation is snow (e.g., –1 °C) [*Hathaway et al.*, 1956;

Tarboton and Luce, 1996]. Given a cumulative density function of elevation

(hypsometric curve), we can evolve the cdf of snow over time (e.g., Figure 5-12). The

relationships of preciptiation and temperature with elevation and the equation predicting

the phase all operate on the cdf of snow water equivalence since there is a 1:1 mapping of

the percentiles of snow water equivalence and the percentiles of elevation. Thus while

we can generally agree that higher elevations receive more precipitation, and it is more

likely to be snow at higher elevations, it is somewhat of a reframing to note that those

places with the most snow will receive the most additional new snow and those with the

least will receive the least new snow. At each time step, then, we evaluate the joint pdf of

w and Δw to give the pdf of w + Δw. A similar concept could be applied in an area with

drifting or other readily observable source of persistent bias in accumulation. This

concept has some similarity to the probability distributed approach presented by *Moore*

[1985], which defines model elements based on one or a few variables and then maps

simulations from variable space to geographic space based on geographic maps of each

variable. The difference is in realizing that pdf or joint pdf of spatially varying

characteristics yields a relationship between the amount of snow on the ground and the

change in snow water equivalence. The pdf derived in this manner is directly useful for

developing depletion curves.

A substantial amount of information is held in depletion curves. The slope of the

curve at any point describes how the snowpack is melting. The slope of the curve is
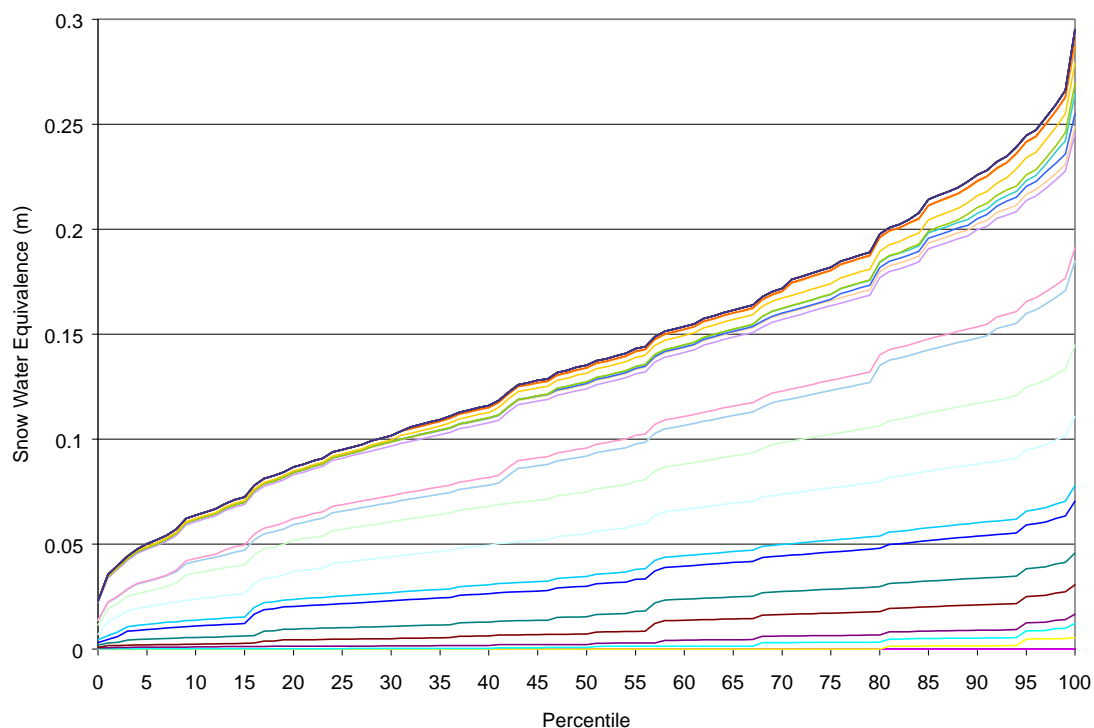
Figure 5-12. Conceptual evolution of the cumulative density function for a snowpack where variability in snow accumulation is modeled by a linear lapse rate for precipitation and temperature with elevation and a threshold temperature for the snow-rain transition. Curves near bottom are near the beginning of the accumulation season and curves near the top are near the end of the season. Elevation and climate data (including average temperature and precipitation lapse rate) are taken from the Tollgate subbasin of the Reynolds Creek watershed for water year 1993.

dA_f/dW_a, which estimates the decrement in area for any decrement in snow water

equivalence. Recall from equation 8 that the basin average snow water equivalence, W_a,

is the fractional snow-covered area, A_f, times the average snow water equivalence of the

snow-covered area, defined as W above, but we will use W_{sc} to clearly differentiate it

from W_a here. Lines radiating from the origin of a depletion curve (e.g., Figure 5-3) then

would be lines of constant W_{sc} with a line of $W_{sc} = 0$ vertical from the origin and $W_{sc} \to \infty$

as it approaches the horizontal axis. From any point along the depletion curve, there is a

line from the point to the origin along which W_{sc} is constant. If the slope of the depletion

curve is the same as this slope, incremental melt yields no change in the average snow water equivalance of snow-covered areas. If the slope of the depletion curve is steeper than that line, the area is decreasing faster than the basin average water equivalence given the current areal coverage, and W_{sc} increases. If the curve is flatter, W_{sc} is decreasing.

Figure 5-13 shows the relationship between W_{sc} and W_a corresponding to the depletion curve shown in Figure 5-3. Using this information, we can intuit the shape of depletion curves readily. The snowpack described by the depletion curve in Figure 5-3 had a great deal of variability, with large areas of shallow snow and a smaller area with very deep snow. A uniform snowpack uniformly melted results in decreases of W_a and W_{sc} with no change in A_f, so would be plotted as a straight line across the top of Figure 5-3 only dropping to 0 area as W_a approaches 0.

This information also shows us that the shape of the depletion curve must be concave downward with a vertical slope at the origin. Any function asymptotic to the horizontal axis will predict a depth of the snow-covered area approaching infinity as the area goes to zero to yield $W_a = 0$. A function arriving along a straight line (not the vertical axis) would imply a finite depth with no area, a situation suggestive of nieves penitentes in the Andes mountains [*Post and LaChapelle*, 1971], but otherwise unrealistic. A function arriving at the vertical axis implies a snow-covered area with no depth, another undefined event. A curve asymptotic to the vertical axis near the origin would have a slope flatter than the direct line to the origin, implying that at the end a decrease in W_{sc} is needed to melt a snowpack away. While there is a temptation to fit a curve such as that seen in Figure 5-3 with a simple function like $A_f = (W_a/W_{amax})^2$, it can be seen from this discussion that it would be a mistake.
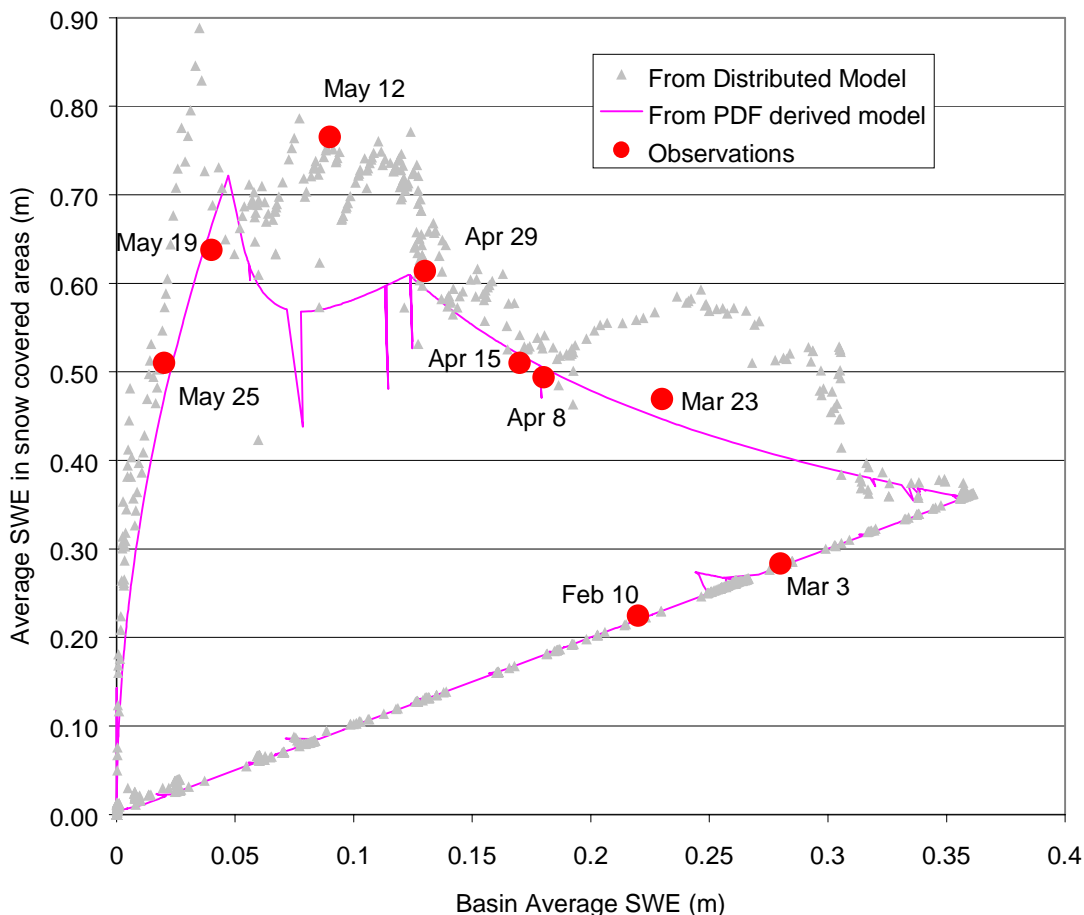
Figure 5-13. Average SWE of snow-covered areas (W_{sc}) versus average SWE in basin (W_a) at Upper Sheep Creek in winter of 1993. Note that there is a hysteresis with time going counter-clockwise around the loop, so that the roughly linear portion along the bottom of the graph is the part representing accumulation and is roughly on the 1:1 line. The reversal in trend of W_{sc} in the upper left corner of the graph is an important feature. Depletion curves that do not approach the origin correctly will result in W_{sc} values going towards a constant or towards ∞. A plot like the one above can be a useful diagnostic in examining alternative depletion curves

2.3. Second Approximation: Differential Solar Radiation with Differential Accumulation

In Figure 5-3 the depletion curve estimated from the above considerations had

less of an initial drop than did either the observations or the depletion curve output by the

distributed model. One reason for that is that the depletion curve derived from the peak of snow accumulation does not reflect differential melt during the later large melt events. At Upper Sheep Creek, the shallow snow is on a south-facing slope and the deep drift is on a north-facing slope. Figure 5-14 shows a scatter plot of the incoming solar radiation on March 21 (equinox) versus the snow water equivalence at peak accumulation. The fact that the initial melt of the basin's snowpack reduced the area more than would be predicted by the distribution of snow depth alone suggests that those areas with relatively shallow snowpack had energy inputs greater than the basin average energy input. According to the reasoning in equation 7 and Figure 5-2 differential melt has conceptually increased the variance. If differential melt is a factor, there is a question as to why the lumped model matches the distributed model so well. Figure 5-15 shows maps of the observed snow water equivalence on nine dates compared to maps simulated by a fully distributed model, including drifting effects, and a distributed model showing only differential energy inputs, primarily solar [*Luce et al.*, 1997; *Luce et al.*, 1998]. What this reveals is that the differential in melt exists, but is very small relative to the differential in accumulation. At Upper Sheep Creek, therefore, a lumped model accounting only for variance induced by differential accumulation makes a fair approximation. At sites with greater differential in energy inputs or less pronounced drifting the approximation may not be as good. It is, therefore, worthwhile to explore how differential melt might be incorporated in lumped models.

To improve the estimate of the snow-covered area for a given basin snow water equivalence, we start by recognizing that the use of M in equations 13-19 is as an index of the amount of energy input required before a site becomes bare. The amount of energy
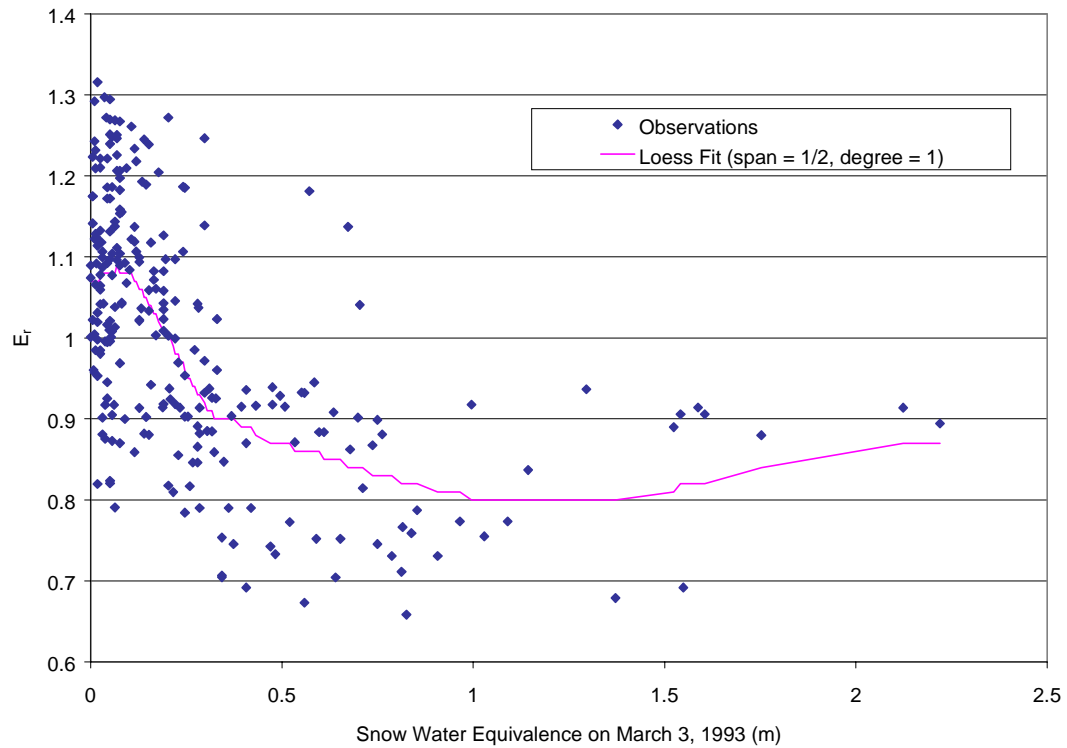
Figure 5-14. Ratio of the daily incoming direct-beam solar radiation at each cell in Figure 5-8 to the basin average daily direct-beam solar radiation versus the snow water equivalence measured on March 3, 1993. The solar radiation calculations were made for spring equinox ~ March 21.

required to melt a location with snow water equivalence, w, is roughly $w\lambda_f$, where λ_f is the latent heat of fusion. If the basin receives an amount of energy during a period, E_{ba} (kJ/m^2), and a location in the basin receives E_l (kJ/m^2), we define a relative energy input (unitless) as

$$E_r = E_l/E_{ba} \tag{23}$$

In this exercise, we define M as the basin average cumulative melt, or $M = E_{ba}/\lambda_f$, and we can calculate that a location will be snow free when

$$M = w/E_r = w_e \tag{24}$$
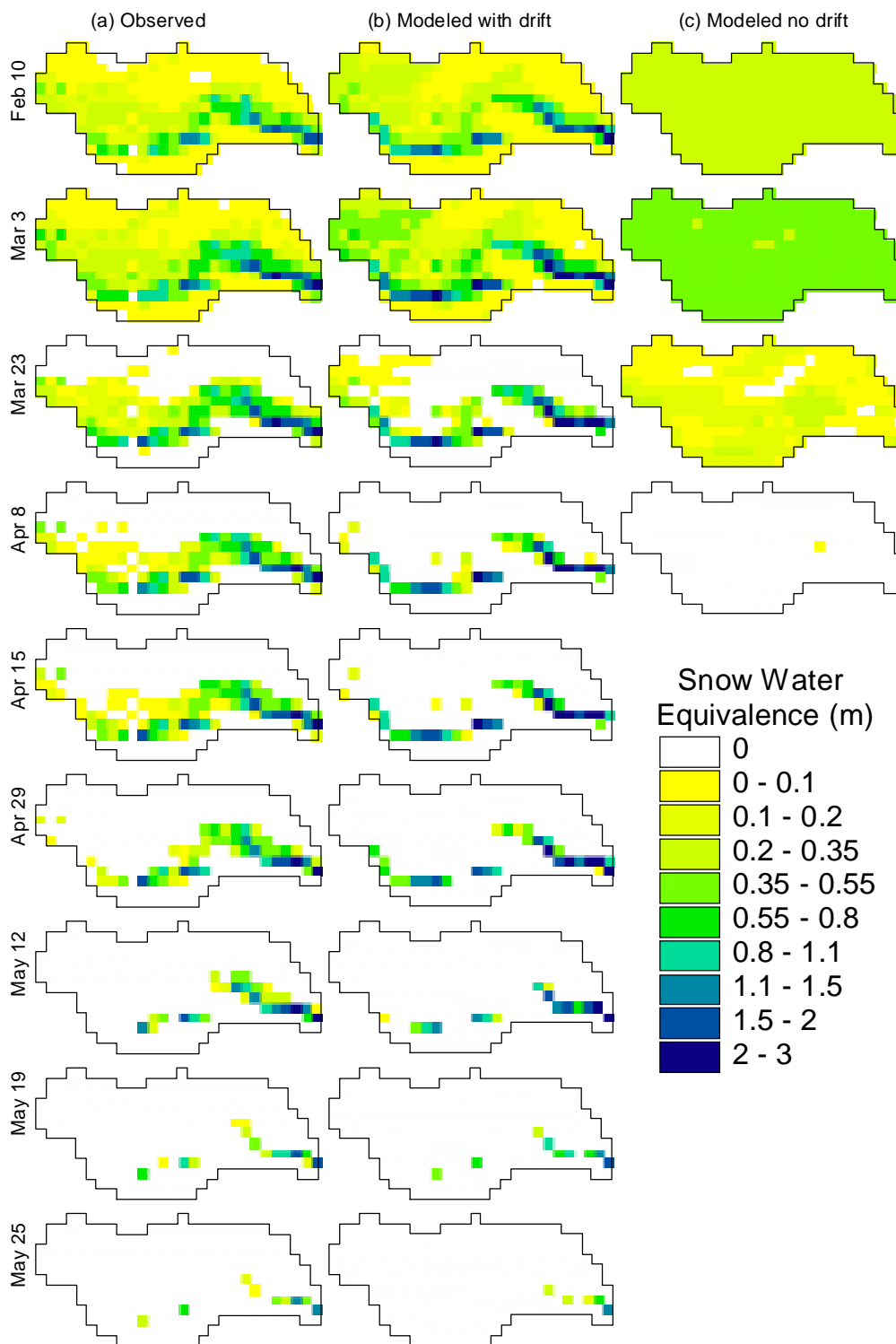
Figure 5-15. Maps of snow water equivalence in the spring of 1993 a) observed, b) simulated by fully distributed model, and c) simulated by fully distributed model except with uniform drift factors over entire basin.

so w_e is the snow water equivalence of each point normalized by the ratio of that point's

energy input to the basin average energy input. We can repeat the analyses described in

equations 13-19 with the distribution of the new variable, w_e, to produce a new areal

depletion curve $A_{dce}(M)$. One difficulty in this approach is that the calculation of melt

over time at each point in the basin can really only be accomplished with a distributed

snowmelt model. We can, however, derive a rough index of the differential melt from

examining the causes of differential melt. If solar radiation is a primary source of energy

for melt, and if there is sufficient relief in a basin to create strong differences in incoming

solar radiation, we could, for example, calculate the ratio of the total incoming solar

radiation at each point to the basin average on a day in the midst of the melt season.

Figure 5-16 shows the depletion curve estimated from the sample of w compared to the a

depletion curve estimated from the distribution of w_e, where E_r was estimated as the ratio

of incoming solar radiation at each point to the average of the basin at spring equinox

(~ March 21). We now have an areal depletion curve that reflects spatial variability in

accumulation and solar radiation. Other approximations could be made for other sources

of differential melt, e.g., patterns of sensible heat transfer based on locations with strong

or light wind.

Liston [1999] described how three pieces of information, the pdf of snow water

equivalence, the time series of element-average melt rate, and the time series of snow-

covered area, are somewhat interchangeable, in that if you know any two, you can

estimate the third. In particular, he described how to estimate the distribution of swe in a

basin from a series of images showing snow-covered area and from a model showing the

basin average melt. As described above this is a reasonable approximation in low relief
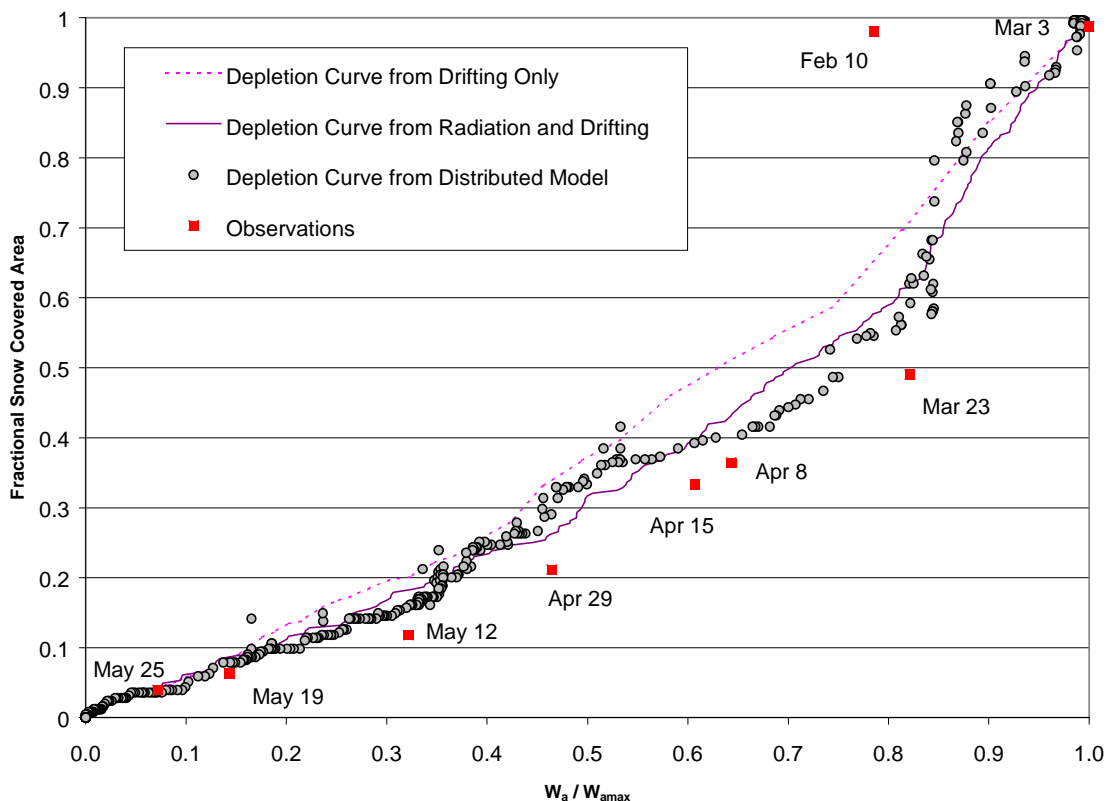
Figure 5-16. Depletion curve derived from the pdf of accumulation using consideration of relative accumulation and relative melt compared to the depletion curve derived from the pdf only and to a depletion curve derived from a distributed snowmelt model and from observations in the basin. The new curve is closer to both the curve from the distributed model and the observations.

landscapes. *Cline et al.* [1998] used images of snow-covered area and a model that accounted for spatial patterns in energy fluxes to back calculate the pdf of snow water equivalence in an alpine basin. The contrast between these two methods is similar to the contrast between the simple approach for estimating the depletion curve and the method just described.

Once we have gone so far as to recognize that differential melt exists, we really have less interest in the snow-covered area per se and a greater interest in the energy balance over the snow that remains. Homogeneous snowpack models (point scale models applied to a model element) assume that the snowpack exchanges energy at the mean rate

of the model element over the entire area of the element, generally resulting in a very fast

melt-out compared to the actual basin average snowmelt. In the lumped model of *Luce et

al*. [1999], the concept used was that the snowpack exchanged energy at a rate equal to

the mean rate of the model element over the fractional area covered by snow. Thus as the

snow melted, the snow remaining received only the element mean solar radiation,

sensible heat, and other fluxes multiplied by the fractional area coverage and the basin

average melt rate was reduced dramatically compared to the homogeneous model. If the

snow remaining does not receive the average basin heat fluxes, then a simple

multiplication by fractional snow-covered area is inadequate.

To illustrate this idea, we can define a fractional solar exposure, S_f (unitless), that

is the ratio of the total solar radiation received over the basin or model element to the

total solar radiation received on the snow-covered areas.

$$S_f = \frac{\int\limits_{B \times A_f} Q_{sn} dA}{\int\limits_{B} Q_{sn} dA} \tag{25}$$

where B denotes the entire basin area, and $B x A_f$ denotes the snow-covered area. In a

uniform, horizontal basin, S_f would be identical to A_f. However, in a basin with

topography and nonrandom accumulation and melt of snow, the ratio, S_f/A_f, can differ

substantially from one as the snow melts (Figure 5-17). When the basin is completely

snow-covered, the ratio is one. The observations in Figure 5-17 were calculated by

noting which locations had snow cover, and which did not, on each of the nine dates.

The curve was estimated by assuming that the elements in the basin melted out in the
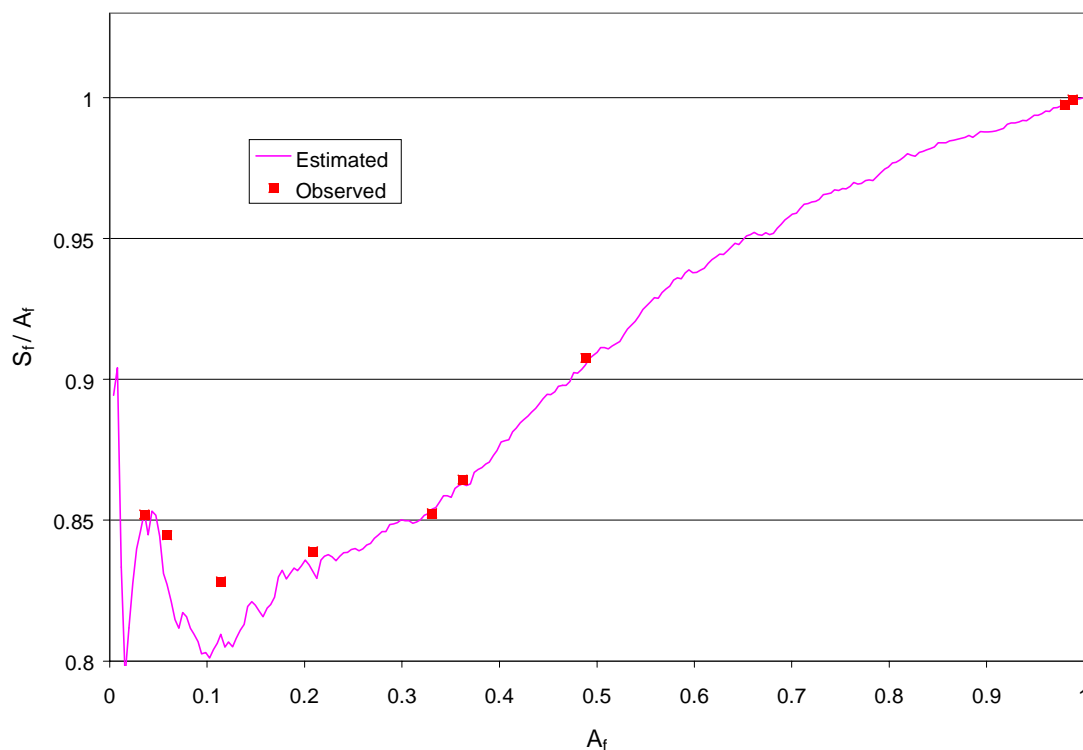
Figure 5-17. The fractional solar exposure is the ratio of the average daily direct-beam radiation over the snow-covered area to the average daily direct-beam radiation over the basin. This figure shows that using fractional snow-covered area alone to estimate net solar radiation for a basin or model element can result in a 20% error, even in a basin with relatively little relief.

order of the w_e values. For both calculations, the daily solar radiation map for March 21 was used to estimate solar radiation to each element.

By incorporating the energy corrected area depletion curve of Figure 5-16 with Figure 5-17, we can show how the ratio, S_f/A_f, varies with the basin average snow water equivalence, W_a (Figure 5-18), and we can go one step further in directly relating the fractional solar exposure, S_f, to W_a (Figure 5-19). We have named this curve a "hiding function." The hiding function serves the same function as the depletion curve did in *Luce et al.* [1999] in giving the appropriate fraction of the energy flux coming into a model element that goes toward melting snow. The term "hiding function" gives a sense
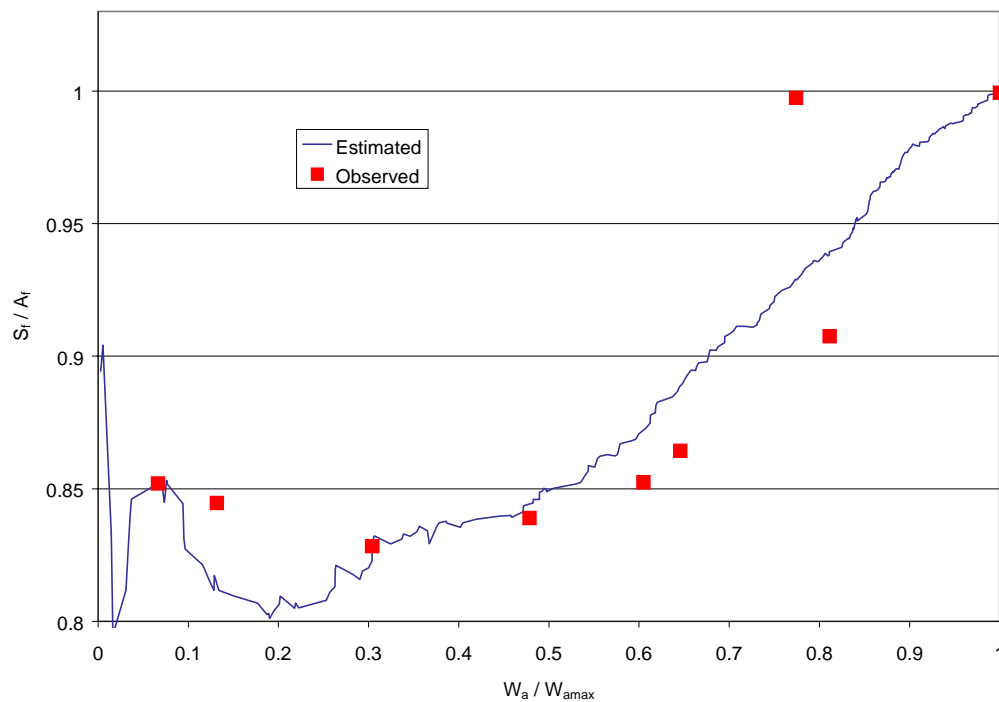
Figure 5-18. The relationship between fractional solar exposure on a per unit area basis and basin average snow water equivalence.
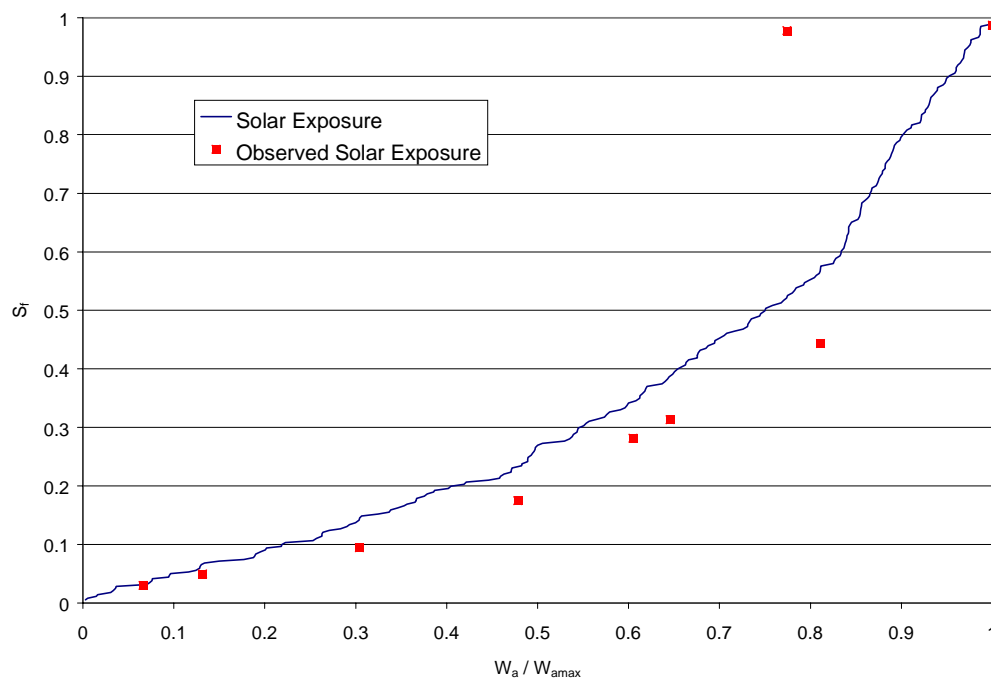
Figure 5-19. A hiding function showing how the solar exposure of snow-covered areas relates to the basin average snow water equivalence.

of the purpose and clearly separates it from the depletion curve terminology, although it

should be noted that in a basin with little relief or differential melt the depletion curve

and hiding function would be identical. The idea is that as the snowmelt season

progresses, we perceive the snow as remaining in patches. These patches are typically

places where the snow has been protected from solar radiation and warm winds, or in

essence "hidden." Snow can hide from these fluxes on steep north slopes, under forest

vegetation, at high elevations (where it is cooler), or even under other snow (as in drifts).

The hiding function better describes the relationship between basin average snow water

equivalence and fluxes like net radiation, and thus is more useful for purposes of

modeling in the fashion detailed in *Luce et al*. [1999] and for modeling the effect of

snow-covered areas on climate exchanges, when spatial heterogeneity in melt and

accumulation are both important processes.

3. SPATIAL SCALE AND THE RELATIVE IMPORTANCE OF DIFFERENTIAL ACCUMULATION AND MELT

Part of the art of modeling hydrologic processes is deciding which processes are

important when developing a model. The above discourse begins with a discussion about

how spatial heterogeneity in snow cover comes about as a result of spatially persistent

heterogeneity in accumulation and melt. In one example basin, about 0.25 km^2 in extent,

it was demonstrated that a model only considering spatial heterogeneity in accumulation

provided a reasonable approximation. Through further examination using distributed

snowmelt models, it was shown that the reason that the simpler model (including spatial

heterogeneity in accumulation but not in melt) worked so well was that the heterogeneity

in accumulation (in terms of the energy represented by the accumulated latent heat of

fusion) was much greater than the heterogeneity in incoming solar radiation. The

elevation range in Upper Sheep Creek is a little less than 200 m, so spatial heterogeneity

in melt caused by temperature differences is probably also small. Upper Sheep Creek has

a small spatial extent and the topography is rolling, and not steep. Strong winds at the

site are responsible for the differential accumulation. It is unlikely that we can say that,

in general, differential accumulation is a more important process to model than

differential melt. The question is, "How can we rationally decide which processes

leading to variability in snow water equivalence are the most important?" The answer to

such a question would also be helpful in determining the shape of depletion curves used

in models such as the National Weather Service River Forecasting System [*Anderson*,

1973], the Precipitation Runoff Modeling System [*Leavesley et al.*, 1983], and that of

Luce et al. [1999].

Important considerations include the degree of variation in incoming solar

radiation, precipitation, drifting, wind speed, and temperature over the model element.

For a model to be completely general for location and element scale, the subgrid

variability parameterization must include all of these. Knowledge of how element

characteristics might affect the relative role of each of these variations in the total

contribution to variability is helpful in evaluating less complete models and in

determining sources of error in predictions. Variation in incoming solar radiation

integrated over the course of the melt season would be strongly related to variability in

aspect, and would be more pronounced in steep terrain than in lower gradient terrain.

Steep terrain also tends to have higher relief and more shadows. Wind speed variability,

which leads to drifting and varying sensible heat, occurs in complex terrain or areas of

patchy thick vegetation. Forest vegetation tends to mute wind speed variability, because

the snowpack is exposed only to light winds. Variability in forest cover, however,

increases variability in exposure to wind. Variability in temperature and precipitation

both would result from large variation in elevation. Large elevation ranges are typically

associated with steep terrain. One characteristic that leads to an increase in the variability

of all items in the list is spatial extent. Larger elements will have more variability in each

of these key components, but the dominant source of variability may change with a

change in scale [*Seyfried and Wilcox*, 1995]

There is a rich and increasing literature discussing optimal scales for modeling,

process scales, and ideas like representative elementary areas [e.g., *Wood et al.*, 1988,

1990; *Fan and Bras*, 1994; *Wolock*, 1995; *Woods et al.*, 1995; *Blöschl*, 1999]. Processes

with characteristic lengths greater than the model element size are explicitly represented

in distributed models by variation in model parameters from element to element, and

processes with characteristic lengths on the order of or smaller than model elements are

parameterized [*Kirnbauer et al.*, 1994; *Blöschl and Sivapalan*, 1995; *Blöschl*, 1999].

This is displayed graphically in Figure 5-1 overlying a power spectrum of some process

(e.g., precipitation), showing that there is generally less power in subgrid processes than

in the explicitly represented processes. As the element scale increases, the subgrid scale

processes become increasingly nonnegligible compared to grid scale processes. If we

shrink the element size too small, however, we run into problems appropriately

distributing parameters and climate information to each element. The search for the

appropriate balance is in the search for the representative elementary area. One of the

means used in this search is to look for minima in the power spectrum to find the

temporal or spatial period which separates processes with different time or space scales.

Thus far, the search for a separation of scales or a "spectral gap" has only turned up good

results for the temporal scale used in climate modeling where there is a separation of

scales supporting use of a 1-hour time step [*Blöschl*, 1996]. For most hydrologic

processes, the power spectrum is monotonic [*Blöschl and Sivapalan*, 1995]. *Wood et al.*

[1990] plot the mean of an observable as a function of element size, stating that the

element size when the mean begins to vary smoothly is the representative elementary

area.

Figure 5-20 is a photograph of the area around Upper Sheep Creek giving a fairly

rhythmic appearance to the snow cover. Figure 5-21 is a map describing the propensity

toward snow drifting based on the model of *Liston and Sturm* [1998] in the Tollgate

Subbasin of Reynolds Creek [*Prasad et al.*, 2000]. From these, it might appear that there

may be a separation of scales in snow drifting. And one could imagine that the mean of

elements of an area having a length scale on the order of the inter-drift distance (in the

direction perpendicular to the drifts) would have little variation, or at least a smooth

variation in the mean. Unfortunately the scale of direct observation is fairly limited

covering only Upper Sheep Creek, or one cycle of what might be the dominant frequency

or spacing. *Seyfried and Wilcox* [1995] state that larger scale effect on precipitation from

elevation and windward-leeward differences may have as much or more influence on the

larger scale hydrology than the drifting. There is in addition the effect of elevation on

temperature affecting which precipitation becomes snow. We have an insufficient

number of measurements over a large spatial extent to be used in either a spectral

analysis or an analysis of mean versus extent. The problems with assumptions in the use

Figure 5-20. Photograph of area around Upper Sheep Creek in the Tollgate Subbasin of Reynolds Creek Experimental Watershed showing drifts on the lee of each ridgeline. (Photograph courtesy of Agricultural Research Service Northwest Watershed Research Center)

of models to approach this problem are well documented, and, for example, the map in Figure 5-21 assumes areally uniform precipitation. In any event, a finding that there is a separation of scales or an element area beyond which variability decreases would be specific to Reynolds Creek. What is more useful is general guidance.

The problems associated with identifying an optimal scale are so great that *Blöschl* [1999] suggested use of an arbitrary elementary area. Questions about how to parameterize sources of variability in snowpacks may help make this choice less arbitrary. As scales change, the processes dominating heterogeneity change [*Seyfried and Wilcox*, 1995]. Some of these processes may be less difficult to parameterize than others.
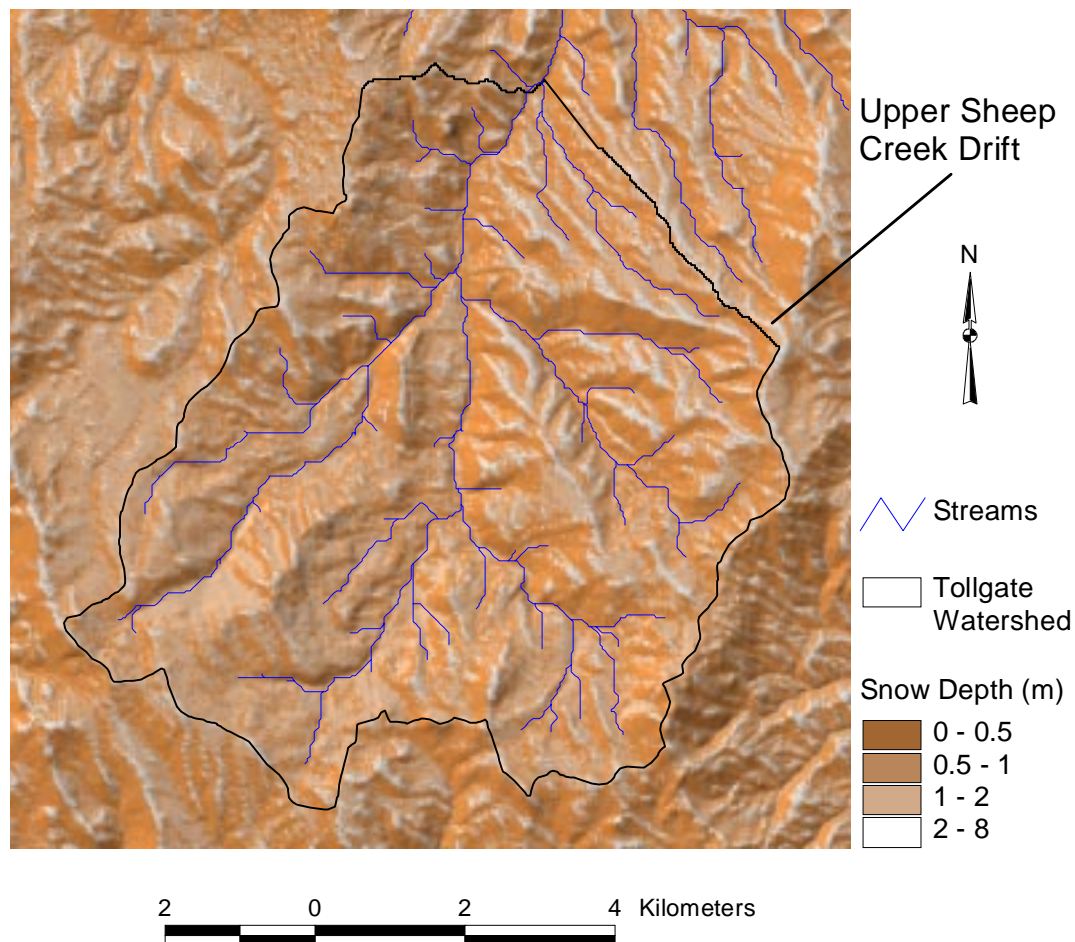
Figure 5-21. Map of relative drifting in the Tollgate Subbasin of the Reynolds Creek Watershed. Lighter colors indicate deeper snow drifts, the slight shading in gray scale indicates shaded relief to give the viewer a sense of topography. Most drifts are close to ridge lines, and the Tollgate basin drains to the north. [Data from *Prasad et al.*, 2000].

For example, differential accumulation by drifting and differential incoming solar radiation, alone or in combination, are more easily parameterized than the temperature differences caused by elevation because elevation-induced temperature differences cause differences in accumulation and differences in melt all at the same time. The difference in the phase of precipitation (water or ice) caused by temperature differences represents a significant amount of energy and a significant nonlinearity. In addition, where drifting may be relatively consistent from year to year when averaged over an area, elevational

patterns of temperature vary storm by storm and the temperature pattern within one storm can result in a significant simultaneous melt and accumulation within one element if the element covers much elevation. Given the already cited problems with using small elements, we can make an argument for using the largest cell size that is easily modeled or parameterized. It may be more practical to have elements that are not square shaped but shaped like elevation bands. In these elements, the radiation and drifting hiding functions can serve to describe within-element variability, where the explicit elevation-driven processes are modeled by the difference in the elevation of each band [e.g., *Bell and Moore*, 1999].

There are important advantages to using large model elements, such as improved accuracy in describing precipitation inputs, a need to specify only distributions or ranges of parameters instead of specifying the parameter value at each cell, and a better match between the scale of observations and the scale of the model. If elements are modeled as homogeneous units, there is a trade-off between the good aspects of large elements and the inaccuracy introduced by the assumption of homogeneity. If subgrid heterogeneity can be reasonably simulated, the nature of the question changes. At this stage, some aspects of subgrid heterogeneity in snow accumulation and melt can be simulated with parameterizations as well as they can be simulated by many small elements. Now we can make elements larger, in so far as we do not violate the assumptions of those subgrid parameterizations or select model elements with other, larger sources of variability. In steep mountains, the difficulties imposed by elevation variability may limit cell size even with drifting and radiation parameterizations. Alternatively in areas with rolling terrain without large elevational changes in short distances (e.g., the great plains), subgrid

parameterizations for drifting and radiation could useful. Asking the question of how large of an element we can use without sacrificing the accuracy of our subgrid scale parameterization is fundamentally different in nature from finding a representative elementary area by separation of scales or mean versus scale studies.

4. CONCLUSIONS

The objective of much snowmelt modeling is for use in prediction of runoff and its timing. This assists in management of water resources for irrigation, drinking water, and hydropower. It can also be helpful for flood prediction and warning. Models are employed for real-time prediction and for simulation of changes following land use changes or climate change. For many of these applications, there is, in fact, little need to have spatially distributed predictions of snowmelt and runoff. The need is generally for integrated information, net flow from a basin over some (brief or long) time period. This information can be generated by numerical integration of distributed point models, or by a model describing the entire basin.

The problem of scaling up models of snowmelt and runoff is a long-standing problem in hydrology.

> It rained steadily all night and as we had no shelter save such as the trees afforded we were pretty well soaked this morning. Stopped raining while we were at breakfast. Notwithstanding the almost constant rain the river is slowly receding from the high stage it has attained. The Indians say this is due to the fact that the snow is rapidly disappearing, and is now nearly gone, from the lower hills and the amount of the rain is not quite sufficient to keep up the river. … All of the hills 1000 ft. above us are white with snow that fell last night.
>
> D. C. Linsley, Civil Engineer, May 30, 1870, while camped along the Skagit River of western Washington [p. 216 in *Majors*, 1981].

The objective of scaling up is to improve the match between the scale of observations and the scale of modeling. Often, in practice, this implies interpreting weather observations at one or a few locations to describe the integrated behavior of a larger area. Sometimes it means interpreting spatially averaged climate output from a GCM to describe the hydrology of the GCM grid cell ground layer. Scaling up snowmelt models is accomplished by creating new parameterizations that describe the subgrid scale processes as functions of observable variables or grid-scale model state variables.

To derive new parameterizations, we must understand the process at the scale of interest, e.g., a scale at which homogeneity is no longer a valid assumption. At scales where spatial variability in snow water equivalence can be substantial, some measure of the variability of the snowpack must be included as a state variable or observable. Changes in snowpack variability derive from persistent patterns in accumulation or melt. Covariance between snow water equivalence and the accumulation rate or melt rate at each point is the source of temporal changes in spatial variance of snow water equivalence. For example, continued drifting in areas where substantial snow buildup has occurred due to drifting will increase the variance. Drifts often occur on north-facing slopes because of winds out of the southwest during synoptic scale cyclones. During the melt season, places with shallow snow melt more rapidly than places with deep, drifted snow, increasing the variance very early in the melt season.

Areal depletion curves can be one approach to parameterizing spatial variability in snow water equivalence caused by persistent accumulation patterns. This approach eliminates the need for knowledge of the location of the drift, but still necessitates information about the pdf of drifting in at least a relative sense. We have shown how

information on radiation can be added, thus accounting for information in the joint pdf of

drifting and exposure to direct-beam solar radiation. The hiding function approach

further corrects for the fact that snowpack evolution no longer depends on element

average energy inputs, but the energy inputs to that portion of the model element that is

covered by snow. If drifting occurs on north-facing slopes, the difference between

fractional area coverage and fractional solar exposure can be substantial. Hiding

functions can be used directly in the approach of *Luce et al*. [1999], where the

assumption was made that the fractional area exposure was an adequate estimate of the

snowpack's exposure to energy causing melt.

A reasonable ability to simulate the effects of subgrid scale heterogeneity allows

us to revisit ideas about optimal element size. Previous work on the subject has focused

finding the process scale as the scale above which the mean of an attribute varies

smoothly. The power spectrum concept has also found some use. The idea that the

nature of spatial heterogeneity changes with a change in scale challenges this concept,

and there is a common undercurrent in several pieces of literature stating that the model

form (e.g., choice of processes to represent) should follow from the choice of element

size, and the choice of element size should follow from available observations. It helps

to work the puzzle from both ends, however. The parameterizations discussed in this

paper represent variability caused by differential accumulation by drifting or by

precipitation differences and variability caused by differential incoming solar radiation,

and these parameterizations probably begin to fail at a scale where elevation differences

have significant bearing on spatial variability. Parameterizations to handle mixed

precipitation phase and mixed accumulation and melt within one element caused by large

within-element variations in elevation and, therefore, temperature, are difficult, and may

functionally default to distributed models with finer spatial resolution. In areas with

enough relief to generate drifting and varying solar irradiation, but not significant

elevation differences, the parameterizations presented here allow matching element size

to data availability with some ease, and in fact represent substantial improvements over

models using no parameterization for subgrid variability. In steep mountainous areas,

however, large-scale snow drifting may occur over spatial scales incorporating significant

elevational change. While the parameterizations we present could be used in fairly large

elements – each having substantial subgrid variability – some of the advantage to using a

subgrid parameterization would be lost because there would also be differences in

drifting between model elements, and the modeler would be required to supply

information about the specific pattern of that large scale variation. If the model elements

are small, it may be difficult to collect observations at a scale that allow parameter

estimation at each element. Given that satellite data on snow cover is more frequent for

elements with larger footprints, the parameterizations we discuss may increase the

support scale of the model enough to allow remotely observed patterns in snow cover to

be used for spatially distributed parameter estimates.

REFERENCES

Anderson, E. A., National weather service river forecast system-snow accumulation and
  ablation model, *NOAA Technical Memorandum NWS HYDRO-17*, U.S. Dept of
  Commerce, Silver Spring, Md., 1973.

Arola, A., and D. P. Lettenmaier, Effects of subgrid spatial heterogeneity on gcm-scale
  land surface energy and moisture fluxes, *J. Climate*, *9*, 1339-1349, 1996.

Barry, R. G., *Mountain Weather and Climate*, 2nd Edition, Routledge, New York, 1992.

Bathurst, J. C., and K. R. Cooley, Use of the she hydrological modelling system to investigate basin response to snowmelt at reynolds Creek, Idaho, *J. Hydrol.*, *175*, 181-211, 1996.

Bell, V. A., and R. J. Moore, An elevation-dependent snowmelt model for upland britain, *Hydrol. Process.*, *13*, 1887-1904, 1999.

Beven, K., Changing ideas in hydrology—the case of physically-based models, *J. Hydrol.*, *105*, 157-172, 1989.

Beven, K., Linking parameters across scales: Subgrid parameterizations and scale dependent hydrological models, *Hydrol. Process.*, *9*, 507-525, 1995.

Beven, K., and A. Binley, The future of distributed models: Model calibration and uncertainty prediction, *Hydrol. Process.*, *6*, 279-298, 1992.

Beven, K. J., and M. J. Kirkby, A physically based variable contributing area model of basin hydrology, *Hydrol. Sci. Bull.*, *24*, 43-69, 1979.

Blöschl, G., *Scale and Scaling in Hydrology*, Habilitationsschrift, Weiner Mitteilungen Wasser Abwasser Gewasser, Wien, 1996.

Blöschl, G., Scaling issues in snow hydrology, *Hydrol. Process.*, *13*, 2149-2175, 1999.

Blöschl, G., and R. Kirnbauer, An analysis of snow cover patterns in a small alpine catchment, *Hydrol. Process.*, *6*, 99-109, 1992.

Blöschl, G., and M. Sivapalan, Scale issues in hydrological modelling: A review, *Hydrol. Process.*, *9*, 251-290, 1995.

Bresler, E., and G. Dagan, Unsaturated flow in spatially variable fields, 2. Application of water flow models to various fields, *Water Resour. Res.*, *19*, 421-428, 1983.

Brutsaert, W., Catchment-scale evaporation and the atmospheric boundary layer, *Water Resour. Res.*, *22*, 39S-45S, 1986.

Cline, D. W., R. C. Bales, and J. Dozier, Estimating the spatial distribution of snow in mountain basins using remote sensing and energy balance modeling, *Water Resour. Res.*, *34*, 1275-1285, 1998.

Conway, H., and R. Benedict, Infiltration of water into snow, *Water Resour. Res.*, *30*, 641-649, 1994.

Cooley, K. R., Snowpack variability on western rangelands, in *Proceedings of the 56th Western Snow Conference*, pp. 1-12, Kalispell, Montana, 1988.

Dagan, G., and E. Bresler, Unsaturated flow in spatially variable fields, *Water Resour. Res.*, *19*, 413-420, 1983.

Daly, C., R. P. Neilson, and D. L. Phillips, A statistical-topographic model for mapping climatological precipitation over mountainous terrain, *J. Appl. Meteorol.*, *33*, 140-150, 1994.

Dingman, S. L., *Physical Hydrology*, Prentice Hall, Englewood Cliffs, N.J., 1994.

Dooge, J. C. I., Looking for hydrologic laws, *Water Resour. Res.*, *22*, 46S-58S, 1986.

Dunne, T., and L. B. Leopold, *Water in Environmental Planning*, W. H. Freeman and Co., San Francisco, 1978.

Elder, K., W. Rosenthal, and R. Davis, Estimating the spatial distribution of snow water equivalence in a montane watershed, *Hydrol. Process.*, *12*, 1793-1808, 1998.

Fan, Y., and R. L. Bras, On the concept of a representative elementary area (rea) in catchment runoff, *Hydrol. Process.*, *9*, 821-832, 1994.

Hanson, C. L., and G. L. Johnson, Spatial and temporal precipitation characteristics in southwest Idaho, in *Management of Irrigation Systems: Integated Perspectives*, edited by R. G. Allen and C. M. U. Neale, pp. 394-401, American Society of Civil Engineers, Park City, Utah, 1993.

Hathaway, G. A., M. Bernard, and U.S. Army Corps of Engineers, Snow hydrology, summary report of the snow investigations, U.S. Army Corps of Engineers, North Pacific Division, Portland, Oregon, 1956.

Johnson, G. L., and C. Hanson, Topographic and atmospheric influences on precipitation variability over a mountainous watershed, *J. Appl. Meteorol.*, *34*, 68-87, 1995.

Kattleman, R., Spatial variability of snowpack outflow at a sierra nevada site, *Ann. Glaciol.*, *13*, 124-128, 1989.

Kirnbauer, R., and G. Blöschl, How similar are snow cover patterns from year to year?, *Dtsch. gewässerkdl. Mitt.*, *37*, 113-121, 1994.

Kirnbauer, R., G. Blöschl, and D. Gutknecht, Entering the era of distributed snow models, *Nord. Hydrol.*, *25*, 1-24, 1994.

Klemeš, V., Dilettantism in hydrology: Transition or destiny, *Water Resour. Res.*, *22*, 177S-188S, 1986.

Leavesley, G. H., R. W. Lichty, B. M. Troutman, and L. G. Saindon, Precipitation-runoff modeling system--users manual, *Water Resources Investigations Report 83-4238*, U.S. Geological Survey, 1983.

Leavesley, G. H., and L. G. Stannard, Application of remotely sensed data in a distributed parameter watershed model, in *Workshop on Applications of Remote*

Sensing in Hydrology, edited by G. W. Kite and A. Wankiewicz, pp. 47-64, National Hydrology Research Institute, Saskatoon, Sask., 1990.

Liston, G. E., Interrelationships among snow distribution, snowmelt, and snow cover depletion: Implications for atmospheric, hydrologic, and ecologic modeling, *J. Appl. Meteorol.*, *38*, 1474-1487, 1999.

Liston, G. E., and M. Sturm, A snow-transport model for complex terrain, *J. Glaciol.*, *44*, 498-516, 1998.

Luce, C. H., D. G. Tarboton, and K. R. Cooley, Spatially distributed snowmelt inputs to a semi-arid mountain watershed, in *Proceedings of the 65th Western Snow Conference*, pp. 77-89, Banff, Alberta, 1997.

Luce, C. H., D. G. Tarboton, and K. R. Cooley, The influence of the spatial distribution of snow on basin-averaged snowmelt, *Hydrol. Process.*, *12*, 1671-1683, 1998.

Luce, C. H., D. G. Tarboton, and K. R. Cooley, Subgrid parameterization of snow distribution for an energy and mass balance snow cover model, *Hydrol. Process.*, *13*, 1921-1933, 1999.

Majors, H. M., A railroad survey of the Sauk and Wenatchee rivers in 1870, *Northwest Discovery*, *2*, 202-266, 1981.

Male, D. H., and R. J. Granger, Snow surface energy exchange, *Water Resour. Res.*, *17*, 609-627, 1981.

Marks, D., and J. Dozier, Climate and energy exchange at the snow surface in the alpine region of the sierra nevada, 2. Snow cover energy balance, *Water Resour. Res.*, *28*, 3043-3054, 1992.

Moore, R. J., The probability-distributed principle and runoff production at point and basin scales, *Hydrolog. Sci. J.*, *30*, 273-297, 1985.

Obled, C., Hydrological modeling in regions of rugged relief, in *Hydrology in Mountainous Regions. I. Hydrological Measurements; the Water Cycle*, edited by H. Lang and A. Musy, pp. 599-613, IAHS Publ. 193, Proc. Lausanne Symp., 1990.

Post, A., and E. LaChapelle, *Glacier Ice*, University of Washington Press, Seattle, Washington, 1971.

Prasad, R., D. G. Tarboton, G. E. Liston, C. H. Luce, and M. S. Seyfried, Testing a blowing snow model against distributed snow measurements at Upper Sheep Creek, *Water Resour. Res.*, in press, 2000.

Seyfried, M. S., and B. P. Wilcox, Scale and the nature of spatial variability: Field examples having implications for hydrologic modeling, *Water Resour. Res.*, *31*, 173-184, 1995.

Shuttleworth, J. W., Macrohydrology-the new challenge for process hydrology, *J. Hydrol.*, *100*, 31-56, 1988.

Stewart, J. B., E. T. Engman, R. A. Feddes, and Y. Kerr (editors), *Scaling Up in Hydrology Using Remote Sensing*, John Wiley and Sons, Chichester, 1996.

Sturm, M., J. Holmgren, and G. E. Liston, A seasonal snow cover classification system for local to global applications, *J. Climate*, *8*, 1261-1283, 1995.

Tarboton, D. G., T. G. Chowdhury, and T. H. Jackson, A spatially distributed energy balance snowmelt model, in *Biogeochemistry of Seasonally Snow-Covered Catchments, Proceedings of a Boulder Symposium*, edited by K. A. Tonnessen, M. W. Williams and M. Tranter, pp. 141-155, IAHS Publ. no. 228, Boulder, Colo., 1995.

Tarboton, D. G., and C. H. Luce, Utah energy balance snow accumulation and melt model (UEB), computer model technical description and users guide, Utah Water Research Laboratory and USDA Forest Service Intermountain Research Station (http://www.engineering.usu.edu/dtarb/), 1996.

Wigmosta, M. S., L. W. Vail, and D. P. Lettenmaier, A distributed hydrology-vegetation model for complex terrain, *Water Resour. Res.*, *30*, 1665-1679, 1994.

Williams, M. W., R. Sommerfeld, S. Massman, and R. Rikkers, Correlation lengths of meltwater flow through ripe snowpacks, colorado front range, USA, *Hydrol. Process.*, *13*, 1807-1826, 1999.

Winstral, A., K. Elder, and R. Davis, Implementation of digital terrain analysis to capture the effects of wind redistribution in spatial snow modeling, in *Proceedings of the 67th Western Snow Conference*, pp. 81-93, South Lake Tahoe, California, 1999.

Wolock, D. M., Effects of subbasin size on topographic characteristics and simulated flow paths in sleepers river watershed, Vermont, *Water Resour. Res.*, *31*, 1989-1997, 1995.

Wood, E. F., M. Sivapalan, and K. Beven, Similarity and scale in catchment storm response, *Rev. Geophys.*, *28*, 1-18, 1990.

Wood, E. F., M. Sivapalan, K. Beven, and L. Band, Effects of spatial variability and scale with implications to hydrologic modeling, *J. Hydrol.*, *102*, 29-47, 1988.

Woods, R., M. Sivapalan, and M. Duncan, Investigating the representative elementary area concept: An approach based on field data, *Hydrol. Process.*, *9*, 291-312, 1995.

CHAPTER 6

EPILOGUE

The impetus for scaling in hydrologic process models has philosophical roots

grounded in the strengths and weaknesses of the so-called "physically based" and "black

box" or "empirical" modeling approaches. Models relate one set of information we have

to another set of information we desire, for example, weather (input) to runoff (output).

Very powerful data-driven approaches such as data mining, neural networks, and genetic

algorithms exist to relate observed inputs to observed outputs. Insofar as we are

concerned with relating inputs and outputs of very similar to those already observed,

these tools can be efficient and accurate. When unique events or sequences of events

occur, however, the predictions may become inaccurate, and these models cannot account

for changes to the system such as a climate change or land use change. In principle,

physically based models circumvent these shortcomings through formulations based on

first-principles and hydrologic laws. The extreme conceptualization of a physically based

model can probably never be realized, however, because real hydrologic systems are very

complex and system properties and boundary conditions cannot be feasibly be mapped at

the ultra-fine scale required for solution of Navier-Stokes equations for flow through

pores. Consequently, most "physically based" models actually use some degree of

lumping, for example Darcy's law to approximate flow through soil pores, or Manning's

or Chezy's equation to describe the effects of surface roughness on water flow. In this

lumping, "the objective is to obtain a simple relationship, in order to replace the

complicated interactions at smaller scales than those employed explicitly in the model" [*Brutsaert*, 1986, p. 40S]. Functionally, such relationships require calibration, and we come to an interesting question, "What is the true nature of the difference between empirical and physically based models?"

Perhaps the answer is in our belief that extrapolation using a physically based empirical model (as opposed to a strictly empirical model) is more "acceptable." Certainly, we have some reassurance that conservation of mass will be maintained, which may not be guaranteed by neural networks. It is also quite a bit easier to know which parameter to adjust in a physically based model than in a neural network or genetically derived algorithm. However, just because the model form is roughly specified does not excuse hydrologists from the concept that extrapolation beyond observations is based on belief. If a physically based model uses parameters that are amenable to experimentation, an effort to relate observable physical attributes to parameter values, such as the texture of a porous media to its hydraulic conductivity [e.g., *Freeze and Cherry*, 1979], assists in extending more complex models to different areas. However, when the unit of analysis (e.g., a hillslope or a 30-m square) becomes larger than the experimental apparatus (e.g., a core or a 1-m^2 plot), there will probably be greater spatial variability, the parameter value derived in the experiments may no longer apply, and the "effective" parameters for each unit of analysis are needed.

One class of physically based models is the distributed model. In this class of model, although the unit of analysis may be much larger than the experimental basis for parameter identification, physical laws, such as conservation of mass, are used as a basis to numerically integrate many small model elements, with the parameters for each

element defined by previous small-scale experimental work. In practice, however, it is unusual to have sufficient topographic information or plant location information to reasonably assign parameter values at scales finer than 30 m (based on the size of USGS DEM's and LANDSAT imagery). This scale is very coarse compared to *experimental* observations of snowmelt estimation or runoff prediction. Consequently, the parameters for distributed model elements must in practice be calibrated, whether it be for the net shading effect of canopy on snowmelt or the effective soil roughness. The distributed snowmelt model used in this study, for example, requires calibration of a drift factor at the element scale. If input-output data are available for each model element within the "unit of analysis," then calibration is potentially a straightforward task. The model elements effectively become the unit of analysis through this approach. If input-output data are not available at each grid cell, then the "distributed" model becomes a form of lumped model, relating large-scale outputs to large-scale inputs using parameters fitted by large-scale input-output data. Extrapolating to changed conditions in a watershed (e.g., through land use or climate change) becomes a speculative affair, because we are no longer certain of element-by-element parameters [see *Beven*, 1989 for similar discussion].

So the reader now recognizes that physically based models are really a functional form to which we fit data. If there is a severe mismatch between the scale of observations supporting a particular set of parameter values and scale of the model elements, the ability to extrapolate is in question. This can occur if the parameter values are identified by relationships derived in small-scale experiments and applied to much larger elements, or if the parameter values are identified by fitting to data with a support

or spacing covering many model elements. Most statisticians would probably explain this as a fairly elementary problem in sampling theory. It is difficult to extrapolate to the population of 30-m or hillslope-length elements from a sample of watersheds, and it is difficult to extrapolate to the population of hillslope-length elements or watersheds from a sample of plots and soil cores.

The purpose of scaling hydrologic models is to create a better match between our units of analysis, the things we sample or observe, and the population to which we wish to extrapolate. This creates a situation more amenable to experimentation or systematic observation to learn more about the population of small watersheds or large units of analysis. In the past, the phrase "lumped empirical" model was frequently used, implying that lumped models must, of necessity, be empirical. Through scaling, it is hoped that we can provide a physical basis to "lumped" models, or more specifically models with larger support scales. Darcy's law is an empirical relationship, "lumped" over many pores, that has some physical basis. The simplification of the problem of complex flow through a pore network produced a relationship amenable to experimentation and systematic observation with samples of porous media. Derivation of equations for saturated groundwater flow based on Darcy's law produced simplifications that were again amenable to experimentation and systematic observation, but this time of larger aquifers. Similar advances are needed for surface water and snow hydrology.

This dissertation is a step in the direction of simplifying distributed snowpack models to increase the ease with which we can describe, measure, or categorize basin-level relationships between a time series of weather observations and snowmelt or snow cover. These four papers represent a beginning for some ideas about spatial scaling of

snowmelt models. Some of the thoughts are equally useful to distributed snowmelt models using large elements. Few will read these papers without some thoughts for improvement. For example, the arguments provided for the importance of being able to increase the spatial support of snowmelt models can be applied to the importance of increasing the temporal support as well. What is the temporal support of average precipitation over a basin if we are working with data from temporally high resolution precipitation gages with 8-inch orifices spaced 10 km apart? If this is our input data, we must realize that any scaling of that data is part of the model. While the issue of temporal support increases was not explicitly discussed, some of the findings on diurnal patterns and low frequency variability in snowpack heating may contribute to this aspect of the problem.

Each of the four papers has a conclusion summarizing its results. The conclusion of the four taken together is not the concatenation of the conclusions of the four papers but is simply that there are great opportunities to learn more about snowpacks at a variety of scales by attempting to quantitatively describe them at different scales. When exploring detailed data from a single site, we learned that by realizing that heating and cooling of the snowpack has a strong diurnal component and a strong low frequency component, a fairly simple, yet reasonably accurate, model of the heat flux into and out of the snowpack, both top and bottom, could be derived. From examining the same site and weather information at a few others, we realized the importance of knowledge about the regional synoptic weather in estimating snowmelt at a point. Because the synoptic weather pattern dictates the presence and persistence of inversions and fog in valleys, it can have a profound influence on the longwave radiation balance in those locations.

Examination of detailed snow water equivalence data from a small basin showed us that effective parameters and even a small number distributed patches or zones is not adequate to address extreme heterogeneity in snow distribution. We also learned that the greatest influence on the spatial variability of snow water equivalence for Upper Sheep Creek, a small semi-arid watershed in the mountains of southwest Idaho, was snow drifting and not differential solar radiation, although solar radiation differences did contribute to spatial variability. Remaining work described the physical basis of parameterizations relating snow drifting and topographic (solar radiation) information to the basin-level snowmelt through the use of depletion curves or hiding functions. In this case study of one basin, the curves are empirical in nature. It is hoped that through systematic observation of other basins, a more general theory relating the shape of these curves to basin topography, vegetation, and climate can be established.

REFERENCES

Beven, K., Changing ideas in hydrology—the case of physically-based models, *J. Hydrol.*, *105*, 157-172, 1989.

Brutsaert, W., Catchment-scale evaporation and the atmospheric boundary layer, *Water Resour. Res.*, *22*, 39S-45S, 1986.

Freeze, R. A., and J. A. Cherry, *Groundwater*, Prentice Hall, Englewood Cliffs, N.J., 1979.

APPENDIX

01-AUG-2000 16:36 FROM JOHN WILEY AND SONS TO 90012083734391 P.01/02

21-AUG-2000 16:36 FROM JOHN WILEY AND SONS TO 90012083734391 P.02/02

~ 1 AUG 2000

--- Begin Forwarded Message ---
Date: Wed, 26 Jul 2000 09:06:55 -0600
From: Charlie Luce <cluce@rmci.net>
Subject: Permission to use papers as chapters in a dissertation
Sender: Charlie Luce <cluce@rmci.net>
To: cs-journals@wiley.co.uk, HP-journal@bristol.ac.uk
Cc: dtarb@cc.usu.edu
Reply-To: Charlie Luce <cluce@rmci.net>
Message-ID: <20000726115O9.JAA38576@sv1.boise.int.fs.fed.us>

Dear Wiley/Hydrological Processes

I have published the following two papers in Hydrological Processes during
my studies towards a PhD degree at Utah State University:

Luce, C. H., D. G. Tarboton and K. R. Cooley. (1998), "The Influence of the
Spatial Distribution of Snow on Basin-Averaged Snowmelt," Hydrological
Processes, 12(10-11): 1671-1683.

and

Luce, C. H., D. G. Tarboton and K. R. Cooley. (1999), "Sub-grid
parameterization of snow distribution for an energy and mass balance snow
cover model." Hydrological Processes, 13(12-13): 1921-1933.

Now I am completing my dissertation and each of these papers will be a
separate chapter. Please let me know what copyright permission or
acknowledgement is needed to include these papers as chapters in my
dissertation.

Thank you,
Charlie Luce

Charles H. Luce   Ph: 208-373-4382
Research Hydrologist   Fax: 208-373-4391
USDA Forest Service   e-mail:cluce@rmci.net
Rocky Mountain Research Station
316 E. Myrtle
Boise, ID 83702

--- End Forwarded Message ---

****

Sue Amesbury
Journal Secretary
Hydrological Processes
Editorial Office
University of Bristol
University Road
BRISTOL BS8 1SS
ENGLAND

phone: +44-(0)117-928-7871   fax: +44-(0)117-928-7878
email: hp-journal@bristol.ac.uk
website: www.interscience.wiley.com/jpages/0885-6087/
****

Permission granted for the use requested.
Proper credit must be given to our publication.

Credit must include the following
components: Title of the work, Author(s)
and/or Editor(s) name(s) Copyright year.
©John Wiley & Sons Limited.
Reproduced with permission.

Permissions Department
John Wiley & Sons Limited
If material appears in our work with credit to another
source, authorisation from that source must be obtained.

1-8-00

(W)
WILEY

John Wiley & Sons Ltd
Baffins Lane, Chichester,
West Sussex, PO19 1UD, UK

Tel: +44 (0)1243 770322 (direct)
Fax: +44 (0)1243 770460 (direct)

FAX MESSAGE

To:	Charles H Luce Research Hydrologist USDA Forest Service Rocky Mountain Research Station 316 E. Myrtle Boise, ID 83702 USA
Fax No:	001 208 373 4391
From:	Lesley Griffin, Permissions Department
Date:	01 August 2000
Subject:	Copyright Permission Request
No. of pages (including this page):	TWO

Dear Charles H Research Hydrologist

Hydrological Processes,1921-1933

Please find attached our response to your permission request.

Yours sincerely

Lesley Griffin

Lesley Griffin
Permission Department
Email: lgriffin@wiley.co.uk

CURRICULUM VITAE

Charles H. Luce

Research Hydrologist   Phone: 208-373-4382
USDA Forest Service   Fax: 208-373-4391
Rocky Mountain Research Station   E-mail: cluce@rmci.net
316 E. Myrtle, Boise, ID 83702

Research Interests
    Scaling Hydrologic and Geomorphic Processes
    Snow Hydrology
    Watershed Hydrology
    Forest Road Effects on Hydrology, Slope Stability, and Erosion
    Slope Stability and Erosion
    Stochastic Climate Simulation

Education
Academic Degreees

Ph.D.   Civil Engineering   Utah State University   2000
        Dissertation: "Scale Influences on the Representation of
        Snowpack Processes", 202 pp.
M.S.   Forest Hydrology   University of Washington   1990
        Thesis: "Analysis of infiltration and overland flow from small
        plots on forest roads", 101 pp.
B.S.   Forest Management   University of Washington   1986
        Thesis: "Literature Review on the Effects of a Forest Canopy on
        Snowpack Structure and Stability", 26 pp.

Additional Training, Special Courses

    Channel Morphology and Stream Restoration, Wildland Hydrology Consultants, 1992
    Watershed Management, University of Washington, 1990
    Statistical Design of Experiments, University of Washington, 1989
    Riparian Area Management, Oregon State University, 1989
    Channel Geomorphology, University of Washington, 1989
    Urban hydrology and erosion, American Water Resources Association, 1988
    Forest Management Effects on Streamflow, University of Washington, 1988
    National Avalanche School, 1985

Professional Experience
    1998- :   Research Hydrologist, Rocky Mountain Research Station, Boise, Idaho.
    1991-1998: Research Hydrologist, Intermountain Research Station, Moscow, Idaho.
    1989-1991: District Hydrologist, Siskiyou National Forest, Powers, Oregon.
    1989-1990: Research Assistant, Dept. of Forestry, University of Washington, Seattle.

1988-1989: Natural Resource Planning Intern, King County, Seattle, Washington.
1985:   Teaching Assistant, Dept. of Forestry, University of Washington, Seattle.
1983-1987   (periodically): Research Assistant, Dept. of Geophysics, Univ. of
            Washington, Seattle.

Professional Distinctions
Awards and Honors
2nd Place, Student Paper Competition, Utah State Chapter American Water Resources
    Association, 1995
Certificate of Merit, USDA Forest Service Intermountain Research Station: "For the
    rapid development of a hydrology model of road surfaces." 1991.
Member of Xi Sigma Pi National Forestry Honor Society, 1985-present

Invitations to Address National and International Meetings
American Geophysical Union Fall Meeting, Session on Snow Hydrology, San
    Francisco, California, 1998.
Assessing Watershed Conditions – A Holistic Approach, American Institute of
    Hydrology, Corvallis, Oregon, 1993.
USDA Forest Service National Hydrology Meeting, Session on Sediment Modeling,
    Phoenix, Arizona, 1992.

Invitations to Address Regional Meetings or Workshops and Government Agencies
USDA Forest Service National Sediment Modeling Workshop, Tucson, Arizona, 2000
Forest Sedimentation Conference, Northwest Forest Soils Council and Western
    Forestry and Conservation Association, Tigard, Oregon, 1999.
USDI Fish and Wildlife Service Snake River Region, Boise, Idaho, 1999.
International Mountain Logging and 10th Pacific Northwest Skyline Symposium,
    International Union of Forestry Research Organizations and Oregon State
    University. Corvallis, Oregon, 1999.
USDI Fish and Wildlife Service Snake River Region, Boise, Idaho, 1998.
National Council of the Paper Industry for Air and Stream Improvement Watershed
    Task Group Research Workshop, Eugene, Oregon, 1998.
Oregon State Dept of Forestry, Forest Practices Advisory Committee, Salem, Oregon,
    1998.
USDA Forest Service Region 6 Road Management Workshop, Eugene, Oregon, 1994.
Water Erosion Prediction Project Validation Meeting. National Soil Erosion Research
    Laboratory, West Lafayette, Indiana, 1992.

Professional Service
Membership in Professional Societies
American Geophysical Union, 1988 to Present
American Society for Civil Engineers, 1992 to Present
Xi Sigma Pi Forestry Honor Society, 1983 to Present
American Water Resources Association, 1988 to 1996
Society of American Foresters, 1983 to 1991

Committee Assignments and Offices
    American Geophysical Union, Surface Water Committee, 1995 to present
    Vice Chair Paradise Creek Watershed Advisory Group, 1996-1998. Appointed by
      State of Idaho.
    American Society for Civil Engineers, Watershed Management Technical Committee,
      1993 to 1997 term
    Xi Sigma Pi Forestry Honor Society, Chapter Vice-President, 1984-1985, and Chapter
      President, 1985-1986

Conference Session Organization
    American Geophysical Union Fall Meeting, Session on Hydrologic and Sedimentation
      Effects of Forest Roads, San Francisco California, 1998.

Editorship
    Guest Editor, Earth Surface Processes and Landforms, Special Issue on Forest Roads,
      1999-2001.

Journal Reviewer for

Water Resources Research	Hydrological Processes
Journal of Hydrologic Engineering	AGU Water Resources Monograph
Journal Environmental Quality	Series
Australian Journal of Soil Research	Journal of the American Water
Water, Air, and Soil Pollution	Resources Association
International Journal of Wildland Fire	Earth Surface Processes and Landforms

Proposal Reviewer for
    National Science Foundation.
    National Aeronautic and Space Administration, Land Surface Hydrology Program.

University Affiliations
    Affiliate Faculty Boise State University Department of Geosciences.
      Committee member for one M.S. student, Patricia Jones, current
    Affiliate Faculty Univ. of Idaho College of Forestry, Wildlife, and Range Sciences.
      Committee member for one M.S. student, David Gloss, 1995

Grants Awarded
    USDI Bureau of Land Management, Oregon State Office, $566,000, Road Erosion
      under Natural Rainfall, Principal Investigator, 1994-present.
    USDI Bureau of Land Management, Eugene District, $110,000, For development of a
      system to use GPS and computer data entry to map road drainage systems and
      culverts for the purpose of erosion prediction using GIS, Principal Investigator,
      1997-present.
    Siuslaw Watershed Council, $22,500, For development of a system to use GPS and
      computer data entry to map road drainage systems and culverts for the purpose of
      erosion prediction using GIS, Principal Investigator, 1999-present.

NASA, Land Surface Hydrology Program, $280,000, Snow Hydrology: the Parameterization of subgrid processes within a physically based snow energy and mass balance model, Co-Principal Investigator, 1999-present.

USDA National Research Initiative Competitive Grants Program, $279,500, Quantifying the Exposure of Streams to Sediment Inputs from Managed Forests, A Risk Based Approach, Subcontractor, 2000-present.

National Council of the Paper Industry for Air and Stream Improvement (NCASI), $44,000, Road Erosion under Natural Rainfall, Principal Investigator, 1994-2000.

USDA Forest Service Technology Development Program, $15,000, Effectiveness of Road Ripping for Restoration of Hydraulic Conductivity, Principal Investigator, 1995.

Interior West Global Change, $50,000, Development of a High Resolution Climate Data Set for the Northern Rockies, Co-Principal Investigator, 1995.

Publications
Refereed Journal Articles

Luce, C.H. and Wemple, (2000), "Introduction to the Special Issue on Hydrologic and Geomorphic Effects of Forest Roads." Earth Surface Processes and Landforms, 26(2), (In Press).

Luce, C.H. and T.A. Black, (2000), "Spatial and Temporal Patterns in Erosion from Forest Roads" *In* Influence of Urban and Forest Land Uses on the Hydrologic-Geomorphic Responses of Watersheds, M.S. Wigmosta and S.J. Burges, Editors, American Geophysical Union, Washington, D.C. (In Press).

Prasad, R., D.G. Tarboton, G. Liston, C. Luce, and M. Seyfried, (2000), "Application of a Wind Blowing Snow Model to Reynolds Creek Experimental Watershed", Water Resources Research (In Press).

Luce, C.H. and T.A. Black, (1999), "Sediment production from forest roads in western Oregon." Water Resources Research 35(8): 2561-2570.

Luce, C. H., D. G. Tarboton and K. R. Cooley, (1999), "Subgrid parameterization of snow distribution for an energy balance snow cover model." Hydrological Processes 13:1921-1933.

Elliot, W.J., R.B. Foltz, C.H. Luce. (1999). Modeling Low-Volume Road Erosion. Transportation Research Record, 1652:244-249.

Tysdal, L.M., W.J. Elliot, C.H. Luce, and T.A. Black. (1999). Modeling Erosion from Insloping Low-Volume Roads with WEPP Watershed Model. Transportation Research Record, 1652:250-256.

Luce, C. H., D. G. Tarboton and K. R. Cooley, (1998), The influence of the spatial distribution of snow on basin-averaged snowmelt. Hydrological Processes 12(10-11):1671-1683.

Luce, C.H., (1997), Effectiveness of Road Ripping in restoring infiltration capacity of forest roads. Restoration Ecology, 5(3): 265-270.

Luce, C. H. and T. W. Cundy, (1994), "Parameter identification for a runoff model for forest roads," Water Resources Research, 30(4):1057-1069.

Luce, C.H. and G.A. Bradley, (1993), "An evaluation of the Washington State Environmental Policy Act." Environmental Impact Assessment Review. 13:1-8.

Burroughs, E.R. Jr., C.H. Luce, and F. Phillips, (1992), "Estimating Interill Erodibility for Forest Soils." Transactions ASAE. 35(5):1489-1495.

Luce, C. H., and T. W. Cundy, (1992), "Modification of the kinematic wave - Philip infiltration overland flow model," Water Resources Research 28(4):1179-1186.

Proceedings

Luce, C.H. and T.A. Black (2000), "Effects of Traffic and Ditch Maintenance on Forest Road Sediment Production." in Proceedings of the Seventh Federal Interagency Sedimentation Conference, March 25-29, 2001, Reno, Nevada. (In Press).

Tarboton, D.G., C.M.U. Neale, K.R. Cooley, G.N. Flerchinger, C.L. Hanson, C.W. Slaughter, M.S. Seyfried, R. Prasad, C. Luce, and G.Crosby (1999), "Scaling up spatially distributed models of semiarid watersheds," In Proceedings, 1999 Water and Watersheds Program Review, April 19-21, 1999, Silver Spring, Maryland, pp. 107-108. National Science Foundation, U.S. Environmental Protection Agency, and U.S. Department of Agriculture.

Luce, C.H. and T.A. Black (2001), "Erosion over time from Gravel-Surfaced Forest Roads in Western Oregon," In Proceedings, Forest Sedimentation Conference, April 14-15, 1999, Tigard, Oregon. Pp. 135-139. Northwest Forest Soils Council and Western Forestry and Conservation Association.

Black, T.A. and C.H. Luce. (1999), "Changes in erosion from gravel surfaced forest roads through time," In Proceedings of the International Mountain Logging and 10th Pacific Northwest Skyline Symposium, March 28-April 1, 1999, Corvallis, Oregon. International Union of Forestry Research Organizations and Oregon State University.

Elliot, W.J., R.B. Foltz, and C.H. Luce. (1997) "Predicting the Impacts of Forest Roads on the Environment." In Proceedings of the no III Simpósio Brasiliero sobre Colheita e Transporte Florestal, Vitória – ES – Brasil, de 8 a 12 dezembro de 1997. pp. 99-119.

Luce, C. H., D. G. Tarboton and K. R. Cooley, (1997). "Spatially Distributed Snowmelt Inputs to a Semi-Arid Mountain Watershed," In Proceedings of the Western Snow Conference, Banff, Canada, May 5-8, 1997.

Tysdal, L.; Elliot, W.; Luce, C.; Black, T., (1997), "Modeling insloping road erosion processes with the WEPP watershed model," Paper 975014 Presented at the 1997 ASAE Annual International Meeting, August 10-14 1997, Minneapolis, MN. St. Joseph, MI: American Society of Agricultural Engineers. 14 pp.

Luce, C.H., (1996), "On the sensitivity of a hillslope subsurface flow model to flow parameterizations." American Water Resources Association, Utah State Chapter, Student Paper Contest 2nd Place. (Refereed).

Elliot, W.J., C.H. Luce, and P.R. Robichaud, (1996), "Predicting Sedimentation from Timber Harvest Areas with the WEPP Model" Proceedings of the Sixth Interagency Sedimentation Conference, March 10-14, 1996, Las Vegas, NV. pp. IX:46-53. (Refereed).

Elliot, W.J.; Foltz, R.B.; Luce, C.H.; Koler, T.E, (1996), "Computer-aided risk analysis in road decommissioning," Proceedings of the AWRA Annual Symposium on Watershed Restoration Management. American Water Resources Association, Syracuse, NY. pp. 341-350. (Refereed).

Luce, C.H., E. Kluzek, and G.E. Bingham, (1995), "Development of a High Resolution Data Set for the Northern Rockies". Proceedings of the Interior West Global Change Workshop, R.W. Tinus, editor. USDA Forest Service, Rocky Mountain Forest and Range Experiment Station, General Technical Report RM-GTR-262. Fort Collins, Colorado. pp. 106-111.

Foltz, R.B., C.H. Luce, and P. Stockton, (1995), "The Kinetic Energy Field Under a Rainfall Simulator." Proceedings of Watershed Management, Planning for the 21st Century. American Society of Civil Engineers, Reston, Virginia. pp. 388-397. (Refereed).

Elliot, W.J., R.B. Foltz, and C.H. Luce, (1995), "Validation of Water Erosion Prediction Project (WEPP) Model for Low-Volume Forest Roads," Proceedings of the Sixth International Conference on Low-Volume Roads, edited by Transportation Research Board. National Academy Press, Washington, D.C. pp. 178-186. (Refereed).

Elliot, W.J., P.R. Robichaud, R.B. Foltz, and C.H. Luce, (1993), "A tool for estimating disturbed forest site sediment production." Proceedings: Interior Cedar-Hemlock-White Pine Forests. Ecology and Management Symposium, Spokane, Washington.

Robichaud, P.R., R.B. Foltz, and C.H. Luce, (1993), "Development of an on-site sediment prediction model for forest roads and timber harvest areas." Proceedings of the IAHS-ICCE Symposium on Sediment Problems: Strategies for monitoring, prediction, and control. July 11-23, 1993. Yokohama, Japan. IAHS publ. no. 217, pp. 135-140. (Refereed).

Robichaud, P.R. and C.H. Luce, (1993), "Variation in Hydraulic Conductivity and Erodibility Between Treatments in Timber Harvest Sites in the Southern Appalachians." Proceedings of the International Russian, United States, Ukrainian Workshop on Quantitative Assessment of Soil Erosion, Moscow, Russia. September 20-24. M.A. Nearing, Editor.

Book Chapters

Tarboton, D.G., G. Blöschl, K. Cooley, R. Kirnbauer, and C. Luce, (2000), Spatial Snow Cover Processes at Kuhtai and Reynolds Creek. Chapter 7 in Spatial Patterns in Hydrological Processes: Observations and Modeling, Edited by R. Grayson and G. Blöschl, Cambridge University Press (In Press).

Luce, C. H., (1995), "Forests and Wetlands," Chapter 8 in Environmental Hydrology. A. D. Ward and W. J. Elliot, editors. CRC Press. Boca Raton, Florida.

Model Handbook Available over Internet

Tarboton, D. G. and C. H. Luce, (1996), "Utah Energy Balance Snow Accumulation and Melt Model (UEB)," Computer model technical description and users guide, Utah Water Research Laboratory and USDA Forest Service Intermountain Research Station. Available at http://www.engineeering.usu.edu/dtarb.

Recent Published Abstracts From Meeting Presentations

Luce, C.H. and T.A. Black (1998), "Erosion from Gravel-Covered Forest Roads in Western Oregon," Eos, Transactions, American Geophysical Union, 79(45): F352, AGU Fall Meeting Suppl.

Luce, C.H., D.G. Tarboton, and K.R. Cooley. (1998), "Sub-grid Parameterization for Modelling Snow Properties and Melt," Eos, Transactions, American Geophysical Union, 79(45): F272, AGU Fall Meeting Suppl.

Clayton, J.L., C.H. Luce, and A.F. Barta. (1998), "Groundwater Level Response in a Riparian Zone to a Temporary Flow Diversion in the Idaho Batholith," Eos, Transactions, American Geophysical Union, 79(45): F352, AGU Fall Meeting Suppl.

Luce, C.H. and T.A. Black. (1998), "Erosion Over Time from Forest Roads in the Oregon Coast Range," In Proceedings of the Watershed Management Council Meeting, Boise, Idaho, September 21-24, 1998.

Black, T.A. and C.H. Luce. (1997), Sediment production from Forest roads in the Oregon Coast Range. Eos, Transactions, American Geophysical Union, 78(46): F314, AGU Fall Meeting Suppl.

Luce, C. H., D. G. Tarboton and K. R. Cooley, (1997), "Spatially integrated snowmelt modeling of a semi-arid mountain watershed," Eos, Transactions, American Geophysical Union, 78(46): F205, AGU Fall Meeting Suppl.

Papers Written and in Internal or Journal Review

Luce, C.H. and D.G. Tarboton, (2000), Scaling up Snow Accumulation and Melt Models. Water Resources Research, in Review.

Prasad, R., D.G. Tarboton, G. Flerchinger, K. Cooley, and C. Luce, (2000), Understanding Hydrologic Behavior of a Small Semi-Arid Mountainous Watershed. Hydrological Processes, in Review.

Luce, C.H., U. Lall, A. Sharma, and B. Rajagopalan, (2000), A Comparison of Parametric and Non-parametric Stochastic Climate Simulations for Use in Erosion Modeling. To be submitted to Water Resources Research, in internal review.

Luce, C.H. and D.G. Tarboton, (2000), Snowpack Energy Fluxes in a Large Mountain Valley. To be submitted to Journal of Hydrometeorology, in internal review.

Peterson, K.C., Luce, C.H., and W.J. Elliot, (2000), The Use of TOPMODEL in a Small, Forested Watershed Under Snowmelt Runoff Conditions. To be submitted to Hydrological Processes, in internal review.

Luce, J., Molnau, M., Robichaud, P., Johnson, S., and Luce, C., (2000), Snowpack Outflow and Streamflow in Northwestern Montana, Rocky Mountain Research Station General Technical Report, in internal review.

Patents

Patent pending for Magnetostrictive Precipitation Gage, Patent application serial number: 09/637,031.